NAVAL POSTGRADUATE SCHOOL
MONTEREY, CALIFORNIA

THESIS

NUMERICAL INVESTIGATION OF SUBSONIC FLOW OVER BODIES OF REVOLUTION AND A TYPICAL MISSILE FOREBODY
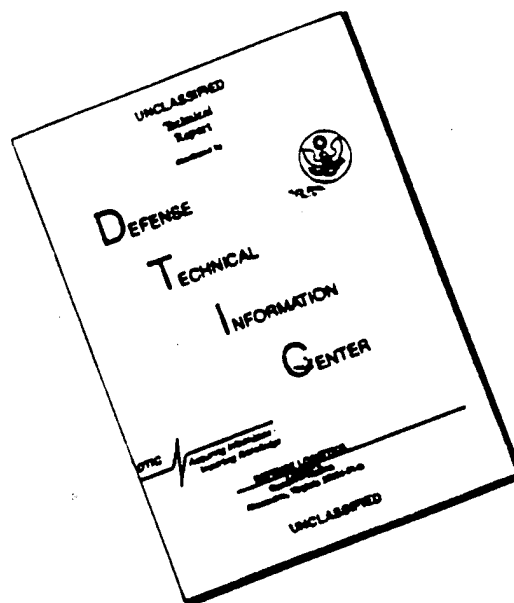
by

Ronald E. Marvin

September, 1995

Thesis Advisor: Max F. Platzer

Approved for public release; distribution is unlimited

DISCLAIMER NOTICE

THIS DOCUMENT IS BEST
QUALITY AVAILABLE. THE COPY
FURNISHED TO DTIC CONTAINED
A SIGNIFICANT NUMBER OF
PAGES WHICH DO NOT
REPRODUCE LEGIBLY.

1. AGENCY USE ONLY (Leave blank)	2. REPORT DATE September 1995	3. REPORT TYPE AND DATES COVERED Engineer's Thesis

4. TITLE AND SUBTITLE NUMERICAL INVESTIGATION OF SUBSONIC FLOW OVER BODIES OF REVOLUTION AND A TYPICAL MISSILE FOREBODY	5. FUNDING NUMBERS
6. AUTHOR(S) Ronald E. Marvin	

7. PERFORMING ORGANIZATION NAME(S) AND ADDRESS(ES) Naval Postgraduate School Monterey CA 93943-5000	8. PERFORMING ORGANIZATION REPORT NUMBER
9. SPONSORING/MONITORING AGENCY NAME(S) AND ADDRESS(ES)	10. SPONSORING/MONITORING AGENCY REPORT NUMBER

12a. DISTRIBUTION/AVAILABILITY STATEMENT Approved for public release; distribution is unlimited.	12b. DISTRIBUTION CODE

13. ABSTRACT (maximum 200 words)

It was the objective of this investigation to study the subsonic flow over a missile forebody. To this end, the NASA Ames developed OVERFLOW, three dimensional, Navier-Stokes Code was applied and detailed results were obtained for the missile forebody. The flow conditions were set at a Mach Number of 0.3 and Reynolds Number of two million for each angle of attack at 0, 2, 6, 10, and 14 degrees. These viscous flow solutions were compared with three inviscid flow solutions, namely Slender Body Theory, von Karman's Method, and the NASA Ames Panel Code called PMARC. As expected, the OVERFLOW and PMARC solutions were in good agreement at zero and small angles of attack. As the angle of attack was increased, the OVERFLOW solution showed the development of the vortical flow separation on the leeward side of the body.

14. SUBJECT TERMS Potential Theory, von Karman, Slender Body, Panel Method, PMARC, Body of Revolution, Computational Fluid Dynamics, OVERFLOW, Missile Forebody	15. NUMBER OF PAGES 128
	16. PRICE CODE

17. SECURITY CLASSIFICATION OF REPORT Unclassified	18. SECURITY CLASSIFICATION OF THIS PAGE Unclassified	19. SECURITY CLASSIFICATION OF ABSTRACT Unclassified	20. LIMITATION OF ABSTRACT UL

NUMERICAL INVESTIGATION OF SUBSONIC FLOW OVER BODIES OF REVOLUTION AND A TYPICAL MISSILE FOREBODY

Ronald E. Marvin
B. S., United States Military Academy, 1966
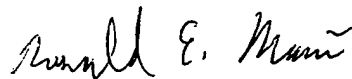
Submitted in partial fulfillment of the
requirements for the degree of

AERONAUTICAL ENGINEER

from the

NAVAL POSTGRADUATE SCHOOL
September 1995
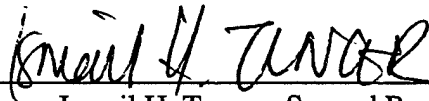
Author: _____
Ronald E. Marvin

Approved by: _____
Max F. Platzer, Thesis Advisor

_____
Ismail H. Tuncer, Second Reader

_____
Daniel J. Collins, Chairman
Department of Aeronautics and Astronautics

ABSTRACT

It was the objective of this investigation to study the subsonic flow over a missile forebody. To this end the NASA Ames developed OVERFLOW, three dimensional, Navier-Stokes Code was applied and detailed results were obtained for the missile forebody. The flow conditions were set at a Mach Number of 0.3 and Reynolds Number of two million for each angle of attack at 0, 2, 6, 10 and 14 degrees. These viscous flow solutions were compared with three inviscid flow solutions, namely Slender Body Theory, von Karman's Method and the NASA Ames Panel Code called PMARC. As expected, the OVERFLOW and PMARC solutions were in good agreement at zero and small angles of attack. As the angle of attack was increased, the OVERFLOW solution showed the development of the vortical flow separation on the leeward side of the body.

TABLE OF CONTENTS

ACKNOWLEDGEMENTS

I. INTRODUCTION

Over the years, a number of methods have been developed to provide the missile aerodynamicist with tools to predict the aerodynamic characteristics of various missile configurations. They range from purely empirical methods and simple slender body theory to panel methods and Navier-Stokes Methods. A recent review of these methods can be found in Reference 1. This review reveals the fact, that the prediction of strong viscous and separated flow effects, presents a great challenge.

Modern missiles tend to have small lifting surfaces. Therefore, the contributions of the body to the forces and moments, and the understanding of the wing-body interference becomes very important. In addition, the missiles are launched at relatively high angles of attack, further exacerbating the problem, due to the vortex shedding from the missile body. As a result, there is a growing need to compute the detailed flow separation and the vortical flow features, which occur over typical modern missile configurations, using the full viscous flow equations.

At NASA-Ames a considerable amount of work was done to study the viscous flow surfaces over blunt-nose bodies of revolution. This work used the NASA-Ames developed OVERFLOW Code for the solution of the thin-layer Navier-Stokes equations. References 2 through 5 document this effort. Recently Reference 6 extended this work, by computing of the flow field about a complete missile at high angle of attack. The results of Reference 6 were compared to experiments, described in Reference 7.

As pointed out, for example in Reference 8, vortices are shed from the forward body and the canards. These vortices affect the pressure distribution and the forces and moments on the missile. Therefore, in this thesis the missile forebody of Reference 6 is investigated in greater detail.

Starting with the solution for zero angle of attack, the angle of attack is gradually increased to 14 degrees. This allows the comparison of the Navier-Stokes solutions with the simpler and faster methods for the more benign flows at small angles of attack, where inviscid methods can be expected to give reasonable results. This comparison allows assessing the range of validity of the simpler methods. Slender Body Theory, von Karman's Method and NASA-Ames panel code PMARC were chosen to compare with the Navier-Stokes calculations from the OVERFLOW Code. These methods are briefly described in Chapters 2 through 4. Chapter 5 presents the major results of this thesis, while Chapter 6 gives the conclusions and recommendations for future work.

1

II. SLENDER BODY METHOD FOR APPROXIMATING FLOW PAST BODIES OF REVOLUTION AT ZERO DEGREE ANGLE OF ATTACK

A.   THEORY

The Slender Body Method is based on the assumptions of incompressible, inviscid and irrotational flow. The governing equation is Laplace's equation for the potential $\phi(x,r,\theta)$ [Reference 9],

$$\frac{\partial^2 \phi}{\partial x^2} + \frac{\partial^2 \phi}{\partial r^2} + \frac{1}{r}\frac{\partial \phi}{\partial r} + \frac{1}{r^2}\frac{\partial^2 \phi}{\partial \theta^2} = 0 \tag{2.1}$$

Equation 2.1 is in cylindrical coordinates (x,r,θ). The body's angle of attack is assumed to be zero, and the body's longitudinal axis is assumed to coincide the x axis.

Source superposition along the x axis, then produces the well-known equation for the disturbance potential,

$$\phi = -\frac{U}{4\pi}\int_0^l \frac{F'(\xi)d\xi}{\left[r^2 + (\xi - x)^2\right]^{3/2}} \tag{2.2}$$

(U) is the free stream speed. (ξ) is the source location on the body's longitudinal axis. The body extends from 0 to l. (F') is the change of the body's cross sectional area along the longitudinal axis. It is given by,

$$F'(x) = 2\pi R(x)\frac{dR(x)}{dx} \tag{2.3}$$

The body radius is given by,

$$r = R(x) \tag{2.4}$$

Equation 2.2 is obtained by imposing the slender body assumption, which requires that the body's maximum diameter is much less than the body's length. Also the absolute magnitude of the change in the body's radius $\left(\dfrac{dR(x)}{dx} \right)$ must be small.

From Reference 10. Equation 2.2 can be rewritten in non-dimensional form, obtaining the non-dimensional longitudinal velocity component,

$$\frac{u_x - U}{U} = -\frac{1}{4\pi} \int_0^1 \frac{F'(\xi)(\xi - x)d\xi}{\left[r^2 + (\xi - x)^2 \right]^{3/2}} \tag{2.5}$$

The non-dimensional radial, velocity component becomes,

$$\frac{u_r}{U} = \frac{r}{4\pi} \int_0^1 \frac{F'(\xi)d\xi}{\left[r^2 + (\xi - x)^2 \right]^{3/2}} \tag{2.6}$$

Using these components, the coefficient of pressure (C_p) becomes,

$$C_p = -2\left(\frac{u_x - U}{U} \right) - \left[\left(\frac{u_r}{U} \right)^2 + \left(\frac{u_x - U}{U} \right)^2 \right] \tag{2.7}$$

Depending on the complexity of the surface function, the integrals in Equations 2.5 and 2.6 can be difficult to integrate analytically. Therefore, the MAPLE Program was used to symbolically integrate Equations 2.5 and 2.6 and solve Equation 2.7.

B.   COMPUTER IMPLEMENTATION OF THE METHOD

MAPLE is a general purpose, commercially available, computer code that can perform symbolic mathematics [Reference 11]. The code may also be used for numerical mathematics. To demonstrate this program's usefulness in potential flow theory, Appendix D lists the implementation of Equations 2.5, 2.6 and 2.7 in Sections 1 through 3 respectively. The MAPLE Procedure, given in these Sections, models the flow over a spindle body of revolution as shown in Figure 1. The spindle is at zero degree angle of attack.
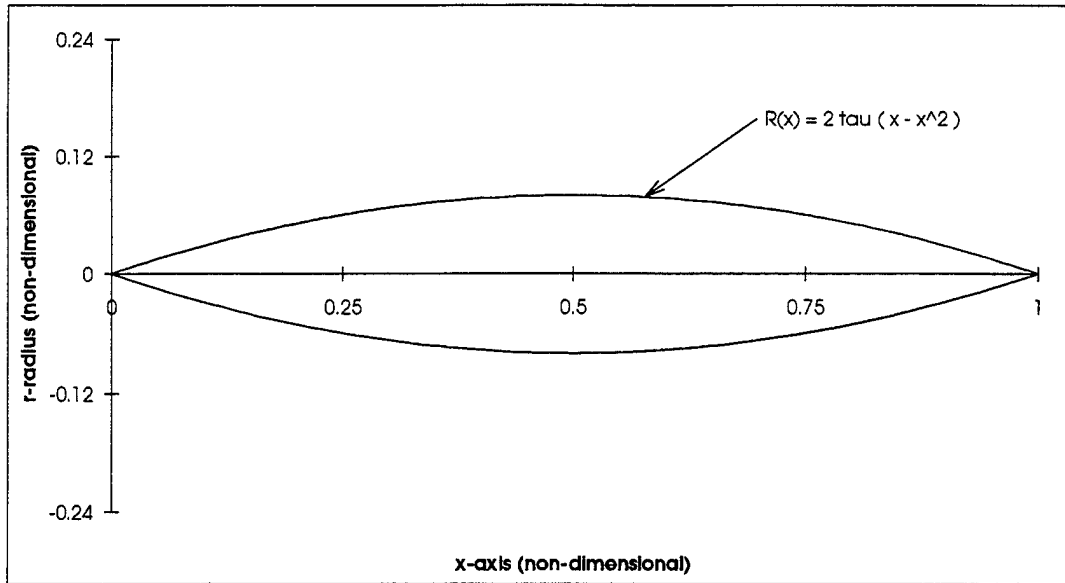
Figure 1. Spindle Body of Revolution Surface Function and Shape.

The geometry is non-dimensional, so that the length is one and maximum diameter (tau) is 16% of the body's length. The maximum diameter occurs at the middle of the body. Velocity components and C_p values for 10 points on the spindle's surface are given in Section 3 of Appendix A.

C.   MAPLE PROCEDURE VERIFICATION

The parabolic spindle shown in Figure 1 is described by,

$$R(x) = 2tau\left(x - x^2\right) \tag{2.8}$$

Its first derivative becomes,

$$\frac{dR(x)}{dx} = 2tau(1 - 2x) \tag{2.9}$$

The absolute magnitude of Equation 2.9 will always be less than one, since the maximum diameter is 0.16. This satisfies the slender body approximation.

To verify the spindle results in Section 3 of Appendix A, Reference 10 gives an approximation of Equation 2.5 of the form,

5

$$\frac{u_x - U}{U} = \frac{1}{2\pi}(F'')\ln r - \frac{1}{2\pi}\left\{(F')\frac{\left(\frac{1}{2}-x\right)}{x(1-x)} + (F'')\left[\ln 2\sqrt{x(1-x)} - 1\right] + \right.$$

$$\left. \frac{1}{2}(F''')\left(\frac{1}{2}-x\right) + \frac{1}{48}(F^{iv})\left[1 + 4\left(\frac{1}{2}-x\right)^2\right]\right\} \qquad (2.10)$$

In this equation (F') is Equation 2.3, while (F''), (F''') and (F^{iv}) represent second, third and fourth derivatives of the body's cross sectional area respectively. Section 4 of Appendix A determines velocity values for Equation 2.10. These are compared to values derived from Equation 2.5, using the surface function for the spindle in Figure 1. Figure 2 shows the comparison between Equations 2.5 and 2.10 for 48 surface points. The agreement is seen to be excellent. Both solutions exhibit the well-known singular behavior of slender body theory at the nose and tail of the body.
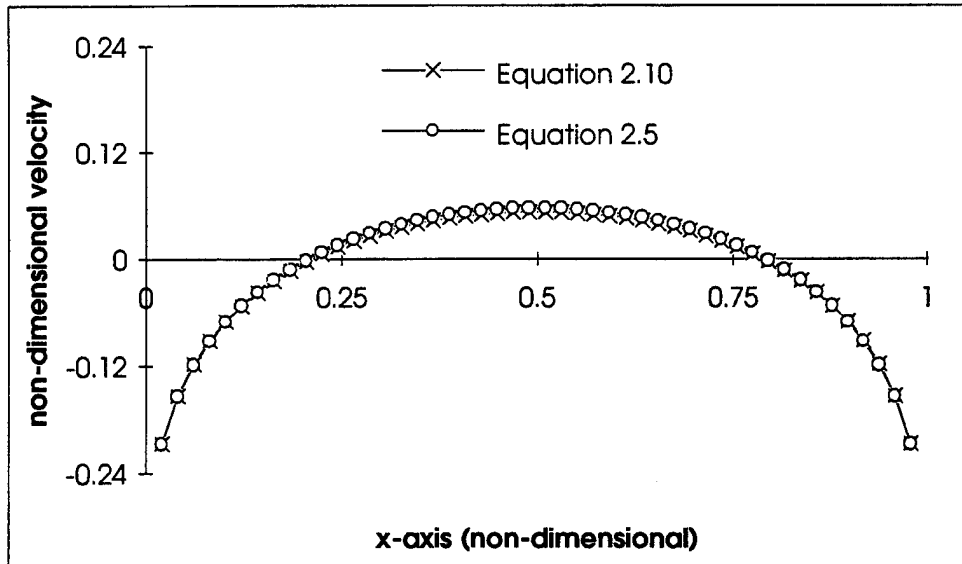
Figure 2. Comparison of Equation 2.5 and 2.10.

D. SUMMARY

This singularity behavior is the result of the integration of Equations 2.5 and 2.6 in Sections 1 and 2 of Appendix A respectively. In both cases integration yields terms containing the logarithmic expression,

$$\ln\left(2\sqrt{x^2+r^2}-2x\right) \tag{2.11}$$

At the spindle's leading or trailing tip the radius approaches zero. At the tips the x coordinate approaches either zero or one respectively. Under these conditions the logarithmic expression becomes indeterminate. As depicted in Figure 2, the velocity components do not have a finite value at the tips of the body. Expression 2.11 also appears in Equation 2.7 (see Section 3 of Appendix A), indicating that the C_p at the tips will not be the expected finite value of one. Another indication of this indeterminate behavior is given in Sections 5 and 6 of Appendix A.

In Section 5 as r and x approach zero, the C_p value peaks at approximately 0.89 The values decrease and do not approach the expected C_p value of one. In Section 6 as r approach's zero and x approach's one, the C_p value oscillates about 0.64, then suddenly decreases at the x coordinate of 0.99927. At this point the MAPLE Program reports a singularity in one of the logarithmic expressions occurring in the solution of Equation 2.7.

This implies that the Slender Body Method is inherently inaccurate near the leading and trailing tips of a body of revolution. The method can be used to confirm computational fluid dynamic (CFD) models in the middle portion of the body, provided that the surface function is relatively simple and continuous. When surface functions can not be easily formulated for complex shapes, the Panel Method might prove more useful.

III. VON KARMAN'S METHOD FOR APPROXIMATING FLOW PAST BODIES OF REVOLUTION

A.   THEORY

von Karman's Method assumes a potential flow about a body of revolution [Reference 12]. The flow is considered incompressible, inviscid and irrotational. The governing equation is Laplace's equation,

$$\frac{\partial^2 \psi}{\partial z^2} + \frac{\partial^2 \psi}{\partial r^2} + \frac{1}{r}\frac{\partial \psi}{\partial r} + \frac{1}{r^2}\frac{\partial^2 \psi}{\partial \theta^2} = 0 \tag{3.1}$$

This represents the flow within a body of revolution in cylindrical coordinates (z, r, θ) [Reference 13]. The solution to this equation may be formed by superposition of elementary flows. These are represented by stream functions (ψ). The stream function for uniform flow of speed (U) z direction is given by,

$$\psi = \frac{1}{2}Ur^2 \tag{3.2}$$

To obtain a solution for flow over a body of revolution at zero angle of attack (non-lifting flow), whose axis coincides with the z axis, it is sufficient to distribute sources along the body axis. The stream function of a source located in the origin of the coordinate system is,

$$\psi = -\frac{mz}{\sqrt{r^2 + z^2}} \tag{3.3}$$

The change in stream function ($d\psi$) at any point in the flow from sources along a small interval ($d\varsigma$) there is,

$$d\psi = -\frac{q_j(z-\varsigma)d\varsigma}{\sqrt{r^2 + (z-\varsigma)^2}} \tag{3.4}$$

9

The interval is measured along the body's longitudinal axis. (q_j) is the source strength per unit length. Integration of Equation 3.4 along this axis yields the induced stream function at any point in the flow. This function is created by sources on the longitudinal axis. The effect of all the source strengths and uniform flow are summed to give the total stream function at any point in the flow. From Reference 13 the summation can be represented as,

$$\psi(r,z) = \frac{1}{2}Ur^2 + \sum_j \left[\sqrt{r^2 + \left(z - z'_{j+1}\right)^2} - \sqrt{r^2 + \left(z - z'_j\right)^2} \right] q_j \qquad (3.5)$$

The $\left(z'_{j+1}\right)$ and $\left(z'_j\right)$ coordinates define the location of the source of constant strength (q_j) on the longitudinal axis. The body of revolution is defined by Equation 2.4. Realizing that the body surface represents the stagnation streamline $\psi = 0$, equating the right hand side of Equation 3.5 to zero provides a means to determine the unknown source strength q_j.

For finite length bodies, the total sum of the source strengths must be zero. This additional condition must be appended to the system given by Equation 3.5. The system therefore becomes,

$$\{\mathbf{const}\} = [\mathbf{dd}]\{\mathbf{q}\} \qquad (3.6)$$

The vector {**const**} is only a function of the known body radius. The coefficient matrix [**dd**] is a function of the known body geometry and source locations, while the vector {**q**} is the unknown source strengths. The resulting system of algebraic equations may now be solved by common equation solves , such as Cramer's Rule, Gaussian Elimination, etc.

Once the source strengths are known on the body's surface, the flow velocity components (u_r, u_z) can be defined through the first derivative of Equation 3.5. From Reference 13 the first derivative with respect to z yields the radial component u_r,. The longitudinal component u_z is obtained from the first derivative with respect to r. Using Bernoulli's Equation, the non-dimensional coefficient of pressure (C_p) is obtained as,

$$C_p = 1 - \left(\frac{u_r}{U}\right)^2 - \left(\frac{u_z}{U}\right)^2 \qquad (3.7)$$

The C_p is the ultimate result of this Method. Since the C_p is a function of the body's geometry, the value will differ at various points in the outer flow field and on the body's

surface. This condition makes the C_p parameter an excellent metric to make comparisons of results from various analytic and computer code techniques.

B.   COMPUTER IMPLEMENTATION OF THE METHOD

Reference 13 lists a computer code that implements von Karman's Method. The code was called SPHERE. A FORTRAN listing of the code is given in Appendix B. This code predicts C_p values about a sphere of radius (a). Since the flow field is symmetrical, the code only calculates C_p values at surface points on the upper half of the sphere. The free stream velocity and the radius of the sphere were assumed to be one. SPHERE used Cramer's Rule to solve the system of equations.

Appendix C and D contain listings of the two output files created by SPHERE. The file called SPH.OUT in Appendix C gives the surface point location (r_i, z_i), calculated (C_p) and exact C_p (C_pex) for various numbers of surface points on the sphere. The exact C_p values are known to be given by,

$$C_pex = 1 - \frac{9}{4}\left(\frac{r_i}{a}\right)^2 \tag{3.8}$$

The derivation of Equation 3.8 may be found in Reference 13. Calculated and exact C_p values were determined for nine surface points as a check of the code. Figure 3 shows that the calculated C_p values plot identically on the exact C_p values for the nine points. However, when the number of surface points is increased, the calculated C_p values diverge from the exact. This is expected because the matrix becomes increasingly ill-conditioned.
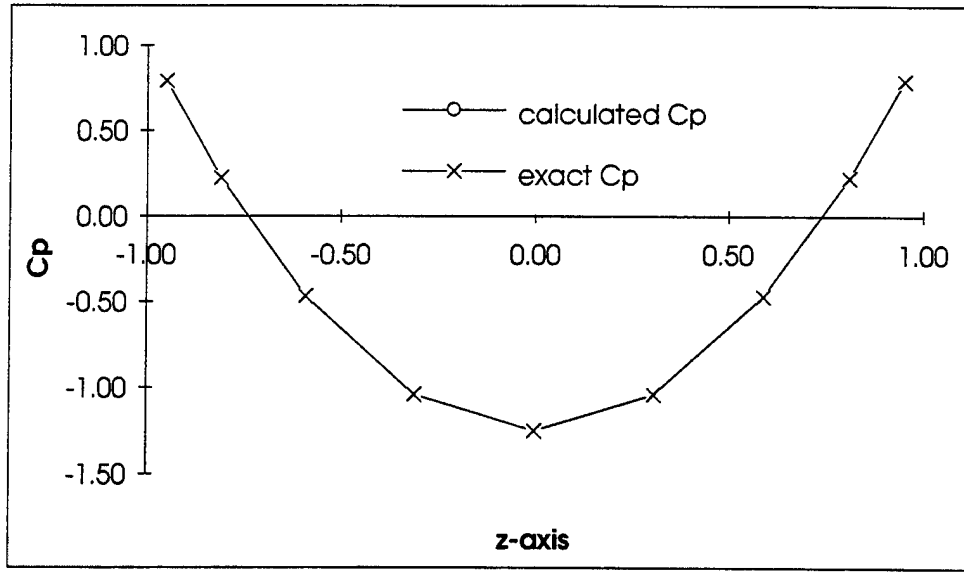
Figure 3. Calculated and Exact C_p Distributions for 9 Surface Points on a Sphere.

C.   ERROR NORM ANALYSIS

Figures 4 and 5 show how the calculated C_p distributions diverge from the exact distribution, as the number of surface points increases. This divergent behavior comes from the ill-conditioning of the coefficient matrix [**dd**] in Equation 2.6. The growth of this ill-conditioning can be defined as,

$$\{\textbf{error}\} = [\textbf{dd}]\{\textbf{q}\} - \{\textbf{const}\} \tag{3.9}$$

$$error\ \ norm = \sqrt{\sum \{\textbf{error}\}^2} \tag{3.10}$$

Appendix D lists the ERR.OUT file from the SPHERE Code. This listing gives the results of Equation 3.10 for various numbers of surface points. Examination of this data and the data's plot in Figure 6 clearly shows the error growth, as the number of surface points increases When the number of surface points exceeds 39, the matrix [**dd**] becomes so ill-conditioned that the code cannot obtain the vector {**q**} in Equation 3.6.

12
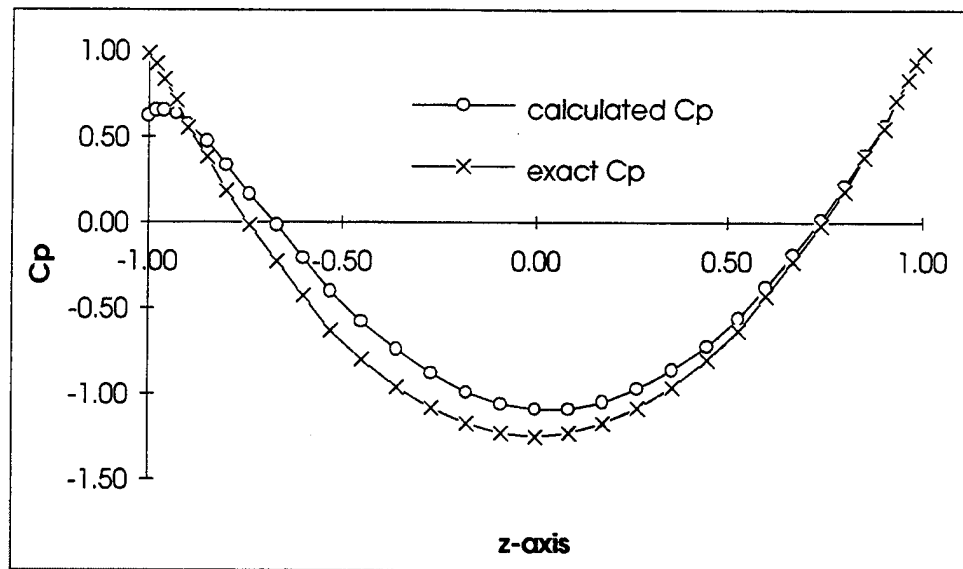
Figure 4. Calculated and Exact C_p Distributions for 33 Surface Points on a Sphere.
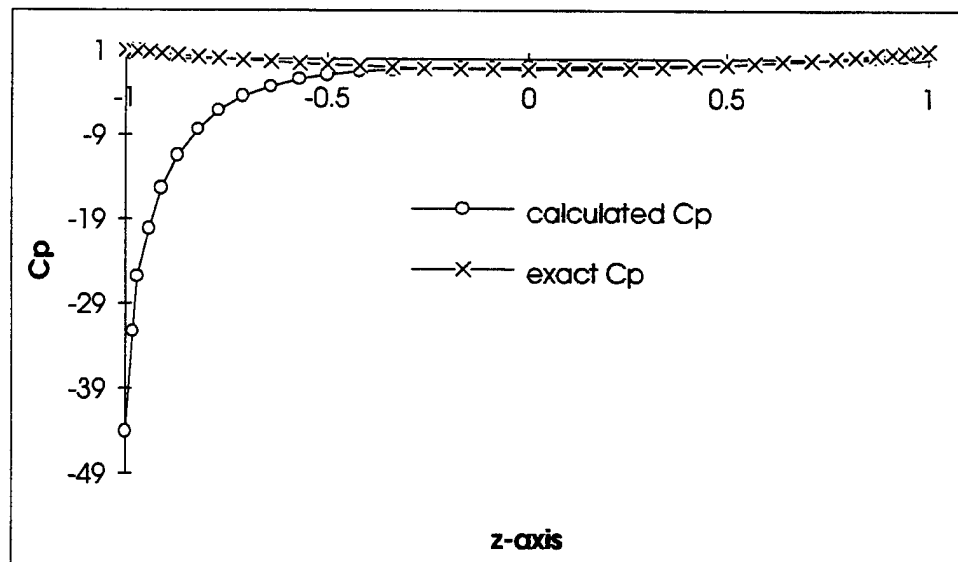
Figure 5. Calculated and Exact C_p Distributions for 35 Surface Points on a Sphere.
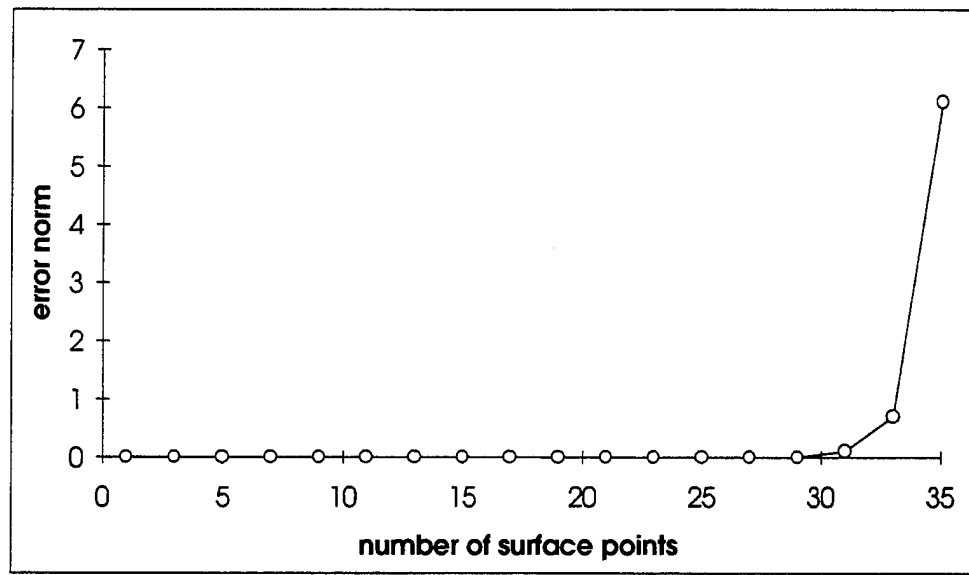
Figure 6. Error Norm verses Number of Surface Points for a Spherical Body of Revolution.

D.   SUMMARY

As shown by von Karman, this method of representing incompressible, inviscid flow over a sphere can be extended to the flow over arbitrary bodies of revolution at zero and small angles of attack. However, the method is limited to slender bodies, because source or doublet distributions are used only along the axis. In contrast to the slender body theory described in Chapter II., it has the advantage of describing the flow over blunt-nosed bodies.

A more general method that eliminates the restriction to slender bodies is afforded by surface distributions of sources and doublets. Such a method is described in the next chapter.

IV. PANEL METHOD FOR APPROXIMATING FLOW PAST BODIES OF REVOLUTION

A.   THEORY

The Panel Method is also based on potential flow theory and generally parallels the development of the Slender Body and von Karman Methods. Reference 14 gives a detailed mathematical description of the Panel Method. This reference also describes how the Method is implemented in the computer code called PMARC (Panel Method Ames Research Center). PMARC assumes an incompressible and irrotational flow. The code does allow a viscous boundary layer on the body, but this option was not used. All of the PMARC results in this thesis were based on inviscid flows. The method solves the three dimensional form of Laplace's equation,

$$\nabla^2 \phi = 0 \qquad\qquad (4.1)$$

As shown in Reference 14, application of Green's Theorem leads to the following integral equation,

$$0 = \left[\iint_{S-P} \mu \bar{n} \bullet \nabla\left(\frac{1}{\bar{r}}\right) dS - 2\pi\mu_P \right] + \iint_S \left(\frac{\sigma}{\bar{r}}\right) + \iint_W \mu_W \bar{n} \bullet \nabla\left(\frac{1}{\bar{r}}\right) dS \qquad (4.2)$$

(μ) and (μ_W) are unknown doublet strengths, on the body's surface element (dS) and on the wake (W) respectively. The doublet strength (μ_P) is zero, if the arbitrary point (P) of interest is off the surface. When the point is on the surface, the strength is 2π. ($\bar{n}$) is the outward surface normal on the body's surface, while ($\bar{r}$) is the vector between P and dS. $\bar{n}$ and $\bar{r}$ are known from the body's geometry. The source strength (σ) is given by,

$$\sigma = \frac{1}{4\pi}\left(V_{norm} - \bar{n} \bullet \bar{V}_\infty\right) \qquad\qquad (4.3)$$

On the body's surface the normal velocity (V_{norm}) is usually zero or may be prescribed. The free stream velocity vector ($\bar{V}_\infty$) is known. Therefore, the source strength is known in Equation 4.2.

Equation 4.2 may be solved numerically by discretizing the body's surface into panels. These panels represent areas of source and doublet strengths, that when known, will define the flow field over the body's surface. This marks the only difference between the Panel Method and those given in Chapters II and III. Previous methods located source strengths inside the body on its' longitudinal axis. In PMARC the source and doublet strengths are assumed to be constant over a panel.

The discretization process results in a system of algebraic equations of the form,

$$\sum_{k=1}^{N_s}\left(\mu_k C_{jk}\right)+\sum_{k=1}^{Ns}\left(\sigma_k B_{jk}\right)+\sum_{l=1}^{N_W}\left(\mu_{W_l} C_{jl}\right)=0\big|_{j=1,N_s} \tag{4.4}$$

The summation terms in Equation 4.4 are analogous to the integrals of Equation 4.2. (B) and (C) become respectively,

$$B_{jk}=\iint_k \frac{1}{\bar{r}} dS \tag{4.5}$$

$$C_{jk}=\iint_k \bar{n} \bullet \nabla\left(\frac{1}{\bar{r}}\right) dS \ , \ C_{jj}=-2\pi \tag{4.6}$$

The first and second terms in Equation 4.4 represent the placement of surface panels on the body. The third term accounts for the wake panels trailing downstream from the body. In PMARC this equation is solved by an iterative technique for very large matrices. The solution occurs in a time stepping fashion, so that either steady or unsteady flows may be calculated. The wake doublet strengths become a function of the surface doublet strengths or,

$$\mu_W = \mu_W(\mu) \tag{4.7}$$

This means that the PMARC time stepping algorithm effectively substitutes Equation 4.7 into Equation 4.4 to yield the surface doublet strengths directly.

These doublet strengths are differenced to obtain the tangential velocity components on the surface of each panel. The velocity components are then used in,

$$Cp_k = 1 - \frac{\bar{V}_k^2}{\bar{V}_\infty^2} + \left(\frac{8\pi}{\bar{V}_\infty^2}\right)\left(\frac{\mu(t) - \mu(t-1)}{\Delta t}\right) \qquad (4.8)$$

Equation 4.8 defines the pressure coefficient (C_{p_k}) at each panel (k). $(\bar{V}_k)$ is the flow velocity magnitude at each panel. The third term in Equation 4.8 accounts for pressure changes when the flow is unsteady. This term is zero for steady flows, so that Equation 4.8 becomes identical to Equations 2.7 and 3.7. Because the theory and PMARC allow the effects of wakes, a problem arises as to how to attach wake panels to bodies of revolution to simulate the effect of flow separation.

B.   MODELING WAKES FROM BODIES OF REVOLUTION

PMARC allows wakes to be excluded from the model. When this occurs PMARC will calculate C_p values, but can not calculate circulation about the body. In this case total aerodynamic forces, such as lift, drag, etc. are not determined. Alternatively, when wakes are included in the model, they must be defined as either *flexible* or *rigid*. Flexible wakes require that the separation line be specified in the input file. Rigid wakes require initial wake panels be defined in regions where the flow is expected to separate.

Reference 14 strongly implies that PMARC's wakes should only be modeled when attached to traditionally defined lifting surfaces, that have sharp, linear trailing edges. This allows a precise definition of a separation line or initial wake panel layout along the edge. The code may then properly apply the Kutta condition at the edge. When wakes are attached to bodies of revolution, without lifting surfaces, the results appear to be questionable, depending on whether the body has a tapered, hemispherical or flat base [Reference 15]. A literature search of References 16 through 19 provided no guidance into acceptable wake modeling for bodies of revolution. Reference 18 claimed to have modeled wakes on a body with no lifting surfaces, but provided no details of the PMARC input file.

In view of this situation the author did not include wakes in any of the PMARC flow models in the thesis. All flow models were considered to be steady. This meant that the third terms of both Equations 4.4 and 4.8 had a value of zero. To evaluate PMARC's ability to compute fully attached flows the code was first applied to the sphere and the spindle, so that the results could be compared with the Slender Body and von Karman's Methods.

C.   VERIFICATION OF PMARC SPHERICAL BODY MODEL

A spherical body was constructed for the PMARC Code. Appendix E lists the input file for the sphere. In the file the name lists &BINP8, &BINP8A and &BINP8B were set to zero in the file. These settings created steady flow. The parameters in the &WAKE1 command were also set to zero. This eliminated the wakes from the model. Figure 7 shows the surface paneling layout.
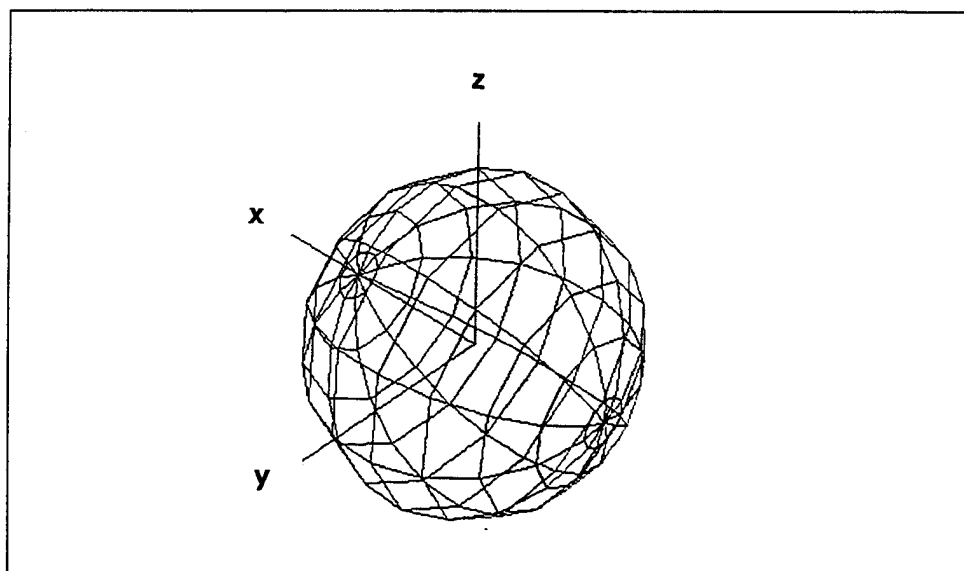
Figure 7. Surface Panel Layout for a Spherical Body.

The panels were positioned on the sphere to yield nine C_p values that corresponded to identical radial and longitudinal locations of the exact C_p values given in Reference 13. All PMARC results shown in this thesis were generated by version 12.21, 4 March 1994, of the code. Figure 8 shows excellent comparison between PMARC and exact C_p values.
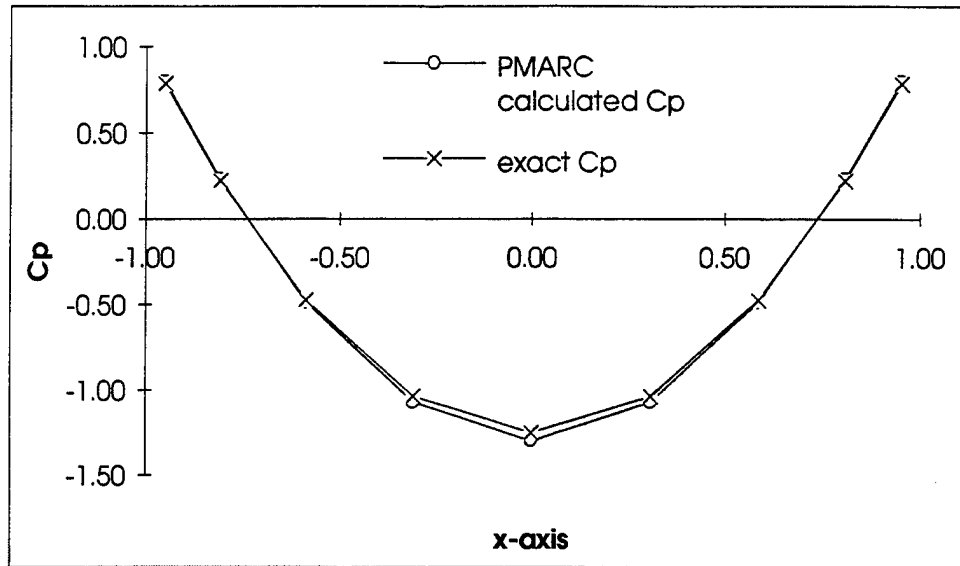
Figure 8. PMARC and Exact C_p Distributions for nine Surface Points on a Sphere without wakes.

D. VERIFICATION OF PMARC SPINDLE BODY MODEL AT ZERO DEGREE ANGLE OF ATTACK

This trend was also confirmed when the spindle body was modeled in steady flow, without wake panels and at zero degree angle of attack. A typical PMARC input file for the spindle is given in Appendix F. Figure 9 displays the PMARC spindle model, using the surface function given in Figure 1. In Figure 9 a positive rotation about the y-axis produces a nose up positive angle of attack, using the right hand rule. The geometry was non-dimensionalized similar to Figure 1. C_p values were calculated and compared to similar values from the Slender Body Method, described in Chapter II. Figure 10 shows that PMARC results compare favorably.
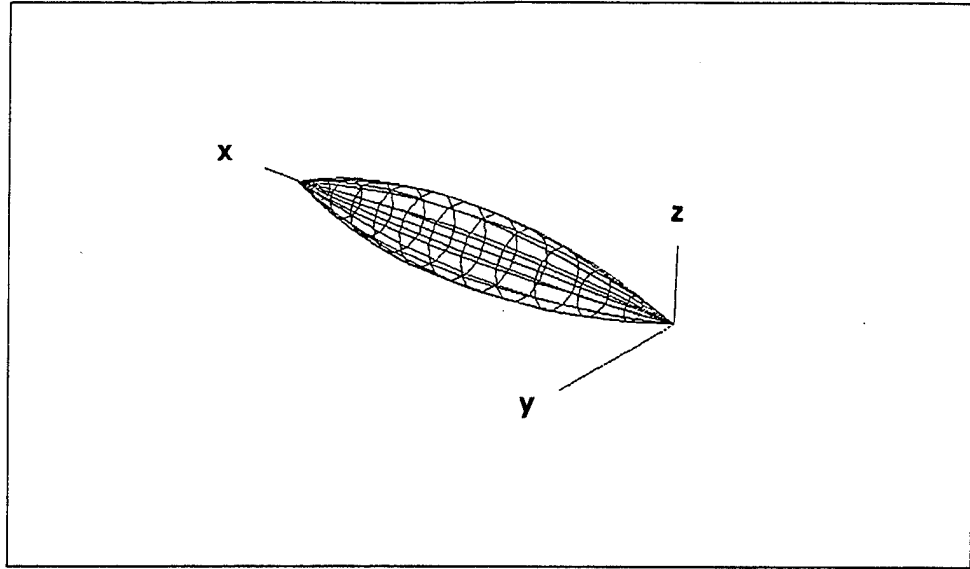
Figure 9. Surface Panel Layout for a Spindle Body.
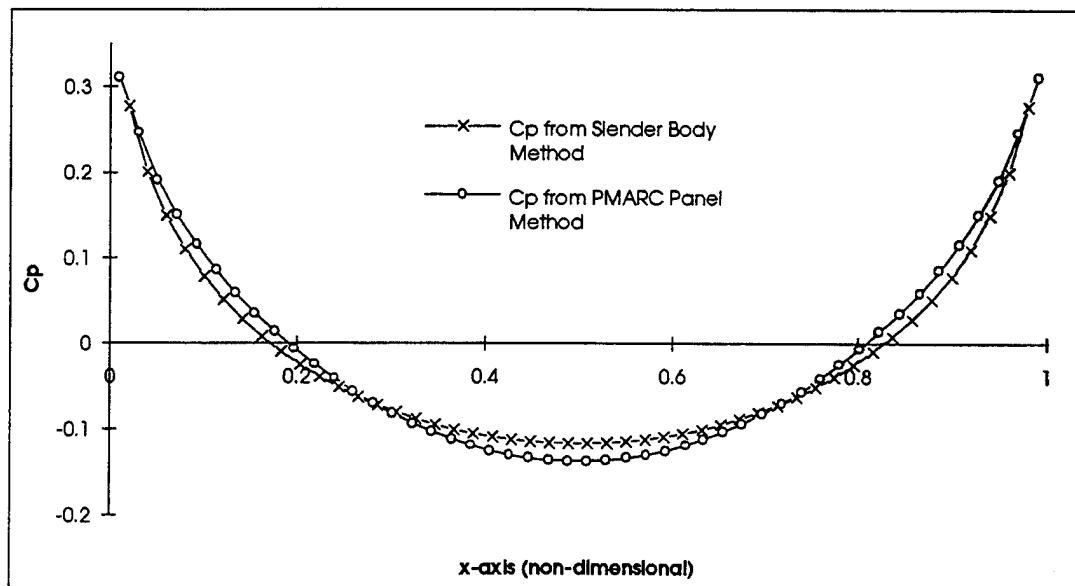
Figure 10. PMARC and Slender Body C_p Distributions for 48 Surface Points on a Spindle at Zero Degree Angle of Attack without Wakes.

20

E. VERIFICATION OF PMARC SPINDLE BODY MODEL AT FIVE DEGREE ANGLE OF ATTACK

The PMARC spindle model was exercised at both zero and five degree angles of attack. This was done to verify the model's physical behavior from a C_p point of view. Figure 11, 12 and 13 compare C_p distributions on longitudinal lines along the body's suction or *top* surface, middle or *mid plane* surface and pressure or *bottom* surface respectively. These longitudinal lines can, alternatively, be defined in Figure 9 as lying in the positive x, z plane for the top surface, the positive x, y plane for the mid plane surface and the positive y, negative z plane for the bottom surface. As expected for a symmetrical spindle, at zero degree angle of attack the C_p distributions are the same longitudinally, regardless of surface orientation.

When the spindle is elevated to an attack angle of five degrees, suction or negative pressures develop on the forward top surface in Figure 11. As expected, the flow accelerates over the forward top surface, creating negative pressures. On the aft top surface the flow experiences an adverse pressure gradient, slowing the flow and creating positive pressure.
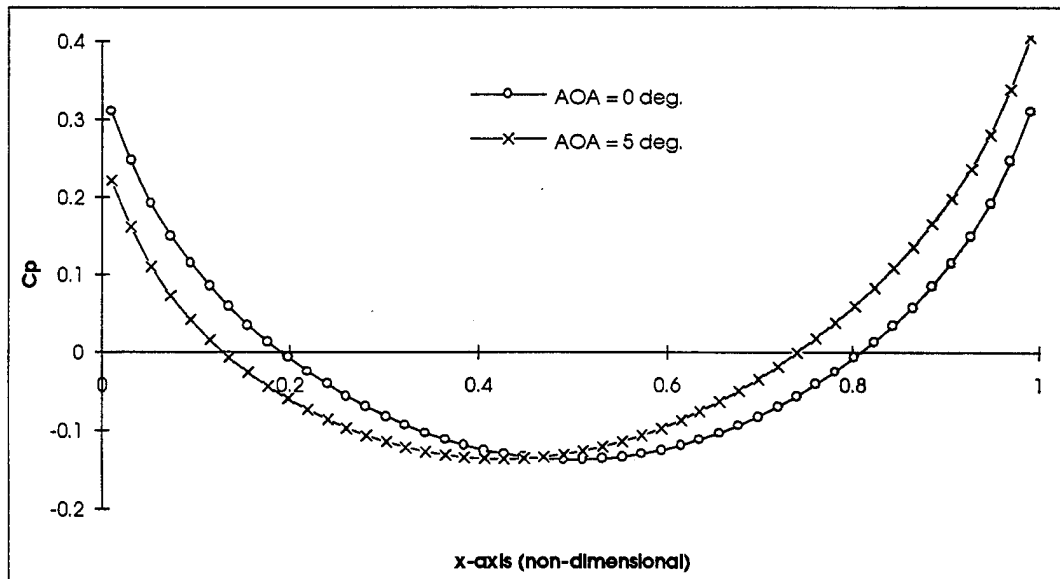
Figure 11. PMARC C_p Distributions for 48 Surface Points on a Spindle at Zero and Five Degrees' Angles of Attack on the Top Surface without Wakes.

21
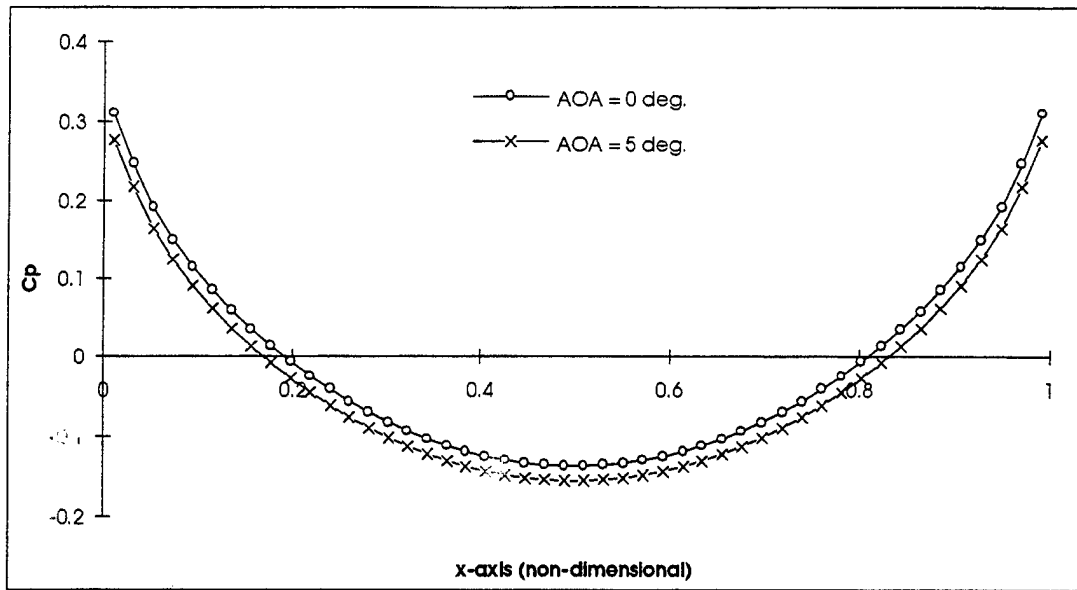
Figure 12. PMARC C_p Distributions for 48 Surface Points on a Spindle at Zero and Five Degrees' Angles of Attack on the Mid Plane Surface without Wakes.
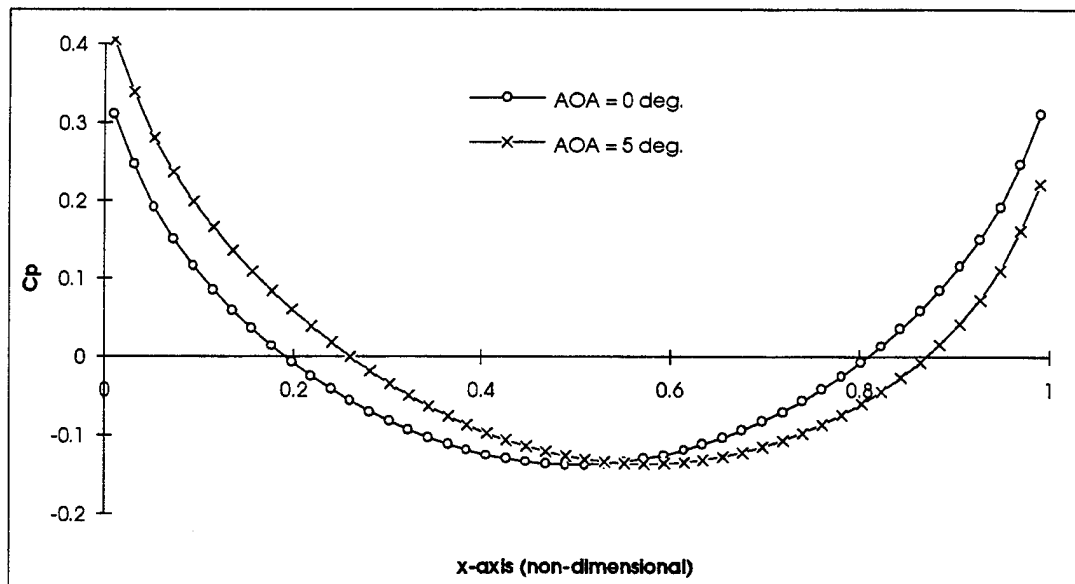
Figure 13. PMARC C_p Distributions for 48 Surface Points on a Spindle at Zero and Five Degrees' Angles of Attack on the Bottom Surface without Wakes.

Figure 12 indicates a relatively constant difference between C_p values at attack angles of zero and five degrees along the spindle's mid plane surface. At zero degree a fluid particle experiences only body fixed, x and y velocity components, as it travels along the body's mid plane surface [see Figure 9]. The particle travels circumferentially and longitudinally along the body's side, when the body is rotated to five degrees. In this case the particle's velocity vector contains all three velocity components in the x, y and z directions. The total velocity is different for either case, producing different C_p distributions.

As expected, in Figure 13 the flow slows on the forward bottom surface, creating positive pressures. On the aft bottom surface the flow experiences a favorable pressure gradient, creating negative pressures.

F.   SUMMARY

The Panel Method, as implemented in the PMARC Code, predicts C_p distributions for bodies of revolution that compare very well with classical potential theories. The code predicts the expected physical behavior of bodies at small angles of attack. Only steady, incompressible, inviscid and irrotational conditions should be considered in the flow. More investigation is needed to understand PMARC's predictions very near the tips of conical shaped bodies. Guide lines should be developed for modeling wakes on bodies of revolution.

Even with these slight deficiencies, PMARC is a suitable tool to confirm pressure fields about CFD models, as long as viscous effects are small. Before explaining how PMARC may be used to verify these models, a brief discussion of the CFD computer code used in this study will be given.

V. A CFD FLOW MODEL OVER A TYPICAL MISSILE FOREBODY

A. A BRIEF THEORY FOR THE OVERFLOW CODE

1. Description of Basic Fluid Dynamic Equations

Due to the experience discussed in Chapter I, the Navier-Stokes flow solver called OVERFLOW was chosen for this study. OVERFLOW is currently in development at the NASA-Ames Research Center.

From Reference 20 the governing equations may be written in the three Cartesian x, y and z coordinates. In the vector form the equation for conservation of the flow mass becomes,

$$\frac{\partial \rho}{\partial t} + \nabla \bullet \rho \bar{V} = 0 \tag{5.1}$$

The conservation of flow momentum in compact form is,

$$\rho \frac{D\bar{V}}{Dt} = \nabla \bullet \sigma_{ij} \tag{5.2}$$

Three momentum equations are obtained, when Equation 5.2 is expanded in each Cartesian direction. The conservation of energy equation in the flow may be written as,

$$\rho \frac{De_i}{Dt} = \nabla \bullet (k\nabla T) + \sigma_{ij} \frac{\partial u_i}{\partial x_j} \tag{5.3}$$

In these five equations (ρ), (t), $(\bar{V})$, (e_i), (k) and (T) are respectively density, time, the velocity vector, internal energy, thermal conductivity and temperature. The fluid stresses (σ_{ij}) are split into pressure and viscous terms as,

$$\sigma_{ij} = p\delta_{ij} + \mu\left(\frac{\partial u_i}{\partial x_j} + \frac{\partial u_j}{\partial x_i}\right) + \delta_{ij}\lambda\nabla \bullet \bar{V} \tag{5.4}$$

The first term in Equation 5.4 is the normal pressure (p) and (δ_{ij}) is the Kronecker Delta Function. This term represents the normal stress components on the fluid element. In the second term (μ) is the molecular viscosity and $\left(\frac{\partial u_i}{\partial x_j} + \frac{\partial u_j}{\partial x_i}\right)$ is the strain in the fluid. In the third term (λ) is the bulk viscosity and is usually assumed equal to $\left(-\frac{2}{3}\mu\right)$ [Reference 21]. When this assumption is made, the last two terms in Equation 5.4 may be combined to form the viscous or shearing stress components on the fluid element.

In OVERFLOW the molecular viscosity in the flow field is approximated by Sutherland's Formula as,

$$\frac{\mu}{\mu_o} \approx \left(\frac{T}{T_o}\right)^{3/2}\left(\frac{T_o + S}{T + S}\right) \tag{5.5}$$

(μ_o) and (T_o) are the reference flow viscosity and temperature respectively. The parameter (S) is assumed to be equal to 194 degrees Rankine for standard air. The turbulent viscosity is determined by the Baldwin and Lomax Turbulence Model in the boundary layer. This turbulent viscosity is added to Equation 5.5. Other turbulence models are available in the code [Reference 20].

Equations' 5.1, 5.2 and 5.3 allow modeling of compressible, viscous and vortical flows, removing the basic assumptions underlying the previous potential flow theory methods. Various mathematical operations are performed on Equations 5.1, 5.2 and 5.3. This effectively places them in a finite difference form suitable for a computer solution.

2. Description of the Major Mathematical Operations

Equations' 5.1, 5.2 and 5.3 are placed in conservative vector form, in order to maintain the accuracy of the solution. The equations become,

$$\frac{\partial Q}{\partial t} + \frac{\partial F}{\partial x} + \frac{\partial G}{\partial y} + \frac{\partial H}{\partial z} = 0 \qquad (5.6)$$

$$Q = \left[\rho, \rho u, \rho v, \rho w, e \right]^T$$

$$F = \left[\rho u, \rho u^2 + p - \tau_{xx}, \rho uv - \tau_{xy}, \rho uw - \tau_{xz}, (e+p)u - u\tau_{xx} - v\tau_{xy} - w\tau_{xz} + q_x \right]^T$$

$$G = \left[\rho v, \rho vu - \tau_{xy}, \rho v^2 + p - \tau_{yy}, \rho vw - \tau_{yz}, (e+p)v - u\tau_{xy} - v\tau_{yy} - w\tau_{yz} + q_y \right]^T$$

$$H = \left[\rho w, \rho wu - \tau_{xz}, \rho wv - \tau_{yz}, \rho w^2 + p - \tau_{zz}, (e+p)w - u\tau_{xz} - v\tau_{yz} - w\tau_{zz} + q_z \right]^T$$

(u), (v) and (w) are the velocity components. $(\tau_{ij}, \quad i,j = x,y,z)$ are the viscous stress components. These stresses can be formed from the last two terms in Equation 5.4. (e) is the total energy and $(q_i, \quad i = x,y,z)$ are the heat transfer terms. Equation 5.6 is non-dimensionalized, so that the different flows may easily be compared, using parameters, such as Mach, Reynolds and Prandtl Numbers. Solutions from non-dimensionalized equations may also be applied to a flow over different size bodies of the same shape. The equations are transformed from the physical domain into computational domain. This transformation is done, so that the equations may eventually be differenced on a uniformly spaced grid [Reference 22]. Equation 5.6 is further simplified by the *thin layer approximation*, which neglects the viscous terms over the body in the streamwise direction.. The equations can now be cast into finite difference form. This leads to a system of algebraic equations, which are solved implicitly in OVERFLOW.

The system in a very simple form may be written as,

$$[lhs]\{\Delta Q\} = \{rhs\} \qquad (5.7)$$

This is called the *delta form* [Reference 4]. The matrix $[lhs]$ and vector $\{rhs\}$ are functions of known flow quantities, such as density, pressure, etc. The vector $\{\Delta Q\}$ is the unknown change in the dependent variables between the current and next time step. For steady flows, when the change in these variables approaches zero, the solution is considered to have *converged* to the best approximation of the original Equations 5.1 through 5.3.

B.   OVERFLOW MISSILE FOREBODY MODEL DESCRIPTION

A flow field about a missile forebody was constructed and exercised in OVERFLOW to obtain an acceptable converged solution. Figure 14 shows the missile forebody's surface, but for clarity it does not show the flow grid extending above the surface. The missile is oriented in an X type configuration to the flow. The axis system is body fixed with the same angle of attack definition given in Figure 9. All of the dimensions of the grid have been non-dimensionalized with respect to the missile's maximum diameter. The maximum diameter is one, while the missile's length is approximately 17.5 diameters. The flow grid extends 39 diameters forward of the nose. The grid extends over the missile body's surface at the aft end to 75 diameters and for computational efficiency only one half of the flow field is modeled. The flow is assumed symmetric about the x, z plane. There is no grid in the negative y direction. There is no grid aft of the missile body's rear base.

The grid over the missile forebody's surface is composed of six sub-grids. These define the in-flow over the missile forebody's nose, the body's mid section, the top and bottom canards, and the out-flow over the body's rear section. The sixth grid is an outer flow grid and covers the mid section. These six grids provide 874,125 total grid points to describe the flow field over the missile's forebody.

All these grids overlap each other to varying extents. In the overlapped regions the *chimera* scheme is used to provide interpolation and grid blanking information [Reference 23]. This information is used to allow OVERFLOW to interpolate the flow variables from one grid to the next. The six grids and the interpolation information are provided to the code in two large files called GRID.IN and FORT.2 respectively. The files were from Reference 24. In addition to these files OVERFLOW requires an input file that describes such things as the number of time steps desired, angle of attack, Mach and Reynolds numbers, time step size, boundary conditions, turbulence model, etc. Appendix G lists a typical OVERFLOW input file for the missile forebody. A description of the various input parameters can be found in Reference 20. All OVERFLOW results shown in this thesis were derived from version 1.6ao, 8 February 1994, of the code. The forebody model was initially exercised at a benign flow condition of zero angle of attack, in order to check the flow physics and solution convergence.

C. OVERFLOW MISSILE FOREBODY FLOW SOLUTION CONVERGENCE STUDY

The initial flow field was set for a free stream Mach Number of 0.3, a Reynolds Number of 2.0 million and zero degree angle of attack. Figures 15 through 20 show the plots of the L_2 norm of the vector $\{\Delta Q\}$ in Equation 5.7 at each iteration. The L_2 norm is the square root of the sum of squares of the vector's elements. As the norm approaches zero, the change in the dependent variable also approaches zero, creating a converged solution. The plots in these figures indicate an acceptable converged solution, after 4000 time steps.

D. PMARC MISSILE FOREBODY MODEL DESCRIPTION

A PMARC flow field of the missile forebody was constructed, using 4836 surface panels. As discussed in Chapter IV, wake panels and boundary layers were not included. The geometry of the PMARC missile forebody in Figure 21 was very similar to the OVERFLOW forebody in Figure 14. Some slight differences existed between the canards of the two forebodes. The PMARC model uses the same body fixed coordinate system and angle of attack definition in Figures 9 and 14. Appendix H lists a typical input file for the PMARC missile forebody. A description of the various input parameters can be found in Reference 14. The PMARC model was exercised at various angles of attack and compared to C_p distributions derived from the OVERFLOW forebody model.

Figure 22 compares typical C_p distributions from both the OVERFLOW and PMARC models. This figure indicates that most of the C_p changes occur in the nose region of the missile. This region extends approximately three to five calibers aft the nose, along the x axis. Figure 23 shows the pressure distribution over the first three calibers and the missile body profile. Similar C_p distribution comparisons were made in this region at various angles of attack, in order to demonstrate where the two models begin to differ.
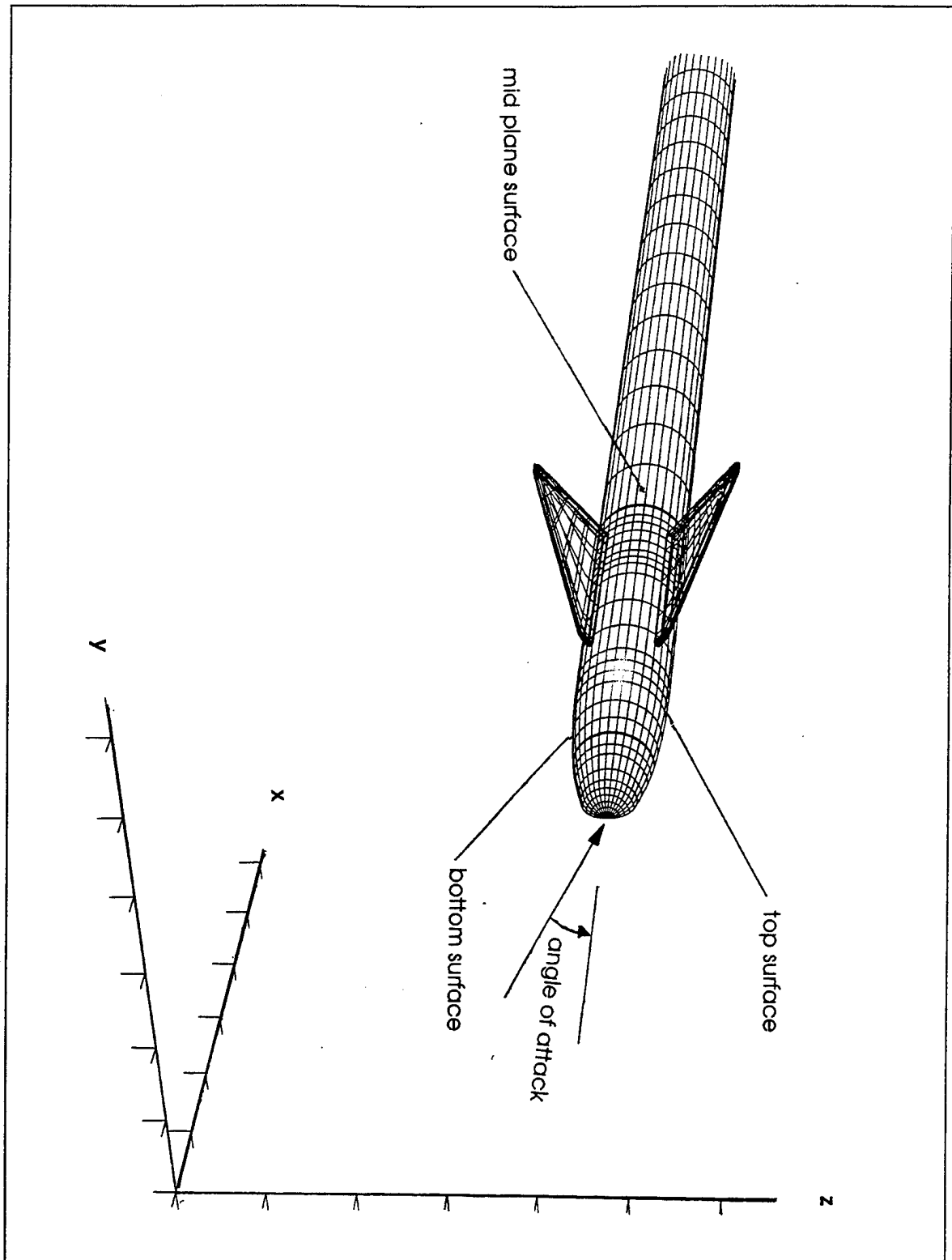
Figure 14. OVERFLOW Missile Forebody Surface.

30
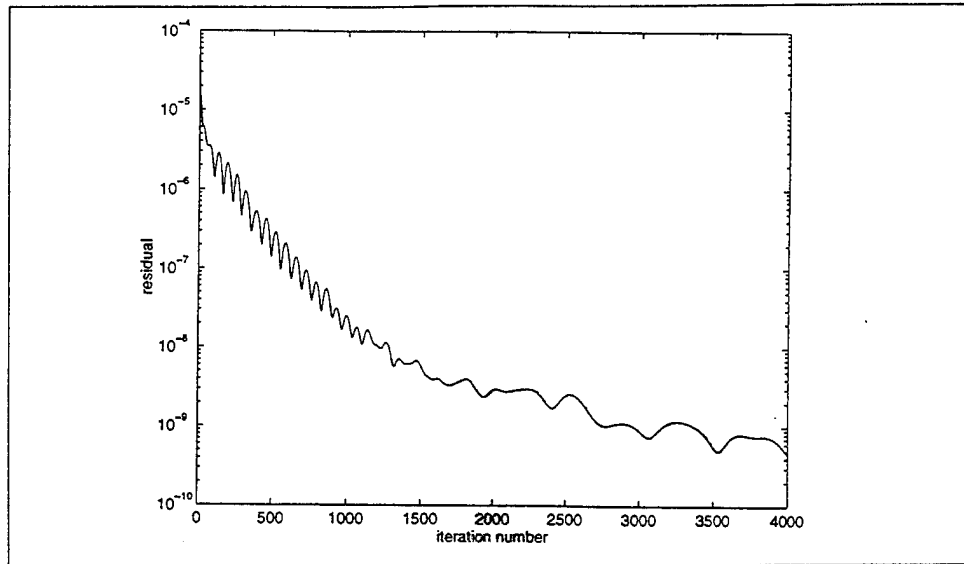
Figure 15. L_2 **Norm for the Nose Grid.**
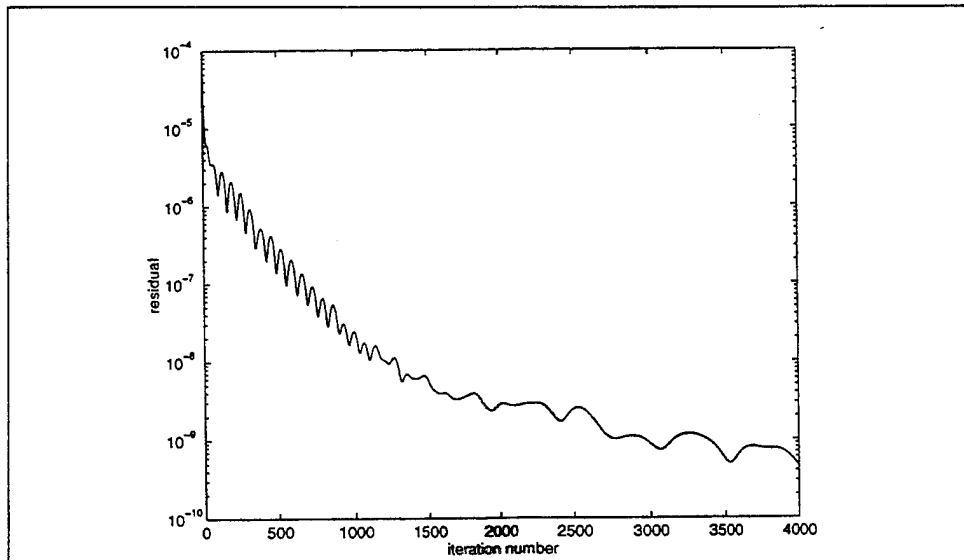
Figure 16. L_2 **Norm for the Mid Section Grid.**

31
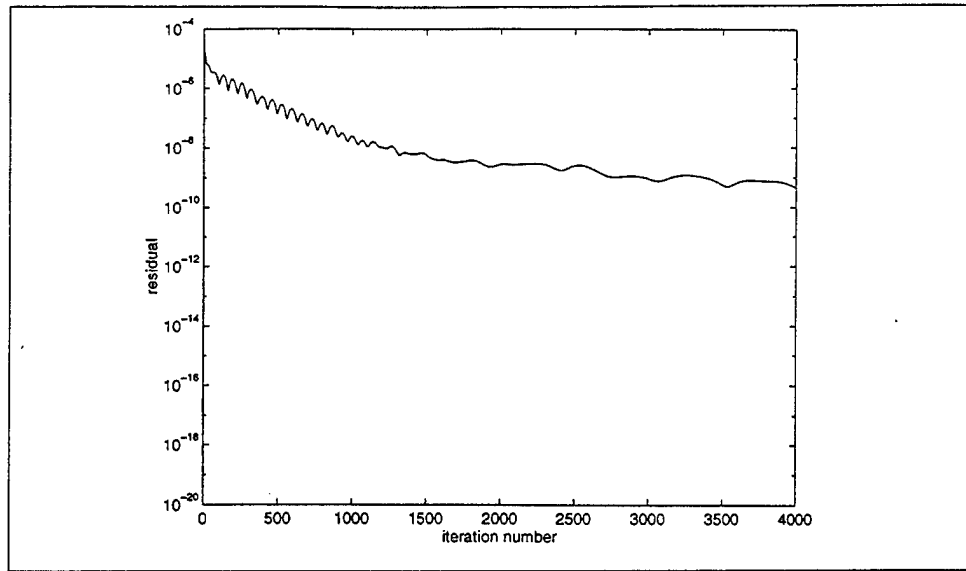
Figure 17. L_2 Norm for the Outer Flow Grid.
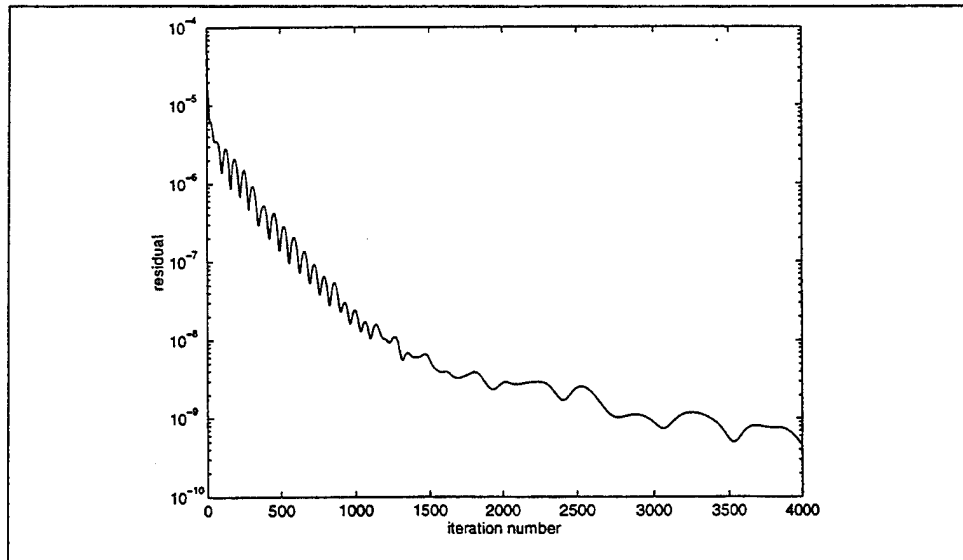
Figure 18. L_2 Norm for the Rear Section Grid.
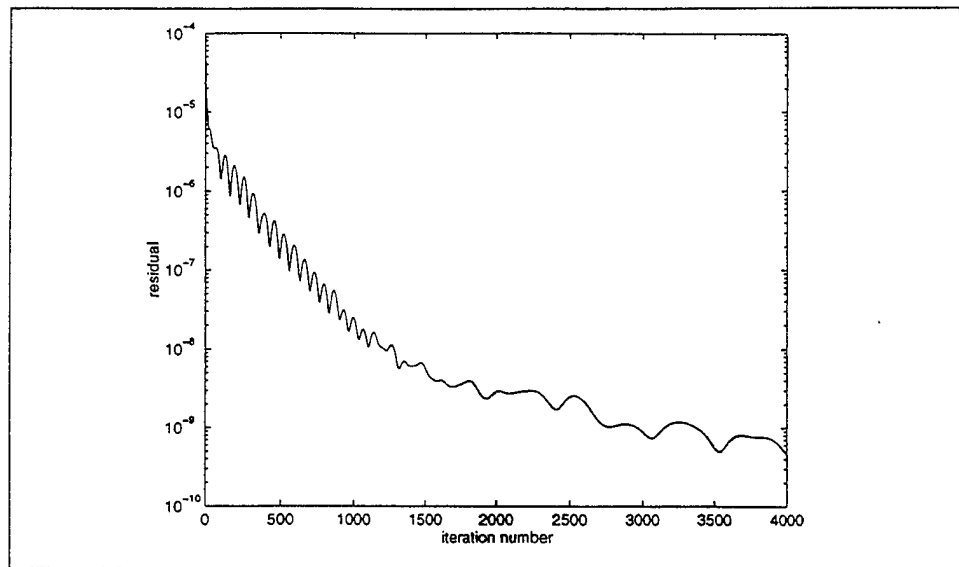
Figure 19. L_2 Norm for the Top Canard Grid.
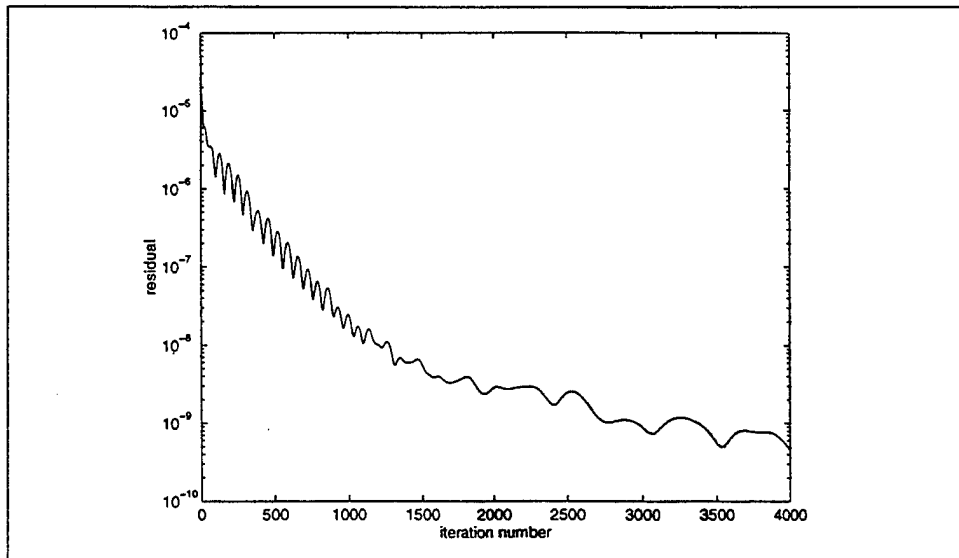
Figure 20. L_2 Norm for the Bottom Canard Grid.

33

E.   COMPUTING TIMES FOR OVERFLOW AND PMARC

Typically OVERFLOW calculations required approximately 10 to 12 cpu days on the Naval Postgraduate School, Cray Y-MP/EL computer for each converged solution. A typical PMARC solution required 1 to 2 cpu days on a Silicon Graphics workstation. The Cray mass storage disk space was accessed across the network for the PMARC runs, since local workstation space was very limited. A PMARC solution could have been obtained much faster, if more local disk space were available.

F.   OVERFLOW AND PMARC C_p DISTRIBUTION COMPARISONS AT VARIOUS ANGLES OF ATTACK

Figures 25 through 38 present C_p distributions for the top , mid plane and bottom surfaces of the nose regions of the two missile forebody models. The models were exercised at 0, 2, 6, 10 and 14 degree angles of attack. The scale used in these figures was the same as used in Figure 23. Figures 39 and 53 are enlargements of figures 25 through 38 in the nose region. These figures show how OVERFLOW and PMARC results diverge as the angle of attack increases.

At zero and two degree angles of attack in Figures 24 through 29 and Figures 39 through 44, there are very good agreement between the two models. At six degree angle of attack in Figure 30 through 32 and Figures 45 through 47, some differences begin to appear along the mid plane surface. The differences in the aft portion of the bottom surface are significant in Figure 32.

Figures 33 through 35 and 48 through 50 show C_p distributions, when the models are at 10 degree angle of attack. Both models are in excellent agreement within the first caliber along the x axis. However, Figures 33 through 35 show differences between both models in the aft portion of the nose region.

Figures 36 through 38 and 51 through 53 present the results of the two models at 14 degree angle of attack. These figures show agreement within the first caliber along the x axis, similar to the 10 degree case. Again there are differences between the OVERFLOW and PMARC models at 14 degree angle of attack in the aft portion of the missile's nose.
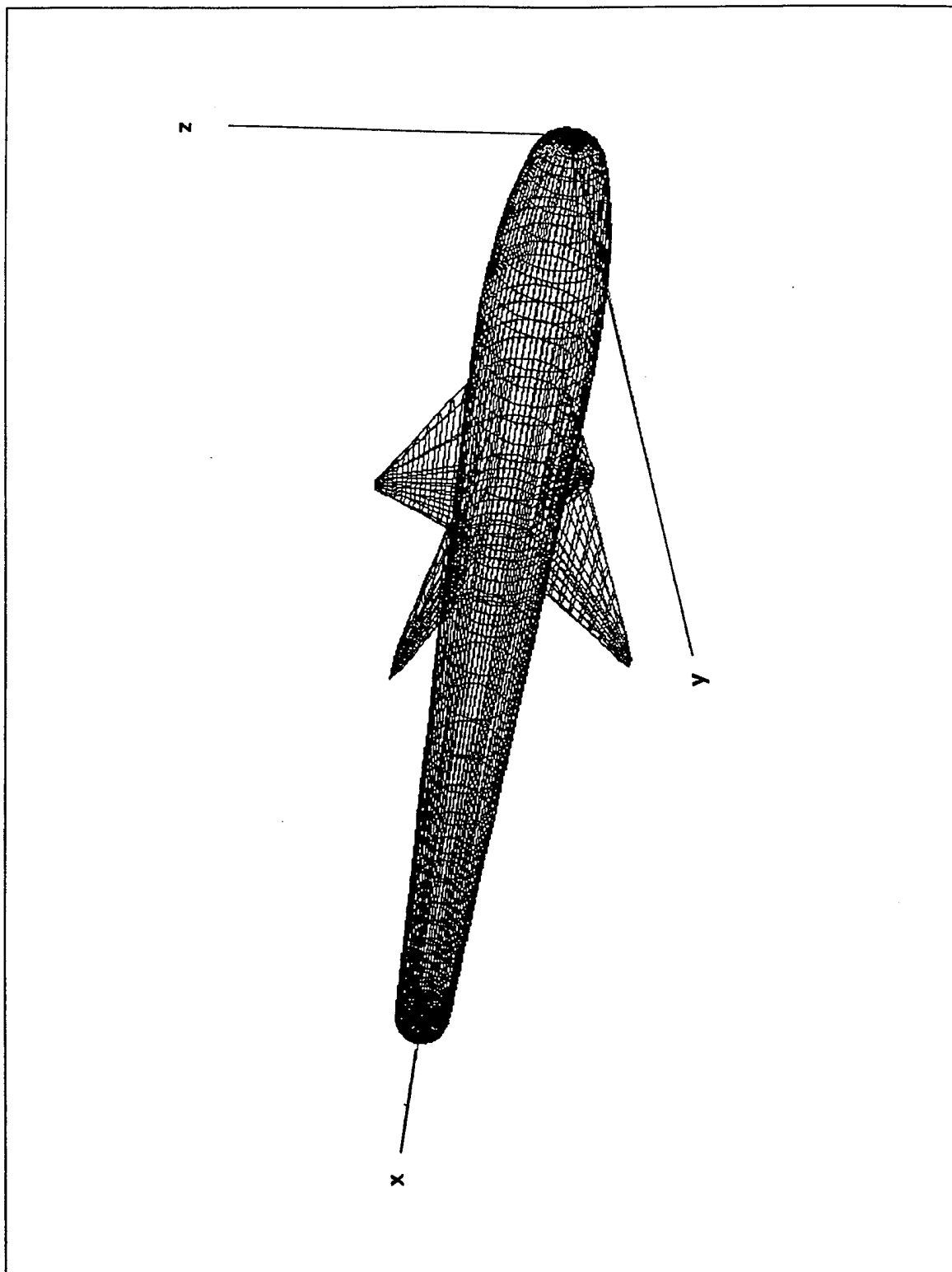
Figure 21. PMARC Missile Forebody Surface.
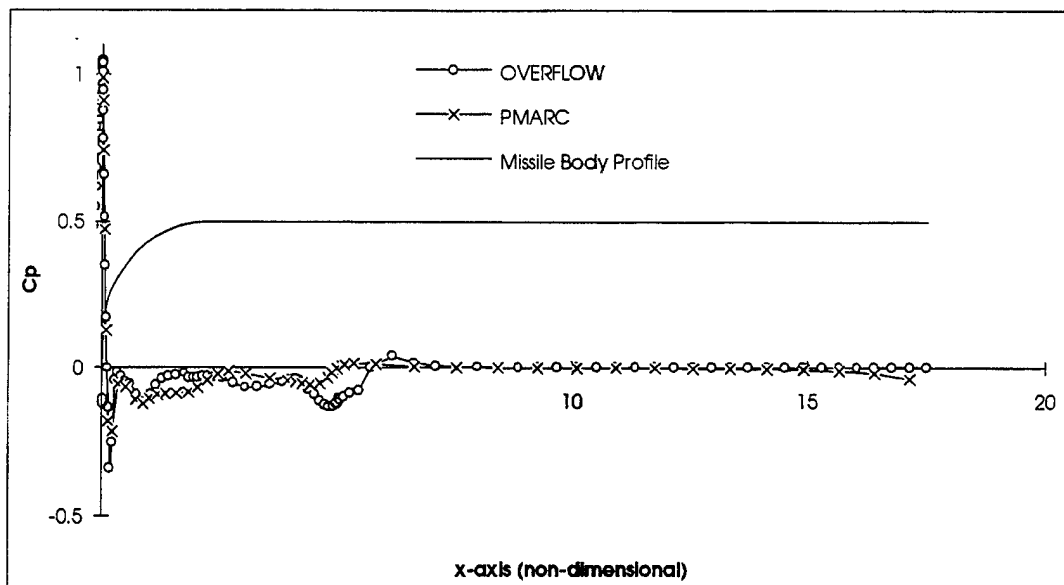
Figure 22. OVERFLOW and PMARC C_p Distributions for the Full Missile Forebody.
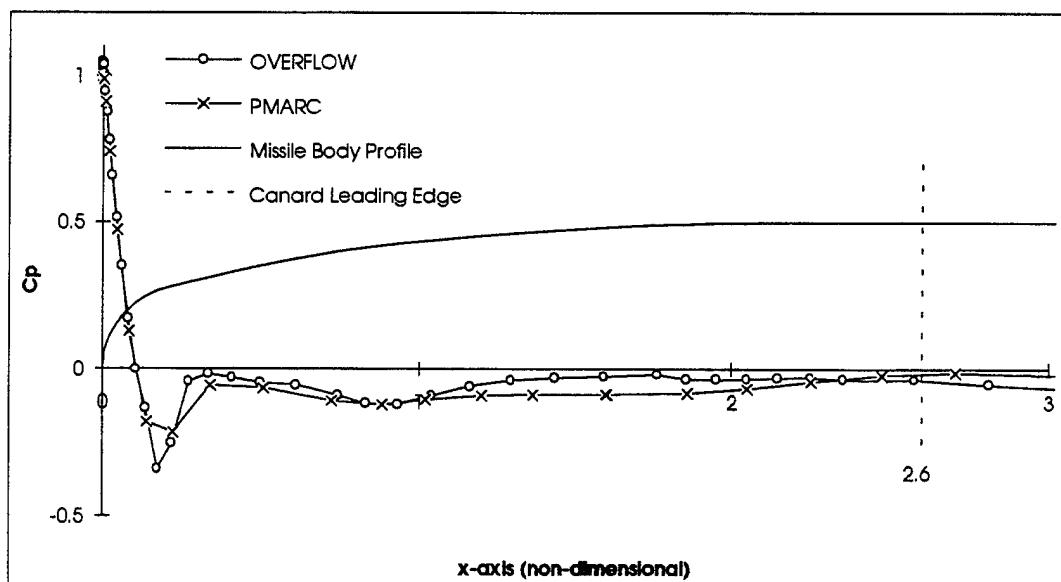
Figure 23. OVERFLOW and PMARC C_p Distributions for the Missile Nose.
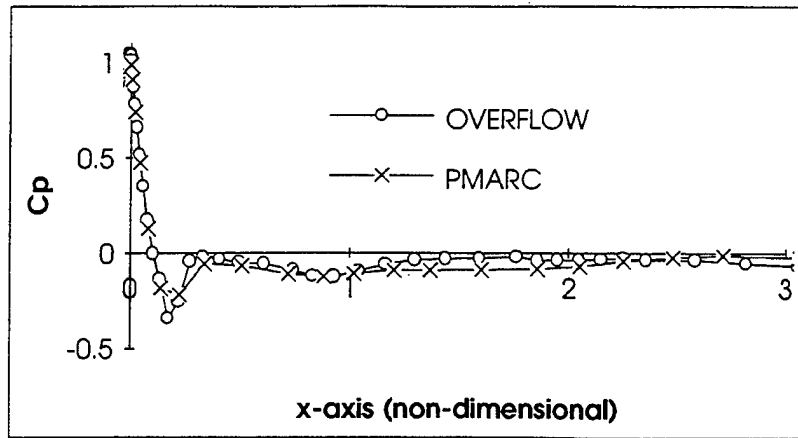
Figure 24. OVERFLOW and PMARC C_p Distributions for the Missile Forebody at Zero Degree Angle of Attack on the Top Surface.
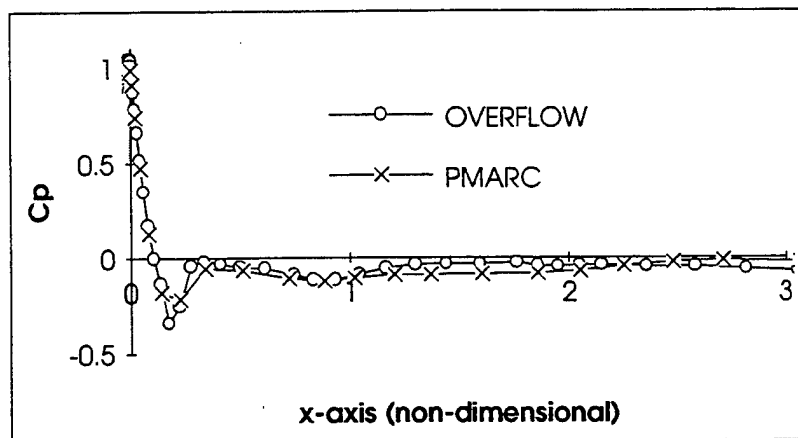
Figure 25. OVERFLOW and PMARC C_p Distributions for the Missile Forebody at Zero Degree Angle of Attack on the Mid Plane Surface.
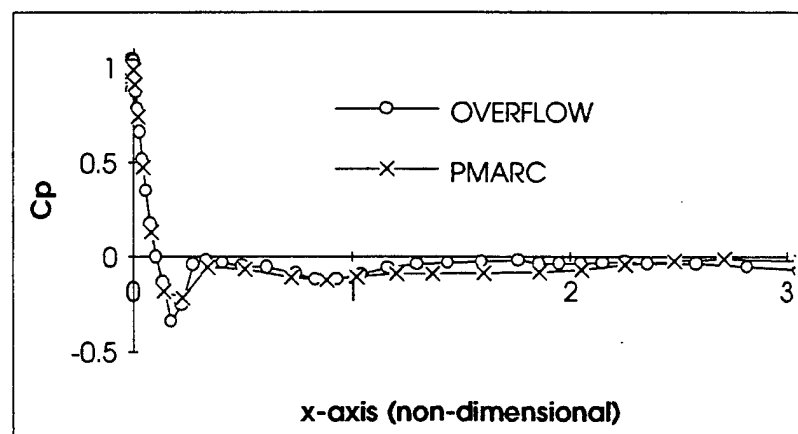
Figure 26. OVERFLOW and PMARC C_p Distributions for the Missile Forebody at Zero Degree Angle of Attack on the Bottom Surface.
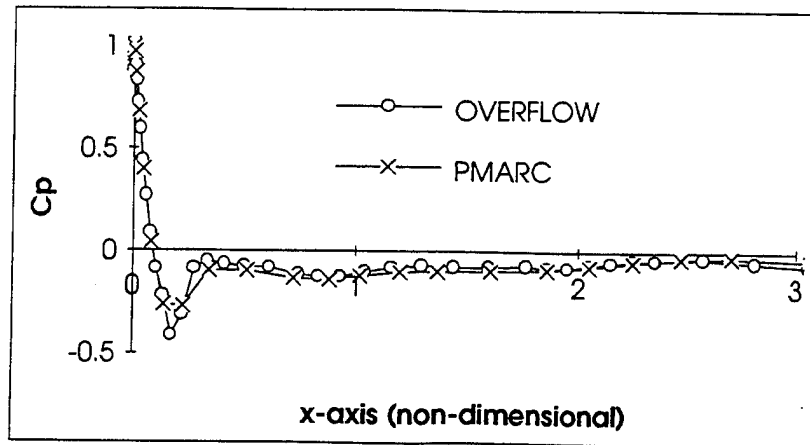
Figure 27. OVERFLOW and PMARC C_p Distributions for the Missile Forebody at Two Degree Angle of Attack on the Top Surface.
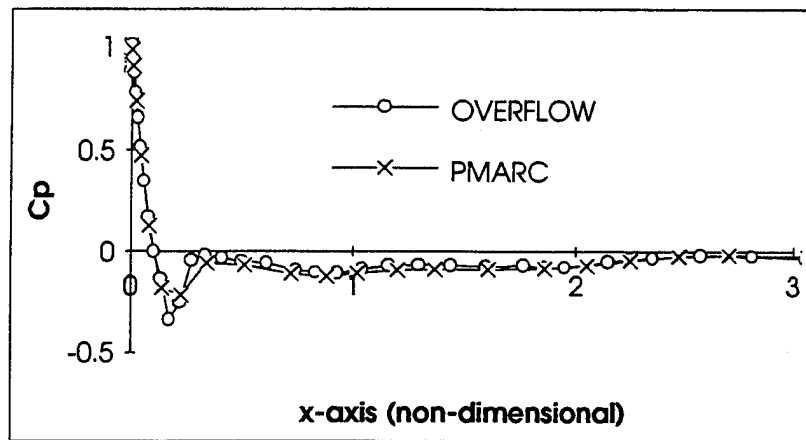
Figure 28. OVERFLOW and PMARC C_p Distributions for the Missile Forebody at Two Degree Angle of Attack on the Mid Plane Surface.
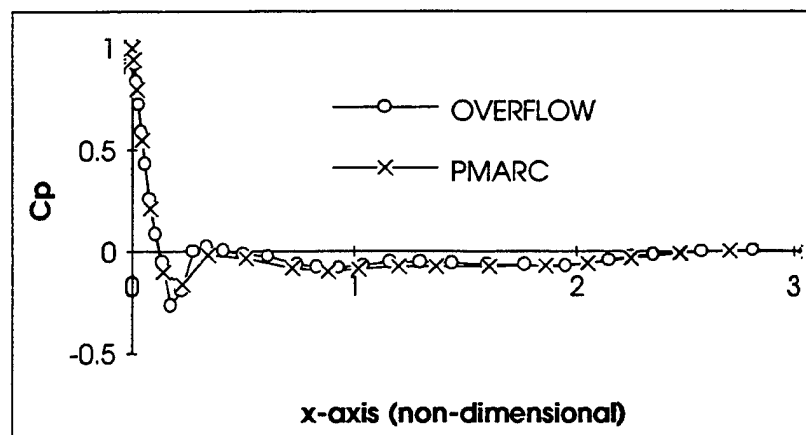
Figure 29. OVERFLOW and PMARC C_p Distributions for the Missile Forebody at Two Degree Angle of Attack on the Bottom Surface.
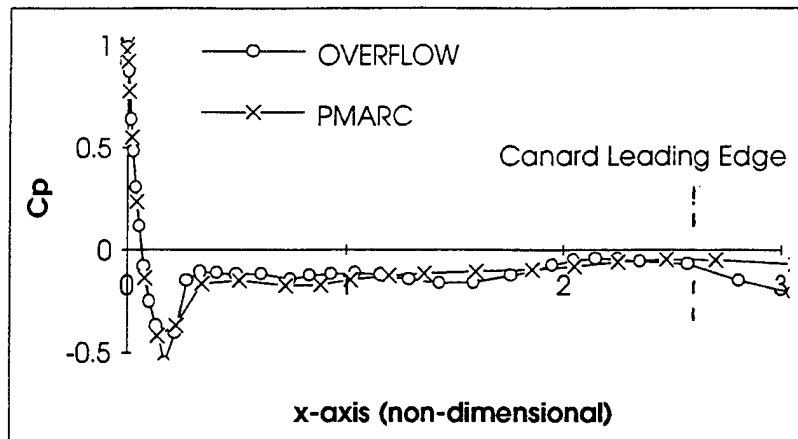
Figure 30. OVERFLOW and PMARC C_p Distributions for the Missile Forebody at Six Degree Angle of Attack on the Top Surface.
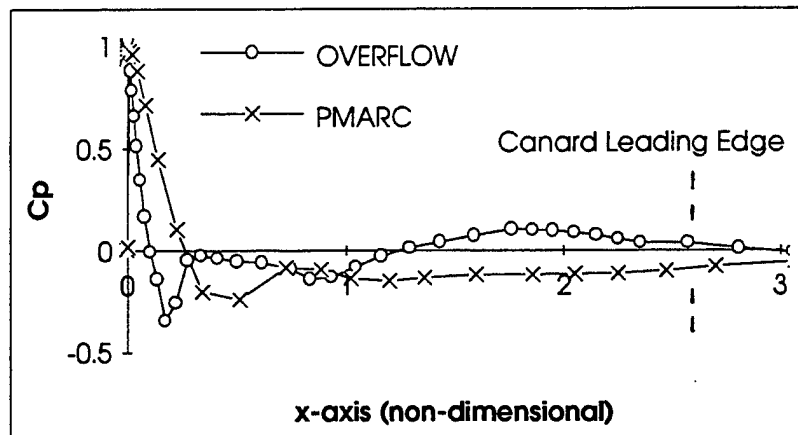
Figure 31. OVERFLOW and PMARC C_p Distributions for the Missile Forebody at Six Degree Angle of Attack on the Mid Plane Surface.
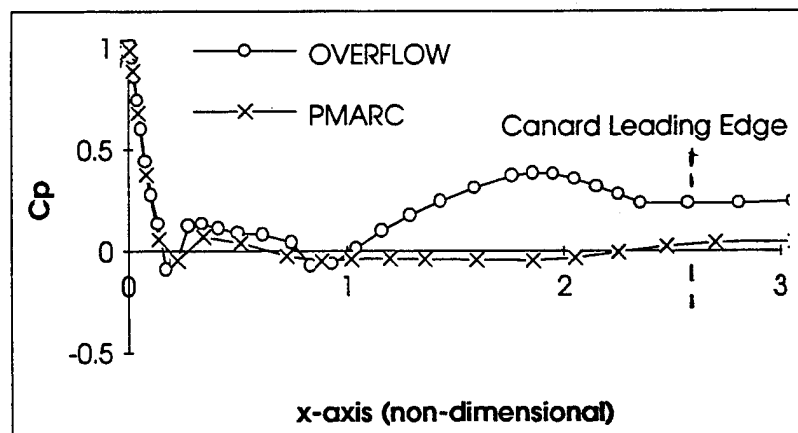
Figure 32. OVERFLOW and PMARC C_p Distributions for the Missile Forebody at Six Degree Angle of Attack on the Bottom Surface.
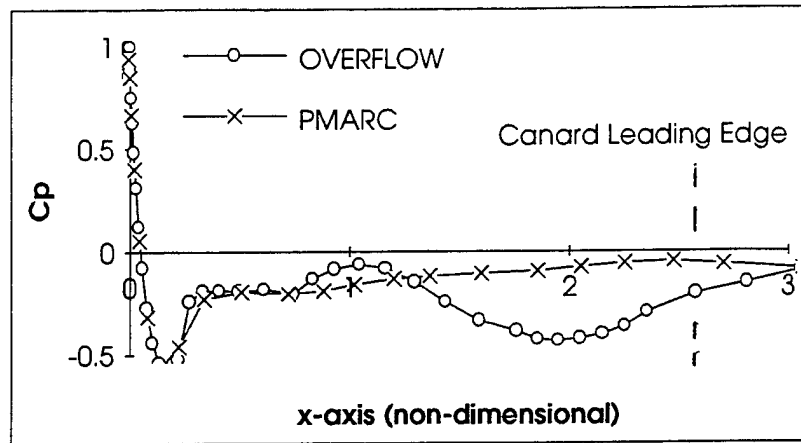
Figure 33. OVERFLOW and PMARC C_p Distributions for the Missile Forebody at Ten Degree Angle of Attack on the Top Surface.
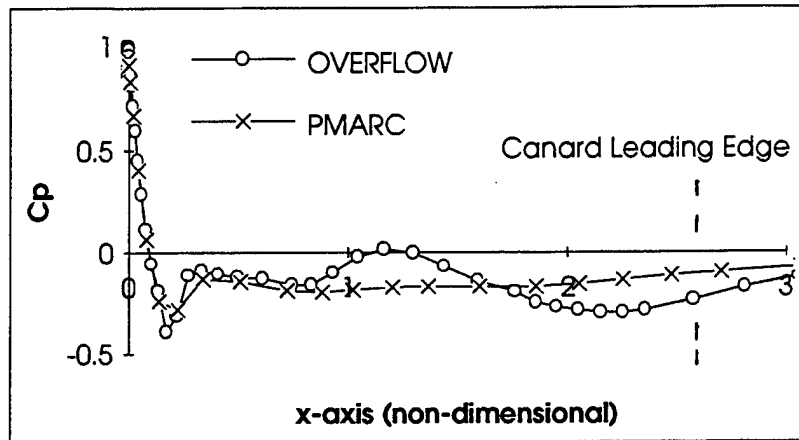
Figure 34. OVERFLOW and PMARC C_p Distributions for the Missile Forebody at Ten Degree Angle of Attack on the Mid Plane Surface.
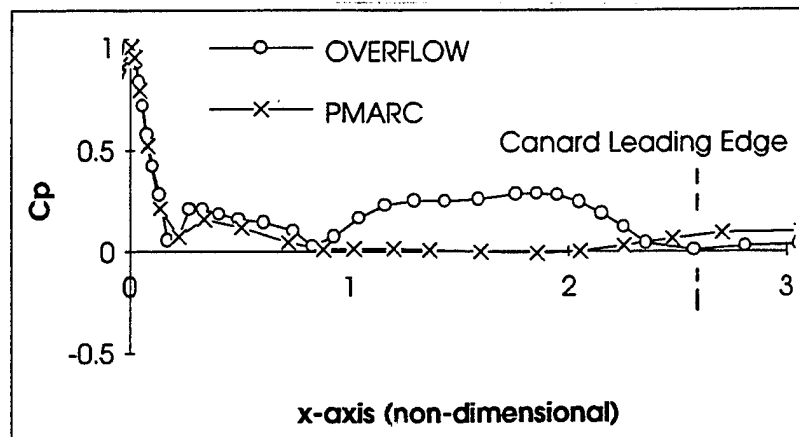
Figure 35. OVERFLOW and PMARC C Distributions for the Missile Forebody at Ten Degree Angle of Attack on the Bottom Surface.
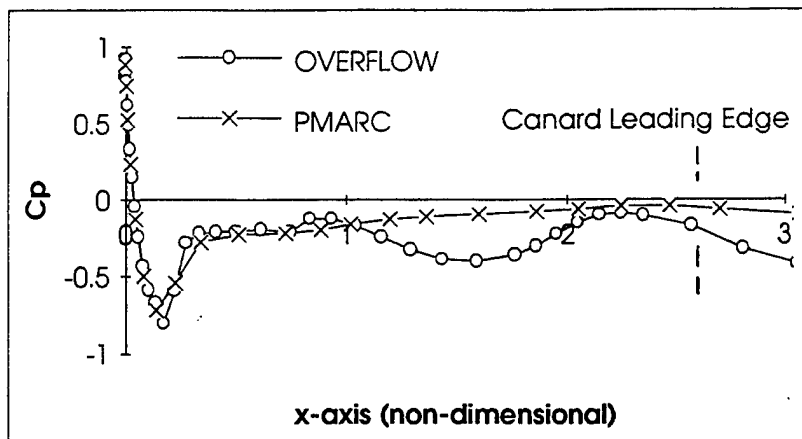
Figure 36. OVERFLOW and PMARC C_p Distributions for the Missile Forebody at Fourteen Degree Angle of Attack on the Top Surface.
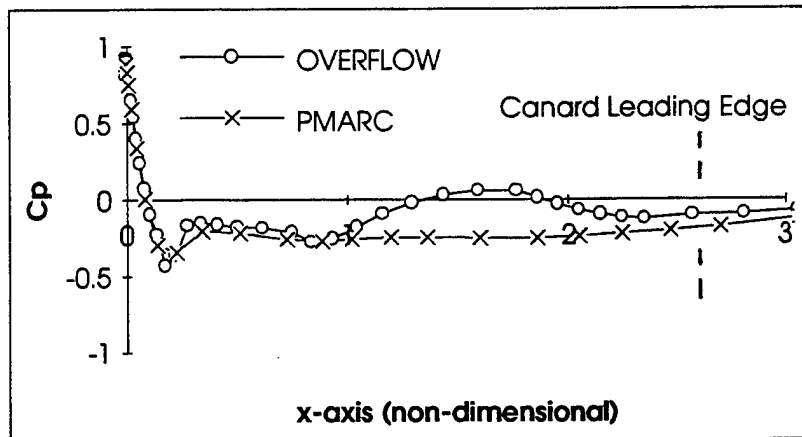
Figure 37. OVERFLOW and PMARC C_p Distributions for the Missile Forebody at Fourteen Degree Angle of Attack on the Mid Plane Surface.
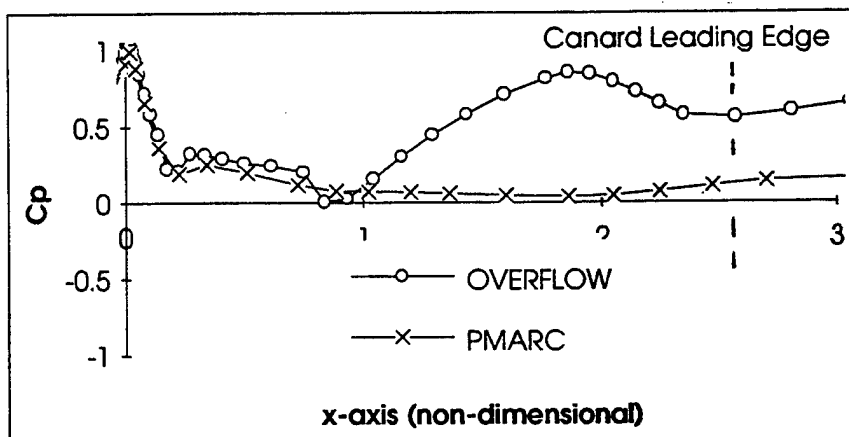
Figure 38. OVERFLOW and PMARC C_p Distributions for the Missile Forebody at Fourteen Degree Angle of Attack on the Bottom Surface.

41
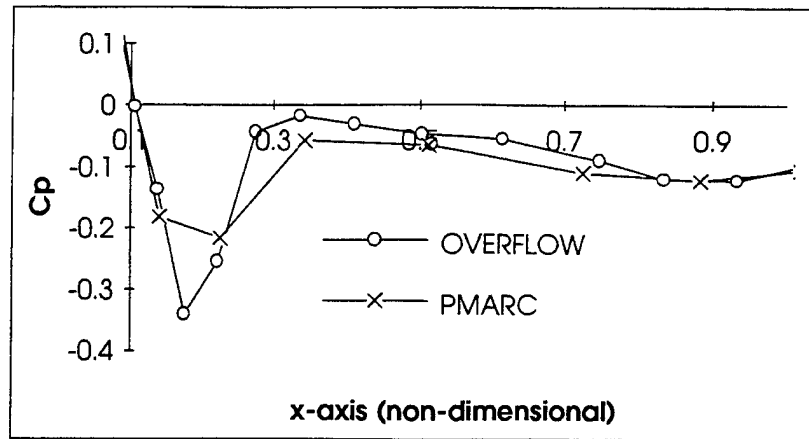
Figure 39. OVERFLOW and PMARC C_p Distributions for the Missile Forebody at Zero Degree Angle of Attack on the Top Surface.
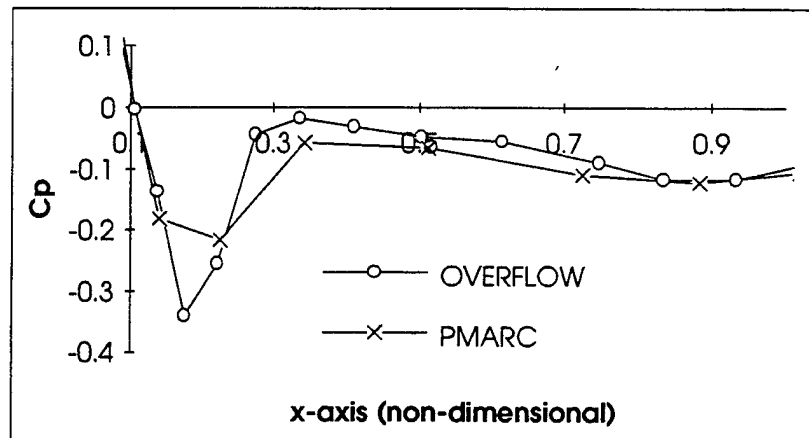
Figure 40. OVERFLOW and PMARC C_p Distributions for the Missile Forebody at Zero Degree Angle of Attack on the Mid Plane Surface.
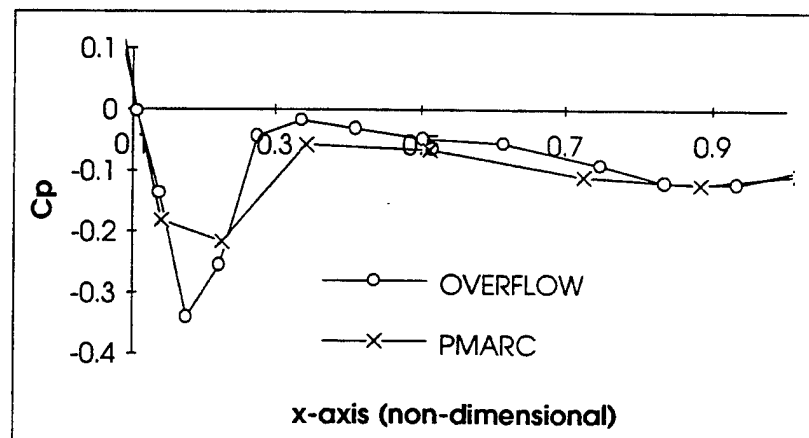
Figure 41. OVERFLOW and PMARC C_p Distributions for the Missile Forebody at Zero Degree Angle of Attack on the Bottom Surface.
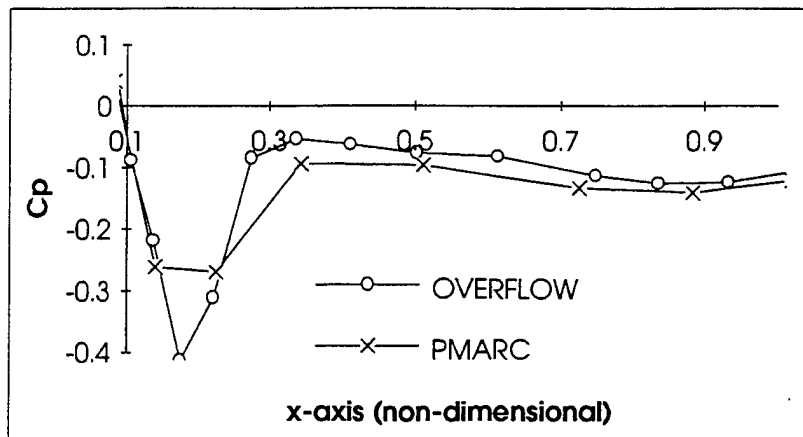
Figure 42. OVERFLOW and PMARC C_p Distributions for the Missile Forebody at Two Degree Angle of Attack on the Top Surface.
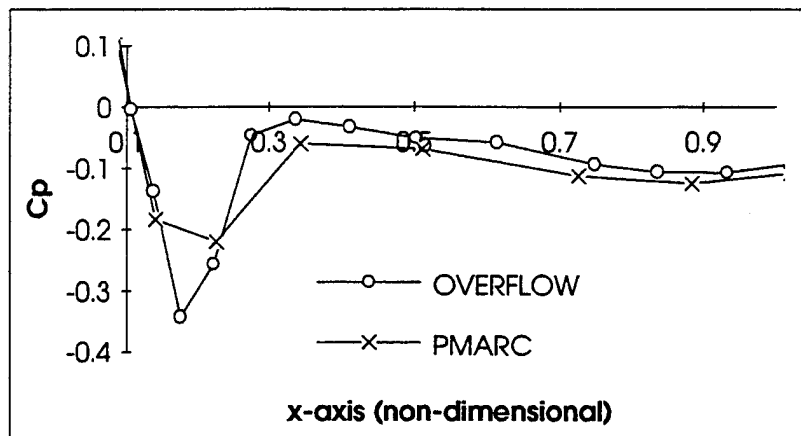
Figure 43. OVERFLOW and PMARC C_p Distributions for the Missile Forebody at Two Degree Angle of Attack on the Mid Plane Surface.
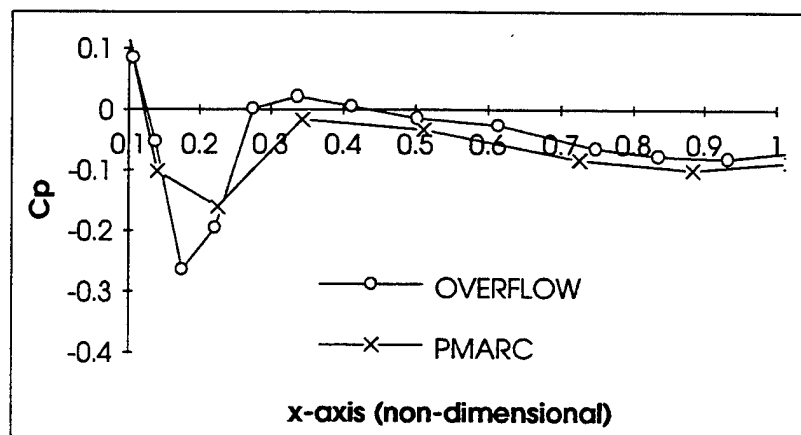
Figure 44. OVERFLOW and PMARC C_p Distributions for the Missile Forebody at Two Degree Angle of Attack on the Bottom Surface.
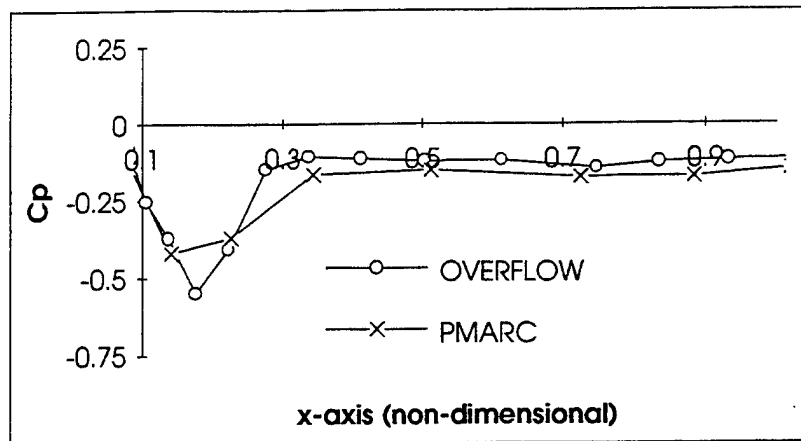
Figure 45. OVERFLOW and PMARC C_p **Distributions for the Missile Forebody at Six Degree Angle of Attack on the Top Surface.**
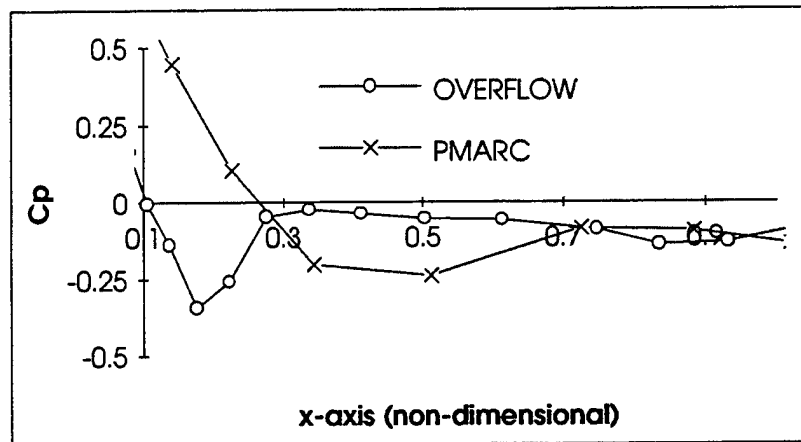
Figure 46. OVERFLOW and PMARC C_p **Distributions for the Missile Forebody at Six Degree Angle of Attack on the Mid Plane Surface.**
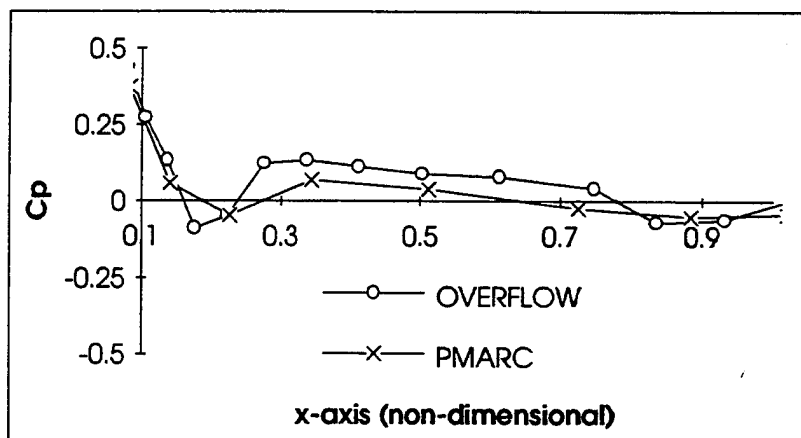
Figure 47. OVERFLOW and PMARC C_p **Distributions for the Missile Forebody at Six Degree Angle of Attack on the Bottom Surface.**
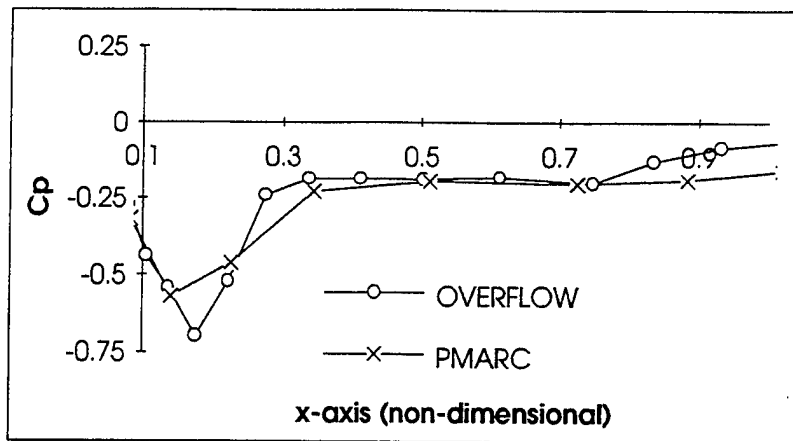
Figure 48. OVERFLOW and PMARC C_p Distributions for the Missile Forebody at Ten Degree Angle of Attack on the Top Surface.
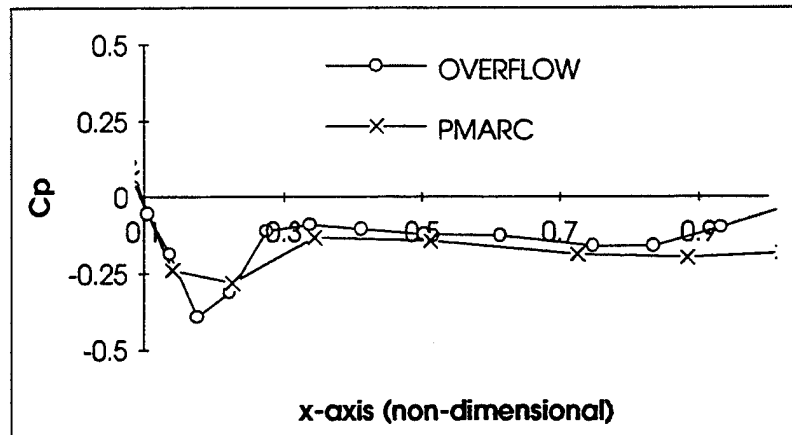
Figure 49. OVERFLOW and PMARC C_p Distributions for the Missile Forebody at Ten Degree Angle of Attack on the Mid Plane Surface.
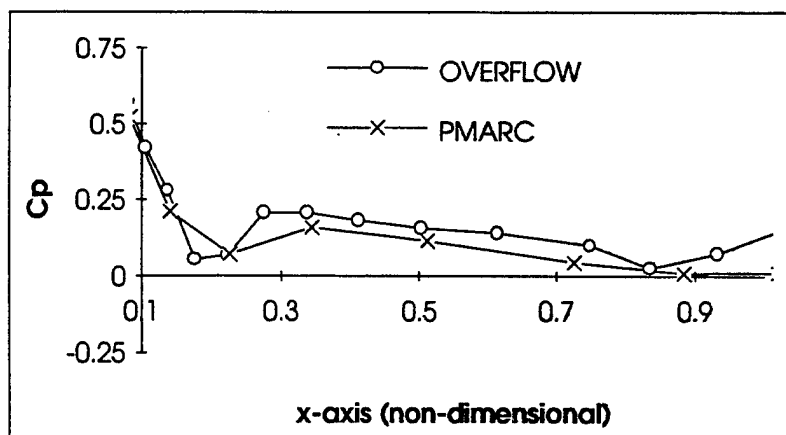
Figure 50. OVERFLOW and PMARC C_p Distributions for the Missile Forebody at Ten Degree Angle of Attack on the Bottom Surface.
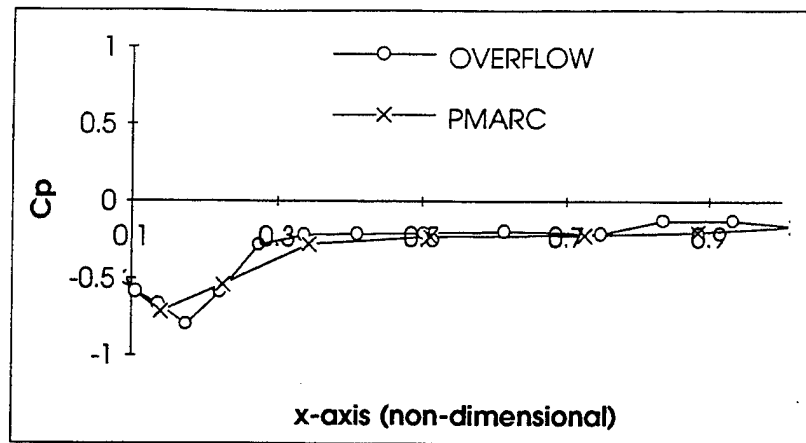
Figure 51. OVERFLOW and PMARC C_p Distributions for the Missile Forebody at Fourteen Degree Angle of Attack on the Top Surface.
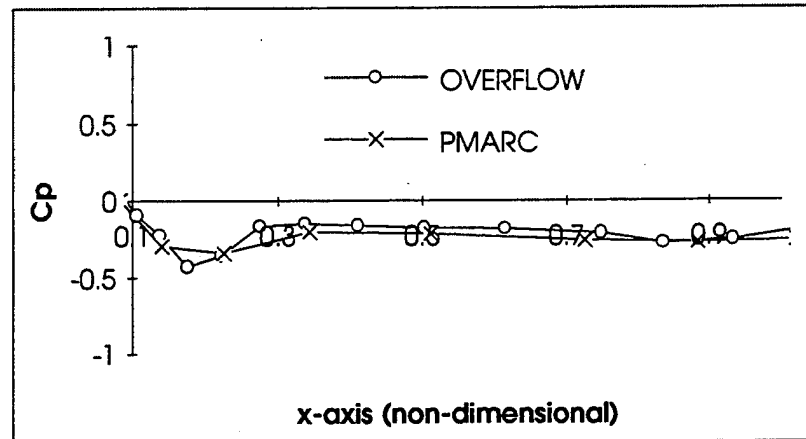
Figure 52. OVERFLOW and PMARC C_p Distributions for the Missile Forebody at Fourteen Degree Angle of Attack on the Mid Plane Surface.
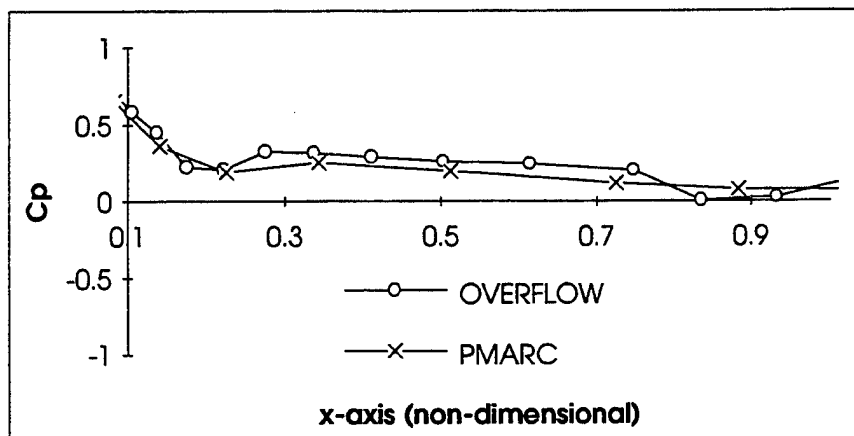
Figure 53. OVERFLOW and PMARC C_p Distributions for the Missile Forebody at Fourteen Degree Angle of Attack on the Bottom Surface.

G. SUMMARY

Missile forebody models were constructed for use in both the OVERFLOW and PMARC Codes. Based on C_p distributions, comparisons were made between these two models for a low Mach number at several angles of attack. Agreement was very good at very low angles of attack. At six degree and higher angles of attack, differences between these two models began to appear.

VI. CONCLUSIONS AND RECOMMENDATIONS

In this thesis the NASA-Ames developed OVERFLOW Navier-Stokes Code was used to obtain solutions for Mach = 0.3 and Reynolds = 2.0e+06 flow over a typical canard configured missile forebody. In the absence of detailed experimental flow and pressure data, the Navier-Stokes computed pressure distributions were compared with potential flow solutions, i.e., Slender Body Theory, von Karman's Method and the NASA-Ames panel code PMARC. As expected, the first two methods were only of limited applicability, but PMARC provides good agreement for zero and small angles of attack. The PMARC and OVERFLOW computed pressure distributions started to deviate in front and close to the canards. This indicates the presence of flow separation and vortical flow development. Further, work is necessary to display the flow features in more detail, so that the underlying flow physics can be better understood.

APPENDIX A. MAPLE PROCEDURE TO CALCULATE Cp VALUES ON A SPINDLE

```
>
>
> # This MAPLE Procedure calculates the Cp values about a spindle body of
> #    revolution at zero degree angle of attack, using potential
> #    theory. The Cp values are determined in Sections 1 through 3.
>
> #    Section 4 determines the non-dimensional longitudinal velocity of
> #    Equation 2.10 and compares it to Equation 2.5 to confirm the
> #    procedure.
>
> #    Sections 5 and 6 investigate the indeterminate behavior of the Cp or
> #    Equation 2.7, as the spindle's radius approaches zero and the x
> #    coordinate either approaches zero or one respectively.
>
```

```
>
> # SECTION 1. Calculate non-dimensional longitudinal velocity component,
> #                using Equations 2.8, 2.3 and 2.5.
>
> tau:=            0.16;
```

$$\tau := .16$$

```
> R:=              2.0*tau* ( (xi) - (xi^2) );
```

$$R := .320\,\xi - .320\,\xi^2$$

```
> derivative_R:=   diff( R, xi );
```

$$derivative\_R := .320 - .640\,\xi$$

```
> eq_2_3:=         2.0 * pi * R * derivative_R;
```

$$eq\_2\_3 := 2.0\,\pi\left(.320\,\xi - .320\,\xi^2\right)(.320 - .640\,\xi)$$

```
> integrand_eq_2_5:= ( eq_2_3 * (x-xi) ) / ( ( (x-xi)^2 + r^2 )^(3/2) );
```

$$integrand\_eq\_2\_5 := 2.0\,\frac{\pi\left(.320\,\xi - .320\,\xi^2\right)(.320 - .640\,\xi)(x-\xi)}{\left((x-\xi)^2 + r^2\right)^{3/2}}$$

```
> Eq_2_5:=         ( (1) / (4.0*pi) ) * ( int( integrand_eq_2_5, xi=0.0..1.0 ) );
```

$$Eq\_2\_5 := .2500000000\,\big(-.2048000000\,\pi$$
$$\left(-21.0\,x^2 - 6.\,x\,\%3\,\sqrt{\%2} + 15.00\,x - 3.000 + 6.\,x^2\,\%3\,\sqrt{\%2} + 9.\,x\,r^2 + 9.\,x^3 - 3.0\,r^2 + \%3\,\sqrt{\%2} - 3.\,r^2\,\%3\,\sqrt{\%2}\right)$$
$$\Big/\sqrt{\%2} + .2048000000\,\pi$$
$$\left(-6.\,r^2 + 9.\,x^3 + 6.\,x^2\,\%1\,\sqrt{x^2+r^2} + 9.\,x\,r^2 - 3.\,r^2\,\%1\,\sqrt{x^2+r^2} - 6.\,x^2 - 6.\,x\,\%1\,\sqrt{x^2+r^2} + \%1\,\sqrt{x^2+r^2}\right)\Big/$$
$$\sqrt{x^2+r^2}\Big)\Big/\pi$$

$$\%1 := \ln\left(2.\,\sqrt{x^2+r^2} - 2.\,x\right)$$

$$\%2 := x^2 - 2.0\,x + 1.00 + r^2$$

$$\%3 := \ln\left(2.\,\sqrt{\%2} + 2.0 - 2.\,x\right)$$

```
>
```

```
>
> # SECTION 2. Calculate non-dimensional radial velocity component,
> #                using Equation 2.6.
```

```
>
> integrand_eq_2_6:= ( eq_2_3 ) / ( ( (x-xi)^2 + r^2 )^(3/2) );
```

$$integrand\_eq\_2\_6 := 2.0\,\frac{\pi\left(.320\,\xi - .320\,\xi^2\right)(.320 - .640\,\xi)}{\left((x - \xi)^2 + r^2\right)^{3/2}}$$

```
> Eq_2_6:=          ( (r) / (4.0*pi) ) * ( int( integrand_eq_2_6, xi=0.0..1.0 ) );
```

$$Eq\_2\_6 := .2500000000\,r\left(-.2048000000\,\pi\left(-4.00\,r^2 + 4.0\,x^2 + 7.0\,x\,r^2 - 5.0\,x^3 - 2.\,x^2 r^2 + 2.\,x^4\right.\right.$$
$$\left.- 6.\,x\ln\left(2.\sqrt{\%1} + 2.0 - 2.\,x\right)r^2\sqrt{\%1} - 4.\,r^4 - 1.0\,x + 3.\,r^2\ln\left(2.\sqrt{\%1} + 2.0 - 2.\,x\right)\sqrt{\%1}\right)/\left(r^2\sqrt{\%1}\right) +$$
$$.2048000000\,\pi\left(2.\,x^4 + r^2 - 2.\,x^2 r^2 + x^2 + 3.\,r^2\ln\left(2.\sqrt{x^2 + r^2} - 2.\,x\right)\sqrt{x^2 + r^2}\right.$$
$$\left.\left.- 6.\,x\ln\left(2.\sqrt{x^2 + r^2} - 2.\,x\right)r^2\sqrt{x^2 + r^2} - 4.\,r^4 - 3.\,x\,r^2 - 3.\,x^3\right)/\left(r^2\sqrt{x^2 + r^2}\right)\right)/\pi$$

$$\%1 := x^2 - 2.0\,x + 1.00 + r^2$$

```
>
>
> # SECTION 3. Calculate the Cp values,
> #                using Equation 2.7.
>
> Cp:=     ( -2.0*(Eq_2_5) ) - ( ((Eq_2_6)**2) + ((Eq_2_5)**2) );
```

$$Cp := -.5000000000\left(-.2048000000\,\pi\right.$$
$$\left(-21.0\,x^2 - 6.\,x\,\%3\sqrt{\%2} + 15.00\,x - 3.000 + 6.\,x^2\,\%3\sqrt{\%2} + 9.\,x\,r^2 + 9.\,x^3 - 3.0\,r^2 + \%3\sqrt{\%2} - 3.\,r^2\,\%3\sqrt{\%2}\right)$$
$$/\sqrt{\%2} + .2048000000\,\pi$$
$$\left(-6.\,r^2 + 9.\,x^3 + 6.\,x^2\,\%1\sqrt{x^2 + r^2} + 9.\,x\,r^2 - 3.\,r^2\,\%1\sqrt{x^2 + r^2} - 6.\,x^2 - 6.\,x\,\%1\sqrt{x^2 + r^2} + \%1\sqrt{x^2 + r^2}\right)/$$
$$\sqrt{x^2 + r^2}\Big)/\pi - .06250000000\,r^2\left(-.2048000000\right.$$
$$\frac{\pi\left(-4.00\,r^2 + 4.0\,x^2 + 7.0\,x\,r^2 - 5.0\,x^3 - 2.\,x^2 r^2 + 2.\,x^4 - 6.\,x\,\%3\,r^2\sqrt{\%2} - 4.\,r^4 - 1.0\,x + 3.\,r^2\,\%3\sqrt{\%2}\right)}{r^2\sqrt{\%2}}$$
$$+ .2048000000\,\frac{\pi\left(2.\,x^4 + r^2 - 2.\,x^2 r^2 + x^2 + 3.\,r^2\,\%1\sqrt{x^2 + r^2} - 6.\,x\,\%1\,r^2\sqrt{x^2 + r^2} - 4.\,r^4 - 3.\,x\,r^2 - 3.\,x^3\right)}{r^2\sqrt{x^2 + r^2}}\Bigg)^{2}/$$
$$\pi^2 - .06250000000\left(-.2048000000\,\pi\right.$$
$$\left(-21.0\,x^2 - 6.\,x\,\%3\sqrt{\%2} + 15.00\,x - 3.000 + 6.\,x^2\,\%3\sqrt{\%2} + 9.\,x\,r^2 + 9.\,x^3 - 3.0\,r^2 + \%3\sqrt{\%2} - 3.\,r^2\,\%3\sqrt{\%2}\right)$$
$$/\sqrt{\%2} + .2048000000\,\pi$$
$$\left(-6.\,r^2 + 9.\,x^3 + 6.\,x^2\,\%1\sqrt{x^2 + r^2} + 9.\,x\,r^2 - 3.\,r^2\,\%1\sqrt{x^2 + r^2} - 6.\,x^2 - 6.\,x\,\%1\sqrt{x^2 + r^2} + \%1\sqrt{x^2 + r^2}\right)/$$
$$\sqrt{x^2 + r^2}\Big)^{2}/\pi^2$$

$$\%1 := \ln\left(2.\sqrt{x^2 + r^2} - 2.\,x\right)$$

$$\%2 := x^2 - 2.0\,x + 1.00 + r^2$$

$$\%3 := \ln\left(2.\sqrt{\%2} + 2.0 - 2.\,x\right)$$

```
>
```

```
> with(linalg):
Warning: new definition for    norm
Warning: new definition for    trace


>
> points:=   10;
```

$$points := 10$$

```
> # points:=   48;
>
> increment:= (1.0) / ( points + 1 );
```

$$increment := .09090909091$$

```
>
> X(1):=     increment;
```

$$X(1) := .09090909091$$

```
>
> r(1):=            2.0 * tau * ( (X(1)) - (X(1)^2) );
```

$$r(1) := .02644628100$$

```
> non_dim_ux(1):= evalf( subs( x=X(1), r=r(1), Eq_2_5 ) );
```

$$non\_dim\_ux(1) := -.08235051778$$

```
> non_dim_ur(1):= evalf( subs( x=X(1), r=r(1), Eq_2_6 ) );
```

$$non\_dim\_ur(1) := .2511767847$$

```
> cp(1):=           evalf( subs( x=X(1), r=r(1), Cp     ) );
```

$$cp(1) := .09482965073$$

```
> for I from 2 by 1 to points do
>
>   X(i):=            X(i-1) + increment:
>   r(i):=            2.0*tau* ( (X(i)) - (X(i)^2) ):
>   non_dim_ux(i):= evalf( subs( x=X(i), r=r(i), Eq_2_5 ) );
>   non_dim_ur(i):= evalf( subs( x=X(i), r=r(i), Eq_2_6 ) );
>   cp(i):=           evalf( subs( x=X(i), r=r(i), Cp     ) );
>
> od:
>
> # writeto( cp );
>
> for I from 0 by 1 to points do
>
>   if (i = 0) then
>     printf('           '):lprint():
>     printf('    tau = %4.2f', tau ):lprint():
>     printf('           '):lprint():
>     printf(' x       r       ux      ur      Cp '):lprint():
>     printf('           '):lprint():
>   else
>     printf(' %8.4f  %8.4f  %8.4f  %8.4f  %8.4f ', X(i),r(i),non_dim_ux(i),non_dim_ur(i),cp(i)):lprint();
>   fi
>
> od;
```

53

```
tau = 0.16
```

x	r	ux	ur	Cp
0.0909	0.0264	−0.0824	0.2512	0.0948
0.1818	0.0476	−0.0136	0.1874	−0.0082
0.2727	0.0635	0.0244	0.1300	−0.0663
0.3636	0.0740	0.0458	0.0766	−0.0996
0.4545	0.0793	0.0557	0.0253	−0.1150
0.5455	0.0793	0.0557	−0.0253	−0.1150
0.6364	0.0740	0.0458	−0.0766	−0.0996
0.7273	0.0635	0.0244	−0.1300	−0.0663
0.8182	0.0476	−0.0136	−0.1874	−0.0082
0.9091	0.0264	−0.0824	−0.2512	0.0948

>
_____

>
> # SECTION 4. Calculate the approximate non-dimensional, longitudinal velocity component,
> #   using Equations 2.10 and compare to Equation 2.5.
>
> Fp1x:= eq_2_3;

$$Fp1x := 2.0\,\pi\left(.320\,\xi - .320\,\xi^2\right)(.320 - .640\,\xi)$$

> Fp2x:= diff(eq_2_3, xi);

$$Fp2x := 2.0\,\pi\,(.320 - .640\,\xi)^2 - 1.2800\,\pi\left(.320\,\xi - .320\,\xi^2\right)$$

> Fp3x:= diff(eq_2_3, xi$2);

$$Fp3x := -3.8400\,\pi\,(.320 - .640\,\xi)$$

> Fp4x:= diff(eq_2_3, xi$3);

$$Fp4x := 2.4576000\,\pi$$

> temp1:= sqrt(xi * (1.0-xi));

$$temp1 := \sqrt{\xi}\,\sqrt{1.0 - \xi}$$

> temp2:= (Fp1x)   * ((0.5-xi) / (xi*(1.0-xi))) ;

$$temp2 := 2.0\,\frac{\pi\left(.320\,\xi - .320\,\xi^2\right)(.320 - .640\,\xi)(.5 - \xi)}{\xi(1.0 - \xi)}$$

> temp3:= (Fp2x)   * (ln(2.0*temp1) - 1.0);

$$temp3 := \left(2.0\,\pi\,(.320 - .640\,\xi)^2 - 1.2800\,\pi\left(.320\,\xi - .320\,\xi^2\right)\right)\left(\ln\left(2.0\,\sqrt{\xi}\,\sqrt{1.0 - \xi}\right) - 1.0\right)$$

> temp4:= (Fp3x/ 2.0) * (0.5-xi);

$$temp4 := -1.920000000\,\pi\,(.320 - .640\,\xi)(.5 - \xi)$$

> temp5:= (Fp4x/48.0) * (1.0 + (4.0*((0.5-xi)**2)));

$$temp5 := .05119999999\,\pi\left(1.0 + 4.0\,(.5 - \xi)^2\right)$$

> Eq_2_10:= (Fp2x/(2.0*pi))*(ln(r))-((1.0/(2.0*pi))*(temp2+temp3+temp4+temp5));

$$Eq\_2\_10 := .5000000000\,\frac{\left(2.0\,\pi\,(.320 - .640\,\xi)^2 - 1.2800\,\pi\left(.320\,\xi - .320\,\xi^2\right)\right)\ln(r)}{\pi} - .5000000000\,\Bigg($$

$$2.0\,\frac{\pi\left(.320\,\xi - .320\,\xi^2\right)(.320 - .640\,\xi)(.5 - \xi)}{\xi(1.0 - \xi)}$$

$$+\left(2.0\,\pi\,(.320-.640\,\xi)^2-1.2800\,\pi\left(.320\,\xi-.320\,\xi^2\right)\right)\left(\ln\!\left(2.0\,\sqrt{\xi}\,\sqrt{1.0-\xi}\right)-1.0\right)$$

$$-1.920000000\,\pi\,(.320-.640\,\xi)\,(.5-\xi)+.05119999999\,\pi\left(1.0+4.0\,(.5-\xi)^2\right)\Bigg\}\Bigg/\pi$$

```
>
> points:=   10;
```

$$points := 10$$

```
> # points:=   48;
>
> increment:= (1.0) / ( points + 1 );
```

$$increment := .09090909091$$

```
>
> X(1):=    increment;
```

$$X(1) := .09090909091$$

```
>
> r(1):=           2.0 * tau * ( (X(1)) - (X(1)^2) );
```

$$r(1) := .02644628100$$

```
> non_dim_ux(1):= evalf( subs( x=X(1), r=r(1), Eq_2_5 ) );
```

$$non\_dim\_ux(1) := -.08235051778$$

```
> approx_eq_2_5(1):= evalf( subs( xi=X(1), r=r(1), Eq_2_10 ) );
```

$$approx\_eq\_2\_5(1) := -.0815224471$$

```
>
> for i from 2 by 1 to points do
>
>  X(i):=           X(i-1) + increment:
>  r(i):=           2.0*tau* ( (X(i)) - (X(i)^2) ):
>  non_dim_ux(i):= evalf( subs( x=X(i), r=r(i), Eq_2_5 ) ):
>  approx_eq_2_5(i):= evalf( subs( xi=X(i), r=r(i), Eq_2_10 ) );
>
> od:
>
> # writeto( eq36ux );
>
> for i from 0 by 1 to points do
>
.>   if (i = 0) then
>     printf('          '):lprint():
>     printf('    tau = %4.2f', tau ):lprint():
>     printf('          '):lprint():
>     printf('  x        r       Eq_2_10    Eq_2_5  '):lprint():
>     printf('          '):lprint():
>   else
>     printf(' %8.4f   %8.4f   %8.4f   %8.4f', X(i),r(i),approx_eq_2_5(i),non_dim_ux(i)):lprint();
>   fi
>
> od;

     tau = 0.16

   x              r           Eq_2_10        Eq_2_5
```

55

```
0.0909      0.0264      -0.0815     -0.0824
0.1818      0.0476      -0.0141     -0.0136
0.2727      0.0635       0.0222      0.0244
0.3636      0.0740       0.0423      0.0458
0.4545      0.0793       0.0514      0.0557
0.5455      0.0793       0.0514      0.0557
0.6364      0.0740       0.0423      0.0458
0.7273      0.0635       0.0222      0.0244
0.8182      0.0476      -0.0141     -0.0136
0.9091      0.0264      -0.0815     -0.0824
```

>
> _____
>
> # SECTION 5. Verify that as r goes to zero and x goes to zero,
> #   Cp values will become indeterminate.
>
> points:=   50;

$$points := 50$$

>
> increment:= (1.0) / (10.0 + 1.0);

$$increment := .09090909091$$

> X(1):=   increment;

$$X(1) := .09090909091$$

> r(1):=   2.0 * tau * ((X(1)) - (X(1)^2));

$$r(1) := .02644628100$$

> cp(1):=   evalf(subs(x=X(1), r=r(1), Cp));

$$cp(1) := .09482965073$$

> for i from 2 by 1 to points do
>
>   X(i):=   X(i-1) * increment:
>   r(i):=   2.0*tau* ((X(i)) - (X(i)^2)):
>   cp(i):= evalf(subs(x=X(i), r=r(i), Cp));
>
> od:
> # writeto(x0);
> for i from 0 by 1 to points do
>
>   if (i = 0) then
>   printf('   '):lprint():
>   printf('   tau = %4.2f', tau):lprint():
>   printf('   '):lprint():
>   printf(' x   r   Cp '):lprint():
>   printf('   '):lprint():
>   else
>   printf(' %18.16e %18.16e %19.16e ', X(i),r(i),cp(i)):lprint();
>   fi
>
> od;

```
    tau = 0.16
```

56

x	r	Cp
9.0909090909999990e-02	2.6446280999999999e-02	9.4829650730000020e-02
8.2644628099999978e-03	2.6227166680000002e-03	3.6136853520000001e-01
7.5131480089999985e-04	2.4024010460000001e-04	5.3521760820000008e-01
6.8301345540000010e-05	2.1854937759999998e-05	6.6798813509999999e-01
6.2092132309999992e-06	1.9869358970000001e-06	7.6933566659999997e-01
5.6447393010000001e-07	1.8063155569999999e-07	8.4041487029999995e-01
5.1315811830000005e-08	1.6421058939999999e-08	8.8133818590000002e-01
4.6650738029999991e-09	1.4928236100000000e-09	8.9211484799999996e-01
4.2409761850000004e-10	1.3571123789999998e-10	8.7274545100000001e-01
3.8554328949999998e-11	1.2337385260000000e-11	8.2323001299999998e-01
3.5049389950000002e-12	1.1215804780000001e-12	7.4356853099999998e-01
3.1863081770000003e-13	1.0196186169999998e-13	6.3376100300000016e-01
2.8966437970000004e-14	9.2692601500000018e-15	4.9380743199999994e-01
2.6333125429999999e-15	8.4266001380000004e-16	3.2370781599999998e-01
2.3939204939999999e-16	7.6605455800000010e-17	1.2346215499999999e-01
2.1762913580000001e-17	6.9641323460000009e-18	-1.0692954999999997e-01
1.9784466890000002e-18	6.3310294039999996e-19	-3.6746730099999997e-01
1.7985878989999998e-19	5.7554812759999995e-20	-6.5815109900000002e-01
1.6350799080000001e-20	5.2322557059999992e-21	-9.7898093900000016e-01
1.4864362800000000e-21	4.7565960960000007e-22	-1.3299568230000001e+00
1.3513057090000002e-22	4.3241782680000007e-23	-1.7110787580000002e+00
1.2284597350000001e-23	3.9310711519999992e-24	-2.1223467270000005e+00
1.1167815770000001e-24	3.5737010460000005e-25	-2.5637607600000001e+00
1.0152559790000002e-25	3.2488191319999990e-26	-3.0353208079999998e+00
9.2295998089999999e-27	2.9534719380000003e-27	-3.5370269280000000e+00
8.3905452809999996e-28	2.6849744900000005e-28	-4.0688790870000000e+00
7.6277684370000006e-29	2.4408859000000001e-29	-4.6308772819999993e+00
6.9343349430000001e-30	2.2189871820000004e-30	-5.2230215270000002e+00
6.3039408569999999e-31	2.0172610740000002e-31	-5.8453118119999994e+00
5.7308553250000002e-32	1.8338737040000003e-32	-6.4977481520000007e+00
5.2098684770000003e-33	1.6671579130000000e-33	-7.1803305270000006e+00
4.7362440700000003e-34	1.5155981020000002e-34	-7.8930589520000005e+00
4.3056764270000000e-35	1.3778164570000001e-35	-8.6359334170000004e+00
3.9142512970000000e-36	1.2525604150000002e-36	-9.4089539470000005e+00
3.5584102699999994e-37	1.1386912859999998e-37	-1.0212120480000001e+01
3.2349184269999993e-38	1.0351738970000002e-38	-1.1045433100000000e+01
2.9408349340000003e-39	9.4106717880000007e-40	-1.1908891739999998e+01
2.6734863040000001e-40	8.5551561719999991e-41	-1.2802496430000001e+01
2.4304420949999996e-41	7.7774147040000000e-42	-1.3726247190000000e+01
2.2094928140000002e-42	7.0703770039999999e-43	-1.4680143960000001e+01
2.0086298310000000e-43	6.4276154600000007e-44	-1.5664186760000002e+01
1.8260271189999999e-44	5.8432867799999995e-45	-1.6678375619999997e+01
1.6600246540000000e-45	5.3120788919999998e-46	-1.7722710589999998e+01
1.5091133220000000e-46	4.8291626299999998e-47	-1.8797191539999996e+01
1.3719212019999997e-47	4.3901478459999999e-48	-1.9901818540000004e+01
1.2472010930000000e-48	3.9910434980000007e-49	-2.1036591570000002e+01
1.1338191749999998e-49	3.6282213599999993e-50	-2.2201510679999995e+01
1.0307447049999999e-50	3.2983830560000001e-51	-2.3396575810000005e+01
9.3704064090000006e-52	2.9985300500000003e-52	-2.4621787019999999e+01
8.5185512810000014e-53	2.7259364099999994e-53	-2.5877144220000002e+01

>
_____
>
> # SECTION 6. Verify that as r goes to zero and x goes to one,

57

```
> #                  Cp values will become indeterminate.
>
> X(1):=  0.9500;
```

$$X(1) := .9500$$

```
> r(1):=    2.0 * tau * ( (X(1)) - (X(1)^2) );
```

$$r(1) := .01520000000$$

```
> cp(1):=  evalf( subs( x=X(1), r=r(1), Cp ) );
```

$$cp(1) := .1752243365$$

```
> X(2):=  0.999900;
```

$$X(2) := .999900$$

```
> r(2):=    2.0 * tau * ( (X(1)) - (X(1)^2) );
```

$$r(2) := .01520000000$$

```
> cp(2):=  evalf( subs( x=X(1), r=r(1), Cp ) );
```

$$cp(2) := .1752243365$$

```
>
> points:=    29;
```

$$points := 29$$

```
>
> increment:= 0.000001;
```

$$increment := .1 \ 10^{-5}$$

```
> for i from 3 by 1 to points do
>
>   X(i):=   X(i-1) + increment:
>   r(i):=    2.0*tau* ( (X(i)) - (X(i)^2) ):
>   cp(i):=  evalf( subs( x=X(i), r=r(i), Cp ) );
>
> od:
Error, (in evalf/ln) singularity encountered

> # writeto( x1 );
> for i from 0 by 1 to points do
>
>   if (i = 0) then
>     printf('         '):lprint():
>     printf('    tau = %4.2f', tau ):lprint():
>     printf('        '):lprint():
>     printf(' x              r                Cp '):lprint():
>     printf('        '):lprint():
>   else
>     printf(' %18.16f  %18.16f  %19.16f ', X(i),r(i),cp(i)):lprint();
>   fi
>
> od;

    tau = 0.16

   x                   r                        Cp

  0.9499999999999998   0.0152000000000000   0.1752243365000000
```

```
0.9998999999999999   0.0152000000000000   0.1752243365000000
0.9999009999999999   0.0000316768640000   0.6476606865000000
0.9999020000000001   0.0000313569280000   0.6553688371999999
0.9999029999999999   0.0000310369920000   0.6422468258999999
0.9999040000000001   0.0000307170560000   0.6393732819000001
0.9999050000000002   0.0000303971200000   0.6585344844000000
0.9999060000000001   0.0000300771840000   0.6561241774000001
0.9999069999999999   0.0000297572480000   0.6536068717000000
0.9999079999999999   0.0000294372800000   0.6398706602999999
0.9999090000000000   0.0000291173440000   0.6489621221999999
0.9999100000000000   0.0000287974080000   0.6580446579000001
0.9999110000000002   0.0000284774720000   0.6431658841000000
0.9999120000000001   0.0000281575360000   0.6400647958000000
0.9999129999999999   0.0000278375680000   0.6507920520000000
0.9999140000000001   0.0000275176320000   0.6343043787000000
0.9999150000000002   0.0000271976960000   0.6448765211000000
0.9999160000000001   0.0000268777280000   0.6425597706000000
0.9999169999999999   0.0000265577920000   0.6392634326000001
0.9999179999999999   0.0000262378560000   0.6357834041000000
0.9999189999999999   0.0000259178880000   0.6482360795000001
0.9999200000000000   0.0000255979520000   0.6293168993000000
0.9999210000000001   0.0000252780160000   0.6416774725000000
0.9999219999999999   0.0000249580480000   0.6547907977000000
0.9999230000000002   0.0000246381120000   0.6354180657000001
0.9999240000000001   0.0000243181440000   0.6494795412000000
0.9999250000000000   0.0000239982080000   0.6623045039000000
0.9999260000000000   0.0000236782400000   0.6253918384000000
0.9999269999999999   0.0000233583040000   -5.8453118119999994
```

> _____
>
> # file = app_a.txt
>
>
>
>

APPENDIX B. FORTRAN LISTING OF THE SPHERE CODE

```fortran
      program sphere
c
c SPHERE calculates the pressure coefficients about a spherical body
c of revolution. It is a slight modification of Chow's implementation of
c vonKarmon's procedure for using line sources along the body's
c symmetric axis to define the body's shape (see Chow, C.Y., "An
c Introduction to Computational Fluid Mechanics", Seminole Publishing,
c corrected edition 1983, pp 105 - 117).
c
c This code differs from Chow's implementation in the following ways,
c   1. SPHERE uses double precision, Chow's code is single precision.
c   2. SPHERE loops through different sets of surface points (PI), in order
c      to investigate the code's convergence properties, Chow's code does
c      not do this.
c   3. SPHERE contains a subroutine to calculate the error norm defined as,
c
c       err = sqrt( sum(((dd)*(q) - (const))**2) )
c
c The number of surface points (m) and the (error) are listed in the
c file "error.out".
c If the (error) grows in magnitude as (m) increases, using double
c precision, then this is an indication that the coefficient
c matrix (dd) is ILL-CONDITIONED.
c
c The file "sphere.out" lists for each set of (m) surface points,
c   1. the (z) and (r) coordinates of each point on the sphere's surface,
c   2. the calculated coefficient of pressure (cp) and the exact
c      coefficient of pressure (cpex) for comparison.
c
c   u  = non-dimensional free stream velocity, assume u = 1.0.
c   a  = non-dimensional total sphere radius, assume a = 1.0
c   m  = number of surface points (PI), assume m = odd number.
c   n  = number of sink/source segments on z-axis,
c        note: n = m + 1, and n = even number.
c
      parameter( kk=250 )
      real*8 u, a, pi, phi(kk), z(kk), r(kk), cp(kk), cpex(kk), err
      integer*4 m, n, j
c
      open( unit=20,file='sph.out',    status='unknown' )
      open( unit=25,file='err.out',    status='unknown' )
c
      open( unit=20,file='sphere.out', status='unknown' )
      open( unit=25,file='error.out',  status='unknown' )
c
c Input the non-dimensional free stream velocity (u) and sphere radius (a).
c
      u = 1.0
      a = 1.0
c
c Write headers for output files
c
      write(20,*)
      write(20,*) ' This is the data output file called SPHERE.OUT'
      write(20,*) '     from the program SPHERE.FOR.'
      write(20,*)
      write(20,*) ' ECHO constant input values for the SPHERE'
      write(20,*)
      write(20,*) ' u (non-dimensional velocity) = ',u
      write(20,*) ' a (non-dimensional length)   = ',a
      write(25,*)
      write(25,*) ' This is the data output file called ERROR.OUT'
      write(25,*) '     from the program SPHERE.FOR,'
      write(25,*)
      write(25,*) '      m,        error norm'
      write(25,*)
c
c Start looping for different sets of surface points (PI)
c
      do 5, m = 1, 51, 2
         n = m + 1
c
c Calculates the surface points, where,
c   (a)  is the sphere's radius,
c   (zi) is the horizontal axis of the sphere,
c   (ri) is the perpendicular distance from (zi).
```

```fortran
c
         pi = 4.0 * atan(1.0)
         do i = 1, m
            phi(i) = (float(m) - float(i)) * ( pi/(float(m)) )
            z(i) = a * cos( phi(i) )
            r(i) = a * sin( phi(i) )
         end do
c
c CHOVON is the main routine to calculate pressure coefficients (cp, cpex)
c and error norm (err) for each set of surface points (z, r).
c
         call chovon( u, a, n, z, r, cp, cpex, err )
c
c Write data to output files.
c
         write(20,*) '     FOR m (surface points) = ',m
         write(20,*) '         z,                r'
         write(20,*)
         do i = 1, m
            write(20,*) z(i), r(i)
         end do
         write(20,*) '         cp,              cpex'
         write(20,*)
         do i = 1, m
            write(20,*) cp(i), cpex(i)
         end do
         write(25,*) m, err
5     continue
      close(unit=20)
      close(unit=25)
      STOP
      END
c
c
      subroutine chovon( u, a, n, z, r, cp, cpex, err )
      parameter( kk=250 )
      real*8 u, a, z(kk), r(kk), zz(kk), s(kk), deleg
      real*8 d(kk,kk), dd(kk,kk), const(kk), q(kk), ur, uz
      real*8 v(kk), vex(kk), cp(kk), cpex(kk), err
      integer*4 i, n, j
c
c create segment (si) and segment end point (zzi) vectors for a sphere
c assume sphere center at origin of coordinate system,
c and a = radius of sphere. (a) is used in the (vex) calculation.
c assume m = odd number of points on sphere surface and
c        n = even number of segments = m + 1
c
      zz(1) = z(1) + ((0.4890)*r(1))
      deleg = abs( zz(1)) / (float(n/2))
      do 10, i = 2, (n+1)
         zz(i) = zz(i-1) + deleg
         s(i-1) = deleg
10    continue
c
c create d(i,j) and dd(i,j) matrices,
c [dd] is the left hand side coefficient matrix in,
c
c          [dd] * (q) = (const)
c
      do 15, i = 1, (n-1)
         do 16, j = 1, (n+1)
            d(i,j) = sqrt( (r(i))**2 + (z(i) - zz(j))**2 )
16       continue
15    continue
      do 17, i = 1, (n-1)
         do 18, j = 1, (n+1)
            dd(i,j) = d(i,j) - d(i,j+1)
18       continue
17    continue
      do 19, j = 1, n
         dd(n,j) = s(j)
19    continue
```

```
c notes in this function (m) has been redefined as a dummy index
c       counter for the array (a).
c

        do 1, i = 1, n
        do 1, j = 1, n
1       a(i,j) = array(i,j)
        m = 1
2       k = m + 1
        do 3, i = k, n
        if (a(m,m).eq. 0.0) then
           write(20,*)             In function DETERM,'
           write(20,*)             at row ',m,' diagonal element= ',a(m,m)
           write(20,*)             causes (ratio) in function to blow up,'
           write(20,*)                  CAN NOT obtain a (q) vector at,'
           write(20,*)             m= ',(n-1),', surface points !!!'
           write(20,*)
        else
        end if
        ratio = a(i,m)/a(m,m)
        do 3, j = k, n
3       a(i,j) = a(i,j) - a(m,j)*ratio
        if( m .eq. n-1 ) go to 4
        m = m+1
        go to 2
4       determ = 1.0
        do 5, i = 1, n
5       determ = determ * a(i,i)
        RETURN
        END

c c c

        subroutine error( n, dd, const, q, err )
        parameter ( kk=250 )
        real*8 dd(kk,kk), const(kk), q(kk), temp1(kk), temp2(kk), sum, err
        integer*4 i, j, n
        do i = 1, n
           temp1(i) = 0.0
        end do
        do i = 1, n
           do j = 1, n
              temp1(i) = (dd(i,j) * q(j)) + temp1(i)
           end do
        end do
        do i = 1, n
           temp2(i)   = const(i) - temp1(i)
        end do
        sum = 0.0
        do i = 1, n
           sum       = sum + ((temp2(i)**2)
        end do
        err = sqrt( sum )
        RETURN
        END

c c c
```

```
c
c Create right hand side or constant vector (const).
c

        do 30, i = 1, (n-1)
          const(i) = ( (r(i))**2 ) / (2.0)
30      continue
        const(n) = 0.0

c
c Solve for the source strengths (q) vector, using Cramer's Rule.
c

        call cramer( dd, const, q, n )

c
c Calc. the error norm (err) between (const) and (q) vectors
c

        call error( n, dd, const, q, err )

c
c Calc. velocities (v), (vex) and pressure coefficients (cp), (cpex).
c   (v) and (cp) are approximated, while (vex) and (cpex) are exact
c   values for comparison.
c

        do 90, i = 1, (n-1)
          ur = 0.0
          us = 1.0
        do 80, j = 1, n
          ur = ur +
          us = us + q(j)/r(j)*(x(s(i)-xs(j+1))/d(i,j+1))-(x(i)-xs(j))/d(i,j))
    $
80      continue
          v(i)    = u  * sqrt(ur**2 + us**2)
          vex(i)  = 1.5 * u * (r(i) / a)
          cp(i)   = 1.0 - (v(i)/u)**2
          cpex(i) = 1.0 - (vex(i)/u)**2
90      continue
        RETURN
        END

c c c

        subroutine cramer( q, a, x, n )
        parameter ( kk=250 )
        real*8 determ, denom, cc(kk,kk), a(kk,kk), q(kk), x(kk)
        integer*4 k, n, i, j
        denom = determ( c, n )
        if (denom .eq. 0.0) then
           write(20,*)             In subroutine CRAMER,'
           denom=', denom
           write(20,*)             causes (x(kk)) in subroutine to blow up,'
           write(20,*)                  CAN NOT obtain a (q) vector at,'
           write(20,*)             m= ',(n-1),', surface points !!!'
           write(20,*)
        else
        end if
        do 3, k = 1, n
        do 1, i = 1, n
        do 1, j = 1, n
1       cc(i,j) = c(i,j)
        do 2, i = 1, n
2       cc(i,k) = a(i)
3       x(k) = determ( cc, n ) / denom
        RETURN
        END

c c c

c DETERM is a function called by this subroutine.
c

        function determ( array, n )
c
c This function calculates the determinate of the matix (array).
c
        parameter ( kk=250 )
        real*8 ratio, determ, array(kk,kk), a(kk,kk)
        integer*4 i, n, j, m, k, l
c
```

APPENDIX C. SPH.OUT FILE FROM THE SPHERE CODE

```
This is the data output file called SPHERE.OUT
from the program SPHERE.FOR.

ECHO constant input values for the SPHERE

u (non-dimensional velocity) =    1.00000000000000000
a (non-dimensional length)   =    1.00000000000000000

FOR m (surface points) =    1

x1,                              r1
6.12303176911886E-017            1.00000000000000000

cp,                              cpex
-2.13495356033629E-001          -1.25000000000000000

FOR m (surface points) =    3

x1,                              r1
-7.07106781186547E-001           7.07106781186547E-001
6.12303176911886E-017            1.00000000000000000
7.07106781186547E-001            7.07106781186547E-001

cp,                              cpex
-1.25722174245158E-001          -1.25000000000000000E-001
-1.24828535309657E-001          -1.25000000000000000
-1.25722174245161E-001          -1.24999999999998E-001

FOR m (surface points) =    5

x1,                              r1
-8.66025403784438E-001           5.00000000000000000E-001
-4.99999999999998E-001           8.66025403784387E-001
5.00000000000001E-001            8.66025403784386E-001
8.66025403784438E-001            4.99999999999998E-001

cp,                              cpex
-1.37499999999993E-001          -1.37499999999932E-001
-6.07500000000001E-001          -6.07500000000018E-001
-6.87500000000001E-001          -4.87500000000099E-001
4.37500000000002E-001           -1.37500000000001E-001

FOR m (surface points) =    7

x1,                              r1
-9.23879532511286E-001           3.82683432365089E-001
-7.07106781186475E-001           7.07106781186475E-001
-3.82683432365089E-017           1.00000000000000000
3.82683432365089E-001            9.23879532511286E-001
7.07106781186475E-001            7.07106781186475E-001
9.23879532511286E-001            3.82683432365089E-001

cp,                              cpex
-9.23879532511286E-001           6.70495128834657E-001
-2.47916545562921E-001          -1.25000000000000000E-001
-3.82683432365089E-017          -9.20495128834656E-001
-1.24995547469213E-001          -1.25000000000000000E-001
7.07106781186475E-001            7.07106781186475E-001
-2.47916545562511E-001           6.70495128834660E-001

FOR m (surface points) =    9

x1,                              r1
```

```
-9.51056516295153E-001           3.09016994374975E-001
-8.09016994374973E-001           5.87785252292473E-001
-5.87785252292473E-001           8.09016994374975E-001
-3.09016994374973E-001           9.51056516295153E-001
6.12303176911886E-017            1.00000000000000000
3.09016994374975E-001            9.51056516295153E-001
5.87785252292473E-001            8.09016994374975E-001
8.09016994374975E-001            5.87785252292473E-001
9.51056516295153E-001            3.09016994374974E-001

cp,                              cpex
7.85293442621123E-001            7.85144118671857E-001
2.25574143979367E-001            2.22644118671856E-001
-4.72625739912781E-001          -4.72644118671859E-001
-1.03515062972125E-001          -1.03514411867181E-001
-1.24999962146078E-001          -1.25000000000000000
-1.03515062972076E-001          -1.03514411867181E-001
-4.72625739912764E-001          -4.72644118671859E-001
2.22574143981165E-001            2.22644118671858E-001
7.85293442621466E-001            7.85144118671859E-001

FOR m (surface points) =    11

x1,                              r1
-9.65925826289068E-001           2.58819045102521E-001
-8.66025403784438E-001           5.00000000000000000E-001
-7.07106781186547E-001           7.07106781186547E-001
-4.99999999999998E-001           8.66025403784387E-001
-1.24999999999998E-001           9.65925826289083E-001
1.72252620153034E-016            1.00000000000000000
-5.00000000000001E-001           9.65925826289082E-001
7.07106781186547E-001            6.66025403784386E-001
-8.66025403784387E-001           7.07106781186475E-001
9.65925826289083E-001            4.99999999999999E-001
                                 2.58819045102521E-001

cp,                              cpex
8.49214882844516E-001            8.49278579257432E-001
4.37523536336221E-001           -3.74999999999999E-001
-1.25000292429414E-001          -1.25000000000000000E-001
-6.87498520962441E-001          -6.87500000000001E-001
                                -1.24992705792574E-001
                                -1.24927922557493E-001
-6.87498520962750E-001           4.99927857925749E-001
-1.25005292485829E-001          -1.24999999999998E-001
-1.37503353445292E-001          -1.37500000000002E-001
8.49216488290143E-001            8.49278579257493E-001

FOR m (surface points) =    13

x1,                              r1
-9.74927912181016E-001           2.22520933956314E-001
-9.00968867902419E-001           4.33883739117582E-001
-7.81831482468039E-001           6.23489801858733E-001
-6.23489801858733E-001           7.81831482468029E-001
-4.33883739117582E-001           9.00968867902419E-001
-1.23031769111886E-017           9.74927912181026E-001
4.33883739117582E-001            7.49279121818234E-001
7.81831482468029E-001            9.00968867902419E-001
9.00968867902419E-001            4.33883739117582E-001
9.74927912181026E-001            2.22520933956314E-001

cp,                              cpex
8.86150687473985E-001            8.85899763902214E-001
5.76417989583464E-001            5.76426027091075E-001
1.25337644305564E-001            1.25336050700085E-001
```

```
 -3.753364245861590E-001  -3.753360507008541E-001
 -8.264259178547433E-001  -8.264260270910755E-001
      -1.138590014156294       -1.138589976390222
      -1.249999971265319       -1.250000000000000
      -1.138590014209914       -1.138589976390222
 -8.264259179573459E-001  -8.264260270910755E-001
 -3.753364247235456E-001  -3.753360507008536E-001
  1.253376441659483E-001   1.253360507008537E-001
  5.764179895080238E-001   5.764260270910752E-001
  8.886150688098057E-001   8.885899763902215E-001

 FOR m (surface points) =          15

  zi,                       ri

 -9.807852804032304E-001   1.950903220161286E-001
 -9.238795325112867E-001   3.826834323650899E-001
 -8.314696123025452E-001   5.555702330196022E-001
 -7.071067811865475E-001   7.071067811865476E-001
 -5.555702330196022E-001   8.314696123025455E-001
 -3.826834323650897E-001   9.238795325112867E-001
 -1.950903220161282E-001   9.807852804032304E-001
  6.123031769111886E-017        1.000000000000000
  1.950903220161283E-001   9.807852804032304E-001
  3.826834323650898E-001   9.238795325112867E-001
  5.555702330196023E-001   8.314696123025452E-001
  7.071067811865476E-001   7.071067811865475E-001
  8.314696123025452E-001   5.555702330196022E-001
  9.238795325112867E-001   3.826834323650898E-001
  9.807852804032304E-001   1.950903220161283E-001

  cp,                       cpex

  9.143543871286477E-001   9.143644740751973E-001
  6.704979296494158E-001   6.704951288348657E-001
  3.055183630936730E-001   3.055188614107261E-001
 -1.249999004366652E-001  -1.250000000000003E-001
 -5.555188881800679E-001  -5.555188614107269E-001
 -9.204951218089557E-001  -9.204951288348656E-001
      -1.164364477600032       -1.164364474075198
      -1.249999998329659       -1.250000000000000
      -1.164364477932414       -1.164364474075198
 -9.204951224391028E-001  -9.204951288348656E-001
 -5.555188890337434E-001  -5.555188614107258E-001
 -1.249999013902985E-001  -1.249999999999998E-001
  3.055183622273460E-001   3.055188614107261E-001
  6.704979291409998E-001   6.704951288348660E-001
  9.143543872151161E-001   9.143644740751976E-001

 FOR m (surface points) =          17

  zi,                       ri

 -9.848077530122080E-001   1.736481776669307E-001
 -9.396926207859083E-001   3.420201433256689E-001
 -8.660254037844386E-001   4.999999999999999E-001
 -7.660444431189779E-001   6.427876096865395E-001
 -6.427876096865393E-001   7.660444431189780E-001
 -4.999999999999999E-001   8.660254037844387E-001
 -3.420201433256687E-001   9.396926207859084E-001
 -1.736481776669303E-001   9.848077530122080E-001
  8.898589330674778E-017        1.000000000000000
  1.736481776669304E-001   9.848077530122080E-001
  3.420201433256688E-001   9.396926207859083E-001
  5.000000000000000E-001   8.660254037844386E-001
  6.427876096865394E-001   7.660444431189780E-001
  7.660444431189780E-001   6.427876096865393E-001
  8.660254037844387E-001   4.999999999999999E-001
  9.396926207859084E-001   3.420201433256687E-001
  9.848077530122080E-001   1.736481776669303E-001

  cp,                       cpex

  9.321582560819821E-001   9.321541983841467E-001
  7.367990183705119E-001   7.367999985088500E-001
  4.375001922878860E-001   4.375000000000002E-001
```

```
  7.035421470635835E-002   7.035419987529622E-002
 -3.203541428621823E-001  -3.203541998752967E-001
 -6.874999481193177E-001  -6.875000000000001E-001
 -9.867999448241237E-001  -9.867999985088505E-001
      -1.182154148773522       -1.182154198384147
      -1.249999955241274       -1.250000000000000
      -1.182154160472416       -1.182154198384147
 -9.867999669576348E-001  -9.867999985088498E-001
 -6.874999771976371E-001  -6.875000000000001E-001
 -3.203541749661064E-001  -3.203541998752967E-001
  7.035418450914792E-002   7.035419987529686E-002
  4.375001688741736E-001   4.375000000000002E-001
  7.367990052812309E-001   7.367999985088503E-001
  9.321582537434007E-001   9.321541983841469E-001

 FOR m (surface points) =          19

  zi,                       ri

 -9.876883405951377E-001   1.564344650402310E-001
 -9.510565162951535E-001   3.090169943749475E-001
 -8.910065241883678E-001   4.539904997395469E-001
 -8.090169943749473E-001   5.877852522924733E-001
 -7.071067811865475E-001   7.071067811865476E-001
 -5.877852522924730E-001   8.090169943749475E-001
 -4.539904997395467E-001   8.910065241883679E-001
 -3.090169943749473E-001   9.510565162951536E-001
 -1.564344650402308E-001   9.876883405951378E-001
  6.123031769111886E-017        1.000000000000000
  1.564344650402309E-001   9.876883405951378E-001
  3.090169943749475E-001   9.510565162951535E-001
  4.539904997395468E-001   8.910065241883678E-001
  5.877852522924731E-001   8.090169943749475E-001
  7.071067811865476E-001   7.071067811865475E-001
  8.090169943749475E-001   5.877852522924731E-001
  8.910065241883679E-001   4.539904997395468E-001
  9.510565162951535E-001   3.090169943749474E-001
  9.876883405951378E-001   1.564344650402309E-001

  cp,                       cpex

  9.449369139835619E-001   9.449385808320477E-001
  7.851444420327133E-001   7.851441186718157E-001
  5.362583108191760E-001   5.362584088290321E-001
  2.226440742758883E-001   2.226441186718156E-001
 -1.250000630274371E-001  -1.250000000000003E-001
 -4.726441859461559E-001  -4.726441186718159E-001
 -7.862584794943457E-001  -7.862584088290325E-001
      -1.035144188348633       -1.035144118671816
      -1.194938646583770       -1.194938580832048
      -1.250000059416345       -1.250000000000000
      -1.194938632513308       -1.194938580832048
      -1.035144161825861       -1.035144118671816
 -7.862584436123664E-001  -7.862584088290320E-001
 -4.726441448582293E-001  -4.726441186718159E-001
 -1.250002111196420E-001  -1.249999999999998E-001
  2.226441137367300E-001   2.226441186718158E-001
  5.362583471604215E-001   5.362584088290323E-001
  7.851444768173613E-001   7.851441186718159E-001
  9.449369434102366E-001   9.449385808320477E-001

 FOR m (surface points) =          21

  zi,                       ri

 -9.898214418809327E-001   1.423148382732852E-001
 -9.594929736144974E-001   2.817325568414297E-001
 -9.096319953545183E-001   4.154150130018863E-001
 -8.412535328311811E-001   5.406408174555978E-001
 -7.557495743542583E-001   6.548607339452852E-001
 -6.548607339452850E-001   7.557495743542583E-001
 -5.406408174555976E-001   8.412535328311811E-001
 -4.154150130018864E-001   9.096319953545184E-001
 -2.817325568414297E-001   9.594929736144974E-001
 -1.423148382732851E-001   9.898214418809328E-001
  3.347474207548995E-017        1.000000000000000
```

cp,

FOR m (surface points) = 23

x1,

cpex

r1

c

cp,

FOR m (surface points) = 25

x1,

cpex

r1

FOR m (surface points) = 27

x1,

cpex

r1

3

cp,

cpex

FOR m (surface points) = 29

x1

r1

cp,

cpex

FOR m (surface points) = 31

x1

r1

4

cp,   cpex

FOR m (surface points) = 33

x1,   r1

cp,   cpex

FOR m (surface points) = 35

x1,   r1

cp,

cpex

FOR m (surface points) = 37

x1,

r1

cp,

cpex

FOR m (surface points) = 39

x1,

r1

68

```
    5.224985647159489E-001    8.526401643540922E-001
    5.877852522924731E-001    8.090169943749475E-001
    6.494480483301837E-001    7.604059656000309E-001
    7.071067811865476E-001    7.071067811865475E-001
    7.604059656000309E-001    6.494480483301837E-001
    8.090169943749475E-001    5.877852522924731E-001
    8.526401643540922E-001    5.224985647159488E-001
    8.910065241883679E-001    4.539904997395468E-001
    9.238795325112867E-001    3.826834323650898E-001
    9.510565162951535E-001    3.090169943749474E-001
    9.723699203976766E-001    2.334453638559054E-001
    9.876883405951378E-001    1.564344650402309E-001
    9.969173337331280E-001    7.845909572784494E-002


       cp,                       cpex

    8.805393639067629E-001    9.861493831695299E-001
    9.027353434792926E-001    9.449385808320477E-001
    8.511179947685362E-001    8.773823397119137E-001
    7.664369495328547E-001    7.851441186718157E-001
    6.564562148195853E-001    6.704951288348657E-001
    5.255108328774930E-001    5.362584088290321E-001
    3.774260578885954E-001    3.857393122069899E-001
    2.161384311068086E-001    2.226441186718156E-001
    4.580818259550300E-002    5.098877317025950E-002
   -1.292247151860526E-001   -1.250000000000003E-001
   -3.045329477985960E-001   -3.009887731702601E-001
   -4.757068227851425E-001   -4.726441186718159E-001
   -6.384599405293646E-001   -6.357393122069905E-001
   -7.887313331453566E-001   -7.862584088290325E-001
   -9.227818362308864E-001   -9.204951288348656E-001
   -1.037282781301297        -1.035144118671816
   -1.129395086758662        -1.127382339711914
   -1.196836872040474        -1.194938580832048
   -1.237937891815081        -1.236149383169530
   -1.251679365058649        -1.250000000000000
   -1.237718124165071        -1.236149383169530
   -1.196394403699731        -1.194938580832048
   -1.128723005893080        -1.127382339711913
   -1.036368004554203        -1.035144118671816
   -9.216015679375731E-001   -9.204951288348656E-001
   -7.872478831464250E-001   -7.862584088290320E-001
   -6.366135399787071E-001   -6.357393122069900E-001
   -4.734060719099040E-001   -4.726441186718159E-001
   -3.016426483135478E-001   -3.009887731702596E-001
   -1.255511579392279E-001   -1.249999999999998E-001
    5.053388664749303E-002    5.098877317025972E-002
    2.222780643714663E-001    2.226441186718158E-001
    3.854537560597832E-001    3.857393122069903E-001
    5.360442244551401E-001    5.362584088290323E-001
    6.703425006687579E-001    6.704951288348660E-001
    7.850426542218033E-001    7.851441186718159E-001
    8.773211116376738E-001    8.773823397119139E-001
    9.449068513375339E-001    9.449385808320477E-001
    9.861318536673343E-001    9.861493831695299E-001


    In subroutine CRAMER,
    denom=   0.000000000000000E+000
    causes {x(k)} in subroutine to blow up,
       CAN NOT obtain a {q} vector at,
       n=         41, surface points !!!
```

APPENDIX D. ERR.OUT FILE FROM THE SPHERE CODE

This is the data output file called ERROR.OUT
from the program SPHERE.FOR.

number of surface points	error norm
1	1.130377350882890E-016
3	4.042327637553116E-015
5	5.884010837789714E-014
7	3.335424922697721E-013
9	7.049768158406932E-013
11	1.204559719731763E-011
13	2.989187292091445E-010
15	2.420649654610353E-009
17	1.827890796692023E-007
19	2.427334109556196E-007
21	4.866208540023427E-006
23	2.494981699304525E-006
25	3.456497292250762E-005
27	2.347015589325810E-003
29	1.638605492134842E-002
31	1.014824650891806E-001
33	6.804778254335419E-001
35	6.117182181739560
37	2.740841302405531E-001
39	1.655699712754890E-002

71

APPENDIX E. PMARC INPUT FILE FOR A SPHERE

```
SPHERE
&BINP2   LSTINP= 2,   LSTOUT= 1,   LSTFRQ= 0,   LENRUN= 0,          &END
         LPLTYP=1,                                                  &END
&BINP3   LSTGEO=1,    LSTNAB= 1,   LSTWAK=0,    LSTCPV=0,           &END
&BINP4   MAXIT=200,   SOLRES=0.0005,                                &END
&BINP5   NTSTPS= 3,   DTSTEP= 0.5,
&BINP6   REYN= 1.0,   RGPR=0.0,    RFF=5.0,     RCORES=0.05
         RCOREW=0.05,                                               &END
&BINP7   VINF= 335.19,   VSOUND= 1117.3,                            &END
&BINP8   ALDEG= 0.0,  YAWDEG=0.0,  PHIDOT=0.0,  THEDOT=0.0,
         PSIDOT=0.0,                                                &END
&BINP8A  PHIMAX=0.0,  THEMAX=0.0,  PSIMAX=0.0,
         WRX=0.0,     WRY=0.0,     WRZ=0.0,                         &END
&BINP8B  DXMAX=0.0,   DYMAX=0.0,   DZMAX=0.0,
         WTX=0.0,     WTY=0.0,     WTZ=0.0,                         &END
&BINP9   CBAR=    2.00,  SREF=    3.1416   SSPAN=    2.00,
         RMPX= 0.0,   RMPY=0.00,   RMPZ=0.00,                       &END
&BINP10  NORSET=0,    NBCHGE=0,    NCZONE=0,                        &END
&BINP11  NORPCH=0,    NC1PCH=0,    NCZONE=0,
         NORF=0,
         NOCF=0,
         NOCF=0,                                                    &END
&BINP12  KPAN=0,      NORL=0,                                       &END
&BINP13  NBLIT=0,     NOCL=0,                                       &END
&ASEM1   ASEMX=0.00,  ABEMX=0.00,  KSIDE=0,  NEWNAB=0,  NEWSID=0,   &END
         ASCAL=1.00,  ATHET=0.00,           NODEA= 5,
&ASEM2   APXX=0.00,   APYT=0.00,            APII=0.00,
         AHXX=0.00,   AHYY=1.00,            AHZZ=0.00,              &END
&COMP1   COMPX= 0.0000,  COMPY= 0.0000,     COMPZ= 0.0000,
         CSCAL=  1.000,  CTHET=   0.0,      NODEC= 5,               &END
&COMP2   CPXX= 0.0000,   CPYY= 0.0000,      CPZZ= 0.0000,
         CHXX= 0.0000,   CHYY= 1.0000,      CHZZ= 0.0000,           &END
&PATCH1  IREV= 0,  IDPAT= 2,  MAKE= 0,  KCOMP= 1,  KASS= 1,  IPATSYM=0,
         IPATCOP=0,
BODY
&SECT1   STX= -0.100000E+01,  STY= 0.0,    STZ= 0.0,   SCALE=  1.0,  &END
         ALF=   0.0,   THETA=  0.0,  TNPS= 0,   TINTS= 3,
         INNODE=  4,   TNODS= 0,  TNPC= 0,  TINTC= 3,
    0.000000E+00   0.464966E-01  -0.158353E+00
    0.000000E+00   0.464966E-01  -0.158353E+00
    0.000000E+00   0.143353E+00  -0.108077E+00
    0.000000E+00   0.143353E+00  -0.234874E-01
    0.000000E+00   0.892263E-01   0.685593E-01
    0.000000E+00   0.150124E+00   0.685593E-01
    0.000000E+00   0.892263E-01   0.118839E+00
    0.000000E+00  -0.144281E-07   0.165038E+00
    0.000000E+00  -0.892263E-01   0.118839E+00
    0.000000E+00  -0.150124E+00   0.685593E-01
    0.000000E+00  -0.892263E-01   0.685593E-01
    0.000000E+00  -0.124727E+00  -0.234873E-01
    0.000000E+00  -0.143353E+00  -0.108077E+00
    0.000000E+00  -0.464967E-01  -0.158353E+00
    0.000000E+00  -0.464964E-01  -0.158353E+00
&BPNODE  TNODE=3,   TNODS= 0,  TNPC= 0,  TINTC= 3,
&SECT1   STX= -0.902100E+00,  STY= 0.0,    STZ= 0.0,   SCALE=  1.0,  &END
         ALF=   0.0,   THETA=  0.0,  TNPS= 0,   TINTS= 3,
         INNODE=  4,   TNODS= 0,  TNPC= 0,  TINTC= 3,
    0.000000E+00   0.134963E+00  -0.459643E+00
    0.000000E+00   0.474172E+00  -0.681752E-01
    0.000000E+00   0.435757E+00  -0.313710E+00
    0.000000E+00   0.258993E+00   0.199004E+00
    0.000000E+00   0.258993E-00   0.403001E+00
```

```
    0.000000E+00  -0.418797E-07   0.479048E+00
    0.000000E+00  -0.258993E+00   0.403001E+00
    0.000000E+00  -0.435757E+00   0.199004E+00
    0.000000E+00  -0.474172E+00  -0.681755E-01
    0.000000E+00  -0.362040E+00  -0.313710E+00
    0.000000E+00  -0.134963E+00  -0.459643E+00
    0.000000E+00  -0.134963E+00  -0.459643E+00
&BPNODE  TNODE=3,   TNPC=0,   TINTC= 3,
&SECT1   STX= -0.715900E+00,  STY= 0.0,   STZ= 0.0,   SCALE=  1.0,  &END
         ALF=   0.0,   THETA= 0.0,  TNPS= 0,   TINTS= 3,
         INNODE=  4,   TNODS= 0,
    0.000000E+00   0.210207E+00  -0.715900E+00
    0.000000E+00   0.563882E+00  -0.488607E+00
    0.000000E+00   0.738529E+00  -0.106184E+00
    0.000000E+00   0.678697E+00   0.309951E+00
    0.000000E+00   0.403385E+00   0.627679E+00
    0.000000E+00  -0.652281E-07   0.746123E+00
    0.000000E+00  -0.403384E+00   0.627679E+00
    0.000000E+00  -0.678697E+00   0.309951E+00
    0.000000E+00  -0.563882E+00  -0.106184E+00
    0.000000E+00  -0.210208E+00  -0.715900E+00
    0.000000E+00   0.210207E+00  -0.715900E+00
&BPNODE  TNODE=3,   TNPC= 0,   TINTC= 3,
&SECT1   STX= -0.459600E+00,  STY= 0.0,   STZ= 0.0,   SCALE=  1.0,  &END
         ALF=   0.0,   THETA= 0.0,  TNPS= 0,   TINTS= 3,
         INNODE=  4,   TNODS= 0,
    0.000000E+00   0.264856E+00  -0.902016E+00
    0.000000E+00   0.710477E+00  -0.615632E+00
    0.000000E+00   0.930527E+00  -0.133790E+00
    0.000000E+00   0.855141E+00   0.390530E+00
    0.000000E+00   0.508254E+00   0.790859E+00
    0.000000E+00  -0.821858E-07   0.940096E+00
    0.000000E+00  -0.508254E+00   0.790859E+00
    0.000000E+00  -0.855141E+00   0.390530E+00
    0.000000E+00  -0.710477E+00  -0.133790E+00
    0.000000E+00  -0.264856E+00  -0.902016E+00
&BPNODE  TNODE=3,   TNPC= 0,   TINTC= 3,
&SECT1   STX= -0.158400E+00,  STY= 0.0,   STZ= 0.0,   SCALE=  1.0,  &END
         ALF=   0.0,   THETA= 0.0,  TNPS= 0,   TINTS= 3,
         INNODE=  4,   TNODS= 0,
    0.000000E+00   0.293655E+00  -0.100010E+01
    0.000000E+00   0.787733E+00  -0.682574E+00
    0.000000E+00   0.103171E+01  -0.148338E+00
    0.000000E+00   0.948128E+00   0.432995E+00
    0.000000E+00   0.563521E+00   0.876855E+00
    0.000000E+00  -0.911225E-07   0.104232E+01
    0.000000E+00  -0.563521E+00   0.876855E+00
    0.000000E+00  -0.948127E+00   0.432996E+00
    0.000000E+00  -0.787733E+00  -0.148337E+00
    0.000000E+00  -0.293655E+00  -0.100010E+01
&BPNODE  TNODE=3,   TNPC= 0,   TINTC= 3,
&SECT1   STX= -0.158400E+00,  STY= 0.0,   STZ= 0.0,   SCALE=  1.0,  &END
         ALF=   0.0,   THETA= 0.0,  TNPS= 0,   TINTS= 3,
         INNODE=  4,   TNODS= 0,
    0.000000E+00   0.293655E+00  -0.100010E+01
    0.000000E+00   0.787733E+00  -0.682574E+00
    0.000000E+00   0.103171E+01  -0.148338E+00
    0.000000E+00   0.948128E+00   0.432995E+00
    0.000000E+00   0.563521E+00   0.876855E+00
    0.000000E+00  -0.911225E-07   0.104232E+01
    0.000000E+00  -0.563521E+00   0.876855E+00
    0.000000E+00  -0.948127E+00   0.432996E+00
    0.000000E+00  -0.787733E+00  -0.148337E+00
    0.000000E+00  -0.293655E+00  -0.100010E+01
&BPNODE  TNODE=3,   TNPC= 0,   TINTC= 3,
&SECT1   STX= -0.459600E+00,  STY= 0.0,   STZ= 0.0,   SCALE=  1.0,  &END
         ALF=   0.0,   THETA= 0.0,  TNPS= 0,   TINTS= 3,
         INNODE=  4,   TNODS= 0,
    0.000000E+00   0.264856E+00  -0.902016E+00
```

```
&WAKE1  IDWAK= 0,   IFLKW= 0,   ITRPTZ= 0,   INTRW= 0,      &END
  BODY WAKE
&WAKE2  KWPACH= 1,  KWSIDE= 3,  KWLINE= 11,  KWPAN1= 0,     &END
  KWPAN2= 0,  MODEW= 5,   INITIAL= 0,                       &END
&CONSTRH  NONSL = 0,  KPSL = 0,                             &END
&BLPARAM  RN = 200000,  VISC = 0.00335,  NSLBL = 0,         &END
&VS1  NVOLR= 0,
&SLIN1  NSTLIN= 0,  NVOLC= 0,
```

```
0.000000E+00    0.710477E+00   -0.615632E+00
0.000000E+00    0.930527E+00   -0.133790E+00
0.000000E+00    0.855141E+00    0.390530E+00
0.000000E+00   -0.508254E+00    0.790859E+00
0.000000E+00   -0.821858E-07    0.940096E+00
0.000000E+00   -0.508254E+00    0.790859E+00
0.000000E+00   -0.855141E+00    0.390530E+00
0.000000E+00   -0.930527E+00   -0.133769E+00
0.000000E+00   -0.710477E+00   -0.615632E+00
0.000000E+00   -0.264856E+00   -0.902015E+00
0.000000E+00    0.264856E+00   -0.902016E+00
&BPNODE  TNODE=3,   TNPC= 0,   TINTC= 3,
&SECT1   STX= 0.715900E+00,  STY= 0.0,   STZ= 0.0,   SCALE= 1.0,   &END
  ALP= 0.0,   THETA= 0.0,
  INMODE= 4,  TNODE= 0,   TNPS= 0,   TINTS= 3,                      &END
0.000000E+00    0.210207E+00   -0.715900E+00
0.000000E+00    0.563882E+00   -0.488607E+00
0.000000E+00    0.738539E+00   -0.106184E+00
0.000000E+00    0.678697E+00    0.309951E+00
0.000000E+00    0.403385E+00    0.627679E+00
0.000000E+00   -0.652281E-07    0.746123E+00
0.000000E+00   -0.403384E+00    0.627679E+00
0.000000E+00   -0.678697E+00    0.309951E+00
0.000000E+00   -0.738539E+00   -0.106184E+00
0.000000E+00   -0.563882E+00   -0.488606E+00
0.000000E+00   -0.210207E+00   -0.715900E+00
&BPNODE  TNODE=3,   TNPC= 0,   TINTC= 3,
&SECT1   STX= 0.902100E+00,  STY= 0.0,   STZ= 0.0,   SCALE= 1.0,   &END
  ALP= 0.0,   THETA= 0.0,
  INMODE= 4,  TNODE= 0,   TNPS= 0,   TINTS= 3,                      &END
0.000000E+00    0.114963E+00   -0.459643E+00
0.000000E+00    0.362040E+00   -0.313710E+00
0.000000E+00    0.474172E+00   -0.681757E-01
0.000000E+00    0.435757E+00    0.199004E+00
0.000000E+00    0.258993E+00    0.403001E+00
0.000000E+00   -0.418797E-07    0.479048E+00
0.000000E+00   -0.435757E+00    0.199004E+00
0.000000E+00   -0.474172E+00   -0.681755E-01
0.000000E+00   -0.362040E+00   -0.313710E+00
0.000000E+00   -0.114963E+00   -0.459643E+00
0.000000E+00    0.134963E+00   -0.459643E+00
&BPNODE  TNODE=3,   TNPC= 0,   TINTC= 3,
&SECT1   STX= 0.999800E+00,  STY= 0.0,   STZ= 0.0,   SCALE= 0.0,   &END
  ALP= 0.0,   THETA= 0.0,
  INMODE= 4,  TNODE= 5,   TNPS= 0,   TINTS= 3,                      &END
0.000000E+00    0.464966E-01   -0.158353E+00
0.000000E+00    0.124727E+00   -0.108077E+00
0.000000E+00    0.163358E+00   -0.234874E-01
0.000000E+00    0.150124E+00    0.685593E-01
0.000000E+00    0.892263E-01    0.138039E+00
0.000000E+00   -0.144281E-07    0.165038E+00
0.000000E+00   -0.150124E+00    0.685593E-01
0.000000E+00   -0.163358E+00   -0.234873E-01
0.000000E+00   -0.124727E+00   -0.108077E+00
0.000000E+00   -0.464967E-01   -0.158353E+00
0.000000E+00    0.464964E-01   -0.158353E+00
&BPNODE  TNODE=3,   TNPC= 0,   TINTC= 3,
```

APPENDIX F. PMARC INPUT FILE FOR A SPINDLE

```
SPINDLE BODY (AOA=0,  PANELS=144)
&BINP2  LSTINP= 2,  LSTOUT= 1,   LSTFRQ= 0,  LENRUN= 0,        &END
        LPLTYP=1,                                              &END
&BINP3  LSTGEO=1,          LSTNAB= 1,  LSTWAK=0,  LSTCPV=0,    &END
&BINP4  MAXIT=200,         SOLRES=0.0005,                      &END
&BINP5  NTSTPS= 3,         DTSTEP= 0.5,                        &END
&BINP6  RSYM= 1.0,    RGPR=0.0,    RFF=5.0,       RCORES=0.05
        RCOREW=0.05,
&BINP7  VINF= 335.19,  VSOUND= 1117.3,                         &END
&BINP8  ALDEG= 0.0,  YAWDEG=0.0,  PHIDOT=0.0,  THEDOT=0.0,     &END
        PSIDOT=0.0,
&BINP8A PHIMAX=0.0,   THEMAX=0.0,   PSIMAX=0.0,                &END
        WRX=0.0,      WRY=0.0,      WRZ=0.0
&BINP8B DXMAX=0.0,    DYMAX=0.0,    DZMAX=0.0,                 &END
        WTX=0.0,      WTY=0.0,      WTZ=0.0,
&BINP9  CBAR=    1.00,   SREF=   0.7854   SSPAN=     1.00,     &END
&BINP10 RMPX= 0.0,    RMPY=0.00,    RMP2=0.00,                 &END
        NORSET=0,    NBCHGE=0,    NCZONE=0,
&BINP11 NCZPCH=0,    C2DUB=0.0,    VREF=0.0,                   &END
        HORPCH=0,
        NORF=0,    NORL=0,
        NOCF=0,    NOCL=0.
&BINP12 VNORM=0.0,                                             &END
        KPAN=0,    KSIDE=0,    NEWNAB=0,    NEWSID=0,          &END
&BINP13 NBLIT= 0,                                              &END
&ASEM1  ASEMX=0.00,   ASEMY=0.00,   ASENZ=0.00,               &END
        ASCAL=1.00,   ATHET=0.00,   NODEA= 5,
&ASEM2  APXX=0.00,    APYY=0.00,    APZZ=0.00,                 &END
        AHXX=0.00,    AHYY=1.00,    AHZZ=0.00,
&COMP1  COMPX= 0.0000,   COMPY= 0.0000,   COMPZ= 0.0000,       &END
        CSCAL= 1.000,    CTHET=   0.0,    NODEC= 5,
&COMP2  CPXX= 0.0000,    CPYY= 0.0000,    CPZZ= 0.0000,        &END
        CHXX= 0.0000,    CHYY= 1.000,     CHZZ= 0.0000,
&PATCH1 IREV= 0,  IDPAT= 2,  MAKE=  0,  KCOMP= 1, KASS= 1, IPATSYM=0,  &END
        IPATCOP=0,
        BODY ( only patch # 1 )
&SECT1  STX= 0.000000E+00,  STY= 0.0,    STZ= 0.0,    SCALE=  0.0,     &END
        ALF=  0.0,    THETA=  0.0,
        INMODE= 4,    TNODS= 0,    TNPS= 0,    TINTS= 3,
        0.000000E+00    0.612669E-02    -0.236115E-01
        0.000000E+00    0.612669E-02    -0.172848E-01
        0.000000E+00    0.172848E-01    -0.612669E-02
        0.000000E+00    0.236115E-01    -0.612669E-02
        0.000000E+00    0.236115E-01    -0.172848E-01
        0.000000E+00    0.172848E-01    -0.236115E-01
        0.000000E+00    0.612669E-02    -0.236115E-01
        0.000000E+00    0.612669E-02    -0.172848E-01
        0.000000E+00    0.172848E-01    -0.612669E-02
        0.000000E+00    0.236115E-01    -0.612669E-02
        0.000000E+00    0.236115E-01    -0.172848E-01
        0.000000E+00    0.172848E-01    -0.236115E-01
&BPNODE TNODE=3,            TNPC= 0,    TNPC= 3,                       &END
&SECT1  STX= 0.833333E-01,  STY= 0.0,    STZ= 0.0,    SCALE=  1.0,     &END
        ALF=  0.0,    THETA=  0.0,
        INMODE= 4,    TNODS= 0,    TNPS= 0,    TINTS= 3,
        0.000000E+00    0.612669E-02    -0.236115E-01
        0.000000E+00    0.612669E-02    -0.172848E-01
        0.000000E+00    0.172848E-01    -0.612669E-02
        0.000000E+00    0.236115E-01    -0.612669E-02
        0.000000E+00    0.236115E-01    -0.172848E-01
        0.000000E+00    0.172848E-01    -0.236115E-01
&BPNODE TNODE=3,            TNPC= 0,    TNPC= 3,                       &END
&SECT1  STX= 0.166667E+00,  STY= 0.0,    STZ= 0.0,    SCALE=  1.0,     &END
        ALF=  0.0,    THETA=  0.0,
        INMODE= 4,    TNODS= 0,    TNPS= 0,    -0.429300E-01
        0.000000E+00    0.115031E-01    -0.314270E-01
        0.000000E+00    0.429300E-01    -0.115031E-01
```

```
        0.000000E+00    0.429300E-01    0.115031E-01
        0.000000E+00    0.314270E-01    0.314270E-01
        0.000000E+00    0.115031E-01    0.429300E-01
        0.000000E+00   -0.115031E-01    0.429300E-01
        0.000000E+00   -0.314270E-01    0.314270E-01
        0.000000E+00   -0.429300E-01    0.115031E-01
        0.000000E+00   -0.429300E-01   -0.115031E-01
        0.000000E+00   -0.115031E-01   -0.429300E-01
&BPNODE TNODE=3,            TNPC= 0,    TNPC= 3,                       &END
&SECT1  STX= 0.250000E+00,  STY= 0.0,    STZ= 0.0,    SCALE=  1.0,     &END
        ALF=  0.0,    THETA=  0.0,
        INMODE= 4,    TNODS= 0,    TNPS= 0,    TINTS= 3,
        0.000000E+00    0.155291E-01    -0.579555E-01
        0.000000E+00    0.424264E-01    -0.424264E-01
        0.000000E+00    0.579555E-01    -0.155291E-01
        0.000000E+00    0.579555E-01    0.155291E-01
        0.000000E+00    0.424264E-01    0.424264E-01
        0.000000E+00    0.155291E-01    0.579555E-01
        0.000000E+00   -0.155291E-01    0.579555E-01
        0.000000E+00   -0.424264E-01    0.424264E-01
        0.000000E+00   -0.579555E-01    0.155291E-01
        0.000000E+00   -0.579556E-01   -0.155291E-01
        0.000000E+00   -0.424264E-01   -0.424264E-01
        0.000000E+00   -0.155292E-01   -0.579555E-01
&BPNODE TNODE=3,            TNPC= 0,    TNTC= 3,                       &END
&SECT1  STX= 0.333333E+00,  STY= 0.0,    STZ= 0.0,    SCALE=  1.0,     &END
        ALF=  0.0,    THETA=  0.0,
        INMODE= 4,    TNODS= 0,    TNPS= 0,    TINTS= 3,
        0.000000E+00    0.184049E-01    -0.686881E-01
        0.000000E+00    0.502832E-01    -0.502831E-01
        0.000000E+00    0.686881E-01    -0.184049E-01
        0.000000E+00    0.686881E-01    0.184049E-01
        0.000000E+00    0.502831E-01    0.502831E-01
        0.000000E+00    0.184049E-01    0.686881E-01
        0.000000E+00   -0.184049E-01    0.686881E-01
        0.000000E+00   -0.502831E-01    0.502831E-01
        0.000000E+00   -0.686881E-01    0.184049E-01
        0.000000E+00   -0.686881E-01   -0.184049E-01
        0.000000E+00   -0.502831E-01   -0.502831E-01
        0.000000E+00   -0.184049E-01   -0.686881E-01
&BPNODE TNODE=3,            TNPC= 0,    STY= 0.0,                      &END
&SECT1  STX= 0.416667E+00,  STY= 0.0,    STZ= 0.0,    SCALE=  1.0,     &END
        ALF=  0.0,    THETA=  0.0,
        INMODE= 4,    TNODS= 0,    TNPS= 0,    TINTS= 3,
        0.000000E+00    0.201304E-01    -0.751276E-01
        0.000000E+00    0.549972E-01    -0.549972E-01
        0.000000E+00    0.751276E-01    -0.201304E-01
        0.000000E+00    0.751276E-01    0.201304E-01
        0.000000E+00    0.549972E-01    0.549972E-01
        0.000000E+00    0.201304E-01    0.751276E-01
        0.000000E+00   -0.201304E-01    0.751276E-01
        0.000000E+00   -0.549972E-01    0.549972E-01
        0.000000E+00   -0.751276E-01    0.201304E-01
        0.000000E+00   -0.751276E-01   -0.201304E-01
        0.000000E+00   -0.549972E-01   -0.549972E-01
        0.000000E+00   -0.201304E-01   -0.751276E-01
&BPNODE TNODE=3,            TNPC= 0,    TNTC= 3,                       &END
&SECT1  STX= 0.500000E+00,  STY= 0.0,    STZ= 0.0,    SCALE=  1.0,     &END
        ALF=  0.0,    THETA=  0.0,
        INMODE= 4,    TNODS= 0,    TNPS= 0,    TINTS= 3,
        0.000000E+00    0.207055E-01    -0.772741E-01
        0.000000E+00    0.565685E-01    -0.565685E-01
        0.000000E+00    0.772741E-01    -0.207055E-01
        0.000000E+00    0.772741E-01    0.207055E-01
        0.000000E+00    0.565685E-01    0.565685E-01
        0.000000E+00    0.207055E-01    0.772741E-01
        0.000000E+00   -0.207055E-01    0.772741E-01
        0.000000E+00   -0.565685E-01    0.565685E-01
        0.000000E+00   -0.772741E-01    0.207055E-01
        0.000000E+00   -0.772741E-01   -0.207055E-01
        0.000000E+00   -0.565685E-01   -0.207055E-01
        0.000000E+00   -0.565685E-01   -0.565685E-01
```

```
0.000000E+00  -0.207055E-01  -0.772741E-01
0.000000E+00  -0.207055E-01  -0.772741E-01
&BPNODE  TNODE=3,  TNPC= 0,  STY= 0.0,  STZ= 0.0,  SCALE= 1.0,  &END
&SECT1  STX= 0.583333E+00,  THETA=  0.0,
   INMODE=  4,  TNODS=  0,  TNPS= 0,  TINTS= 3,
   ALF=  0.0,
0.000000E+00   0.201304E-01  -0.751276E-01
0.000000E+00   0.549972E-01  -0.549972E-01
0.000000E+00   0.751276E-01  -0.201304E-01
0.000000E+00   0.751276E-01   0.201304E-01
0.000000E+00   0.549972E-01   0.549972E-01
0.000000E+00   0.201304E-01   0.751276E-01
0.000000E+00  -0.201304E-01   0.751276E-01
0.000000E+00  -0.549972E-01   0.549972E-01
0.000000E+00  -0.751276E-01   0.201304E-01
0.000000E+00  -0.751276E-01  -0.201304E-01
0.000000E+00  -0.549972E-01  -0.549972E-01
0.000000E+00  -0.201304E-01  -0.751276E-01
&BPNODE  TNODE=3,  TNPC= 0,  STY= 0.0,  STZ= 0.0,  SCALE= 1.0,  &END
&SECT1  STX= 0.666667E+00,  THETA=  0.0,
   INMODE=  4,  TNODS=  0,  TNPS= 0,  TINTS= 3,
   ALF=  0.0,
0.000000E+00   0.184049E-01  -0.686881E-01
0.000000E+00   0.502831E-01  -0.502831E-01
0.000000E+00   0.686881E-01  -0.184049E-01
0.000000E+00   0.686881E-01   0.184049E-01
0.000000E+00   0.502832E-01   0.502832E-01
0.000000E+00   0.184049E-01   0.686881E-01
0.000000E+00  -0.184049E-01   0.686881E-01
0.000000E+00  -0.502831E-01   0.502831E-01
0.000000E+00  -0.686881E-01   0.184049E-01
0.000000E+00  -0.686881E-01  -0.184049E-01
0.000000E+00  -0.502832E-01  -0.502832E-01
0.000000E+00  -0.184049E-01  -0.686881E-01
&BPNODE  TNODE=3,  TNPC= 0,  STY= 0.0,  STZ= 0.0,  SCALE= 1.0,  &END
&SECT1  STX= 0.750000E+00,  THETA=  0.0,
   INMODE=  4,  TNODS=  0,  TNPS= 0,  TINTS= 3,
   ALF=  0.0,
0.000000E+00   0.155291E-01  -0.579555E-01
0.000000E+00   0.424264E-01  -0.424264E-01
0.000000E+00   0.579555E-01  -0.155291E-01
0.000000E+00   0.579555E-01   0.155291E-01
0.000000E+00   0.424264E-01   0.424264E-01
0.000000E+00   0.155291E-01   0.579555E-01
0.000000E+00  -0.155291E-01   0.579555E-01
0.000000E+00  -0.424264E-01   0.424264E-01
0.000000E+00  -0.579556E-01   0.155291E-01
0.000000E+00  -0.579556E-01  -0.155291E-01
0.000000E+00  -0.424264E-01  -0.424264E-01
0.000000E+00  -0.155292E-01  -0.579555E-01
&BPNODE  TNODE=3,  TNPC= 0,  STY= 0.0,  STZ= 0.0,  SCALE= 1.0,  &END
&SECT1  STX= 0.813333E+00,  THETA=  0.0,
   INMODE=  4,  TNODS=  0,  TNPS= 0,  TINTS= 3,
   ALF=  0.0,
0.000000E+00   0.115031E-01  -0.429301E-01
0.000000E+00   0.314270E-01  -0.314270E-01
0.000000E+00   0.429301E-01  -0.115031E-01
0.000000E+00   0.429301E-01   0.115031E-01
0.000000E+00   0.314270E-01   0.314270E-01
0.000000E+00   0.115031E-01   0.429301E-01
0.000000E+00  -0.115031E-01   0.429301E-01
0.000000E+00  -0.314270E-01   0.314270E-01
0.000000E+00  -0.429301E-01   0.115031E-01
0.000000E+00  -0.429301E-01  -0.115031E-01
0.000000E+00  -0.314270E-01  -0.314270E-01
0.000000E+00  -0.115031E-01  -0.429301E-01
&BPNODE  TNODE=3,  TNPC= 0,  STY= 0.0,  STZ= 0.0,  SCALE= 1.0,  &END
&SECT1  STX= 0.916667E+00,  THETA=  0.0,
   INMODE=  4,  TNODS=  0,  TNPS= 0,  TINTS= 3,
   ALF=  0.0,
0.000000E+00   0.612669E-02  -0.236115E-01
0.000000E+00   0.172848E-01  -0.172848E-01
```

```
0.000000E+00   0.236115E-01  -0.632669E-02
0.000000E+00   0.236115E-01   0.632669E-02
0.000000E+00   0.172848E-01   0.172848E-02
0.000000E+00  -0.632669E-02  -0.632669E-02
0.000000E+00  -0.632669E-02   0.236115E-01
0.000000E+00  -0.236115E-01   0.632669E-02
0.000000E+00  -0.632670E-02  -0.172848E-01
0.000000E+00  -0.236115E-01  -0.236115E-01
0.000000E+00  -0.632670E-02  -0.236115E-01
&BPNODE  TNODE=3,  TNPC= 0,  STY= 0.0,  STZ= 0.0,  SCALE= 0.0,  &END
&SECT1  STX=-0.100000E+01,  THETA=  0.0,
   INMODE=  4,  TNODS= 5,  TNPS= 0,  TINTS= 3,
   ALF=  0.0,
0.000000E+00   0.632669E-02  -0.236115E-01
0.000000E+00   0.172848E-01  -0.172848E-01
0.000000E+00   0.236115E-01  -0.632669E-02
0.000000E+00   0.236115E-01   0.172848E-01
0.000000E+00  -0.612669E-02   0.236115E-01
0.000000E+00  -0.236115E-01   0.632669E-02
0.000000E+00  -0.172848E-01  -0.172848E-01
0.000000E+00  -0.632670E-02  -0.236115E-01
&BPNODE  TNODE=3,  TNPC= 0,  TINTC=3,                                   &END
&WAKE1  IDWAK= 0,  IFLKW= 0,  ITRFTZ= 0,  IHTRM= 0,                     &END
BODY WAKE
&WAKE2  KWPACH= 1,  KWSIDE= 3,  KWLINE= 12,  KWPAN1= 0,                 &END
        KWPAN2= 0,  NODEM= 5,  INITIAL= 0,                             &END
&ONSTRM  NONSL= 0,  KPSL = 0,                                           &END
&BLPARAM  RN = 200000,  VISC = 0.00135,  NSLBL = 0,                     &END
&VS1    NVOLR= 0,  NVOLC= 0,                                            &END
&SLIN1  HSTLIN= 0,                                                      &END
```

APPENDIX G. OVERFLOW INPUT FILE FOR A MISSILE FOREBODY

```
$GLOBAL
  NSTEPS= 1000, RESTRT= .F., NSAVE = 50, CHIMRA= .T., NQT = 0, $END
$FLOINP
  ALPHA = 0.0, FSMACH= 0.3000, REY= 2.0E+06, TINF= 520.000, $END
$VARGAM $END

$GRDNAM
  NAME = 'HEMISPHERE CYL. NOSE ( gr_1, 23x93x71 )', $END
$NITERS $END
$METPRM
  IRHS   = 1,    ILHS = 1,    IDISS = 1, $END
$TIMACU
  DT   = 0.20, ITIME= 1, CFLMIN=2, CFLMAX=200, TFOSO = 1.00, $END
$SMOACU
  ISPEC = 2, DIS2 = 2.00, DIS4 = 0.02,
  SMOO = 1.000, EPSE = 0.060, $END
$VISINP
  VISCJ = .F., VISCK = .T., VISCL = .T.,
  NTURB = 1,
  ITTYP = 1,
  ITDIR = 3,
  JTLS  = 2,
  JTLE  = 23,
  KTLS  = 1,
  KTLE  = 93,
  LTLS  = 1,
  LTLE  = 71,
  TLPAR1= 0.9, $END
$BCINP
  NBC   = 5,
  IBTYP = 12,   5,   40,
  IBDIR = 2,   -1,   -3,
  JBCS  = 1,   23,   -1,
  JBCE  = 23,  23,   1,
  KBCS  = 93,  1,   93,
  KBCE  = 1,   1,
  LBCS  = 71,  71,   71,
  LBCE  = 1,   1,
  $END
$BCSINP $END

$GRDNAM
  NAME = ' Bot. Middle Cyl, mis. surface ( gr_2, 39x93x49 )', $END
$NITERS $END
$METPRM
  IRHS   = 1,    ILHS = 1,    IDISS = 1, $END
$TIMACU
  DT   = 0.20, ITIME= 1, CFLMIN=0, CFLMAX=200, TFOSO = 1.00, $END
$SMOACU
  ISPEC = 2, DIS2 = 2.00, DIS4 = 0.02,
  SMOO = 1.000, EPSE = 0.060, $END
$VISINP
  VISCJ = .F., VISCK = .T., VISCL = .T.,
  NTURB = 1,
  ITTYP = 1,
  ITDIR = 3,
  JTLS  = 1,
  JTLE  = 39,
  KTLS  = 1,
  KTLE  = 93,
  LTLS  = 1,
  LTLE  = 49,
  TLPAR1= 0.9,
  $END
$BCINP
  NBC   = 3,
  IBTYP = 12,   5,
  IBDIR = 2,   -1,   3,
  JBCS  = 1,   39,
  JBCE  = 39,  39,
  KBCS  = 93,  1,
  KBCE  = 1,   1,
  LBCS  = 1,   93,
  $END
```

```
  LBCE  = 49,    1,
  $END
$BCSINP $END

$GRDNAM
  NAME = ' Top Middle Cyl. ( gr_3, 12x93x21 )', $END
$NITERS $END
$METPRM
  IRHS   = 1,    ILHS = 1,    IDISS = 1, $END
$TIMACU
  DT   = 0.20, ITIME= 1, CFLMIN=0, CFLMAX=200, TFOSO = 1.00, $END
$SMOACU
  ISPEC = 2, DIS2 = 2.00, DIS4 = 0.02,
  SMOO = 1.000, EPSE = 0.060, $END
$VISINP
  VISCJ = .F., VISCK = .T., VISCL = .T.,
  NTURB = 1,
  ITTYP = 1,
  ITDIR = 3,
  JTLS  = 1,
  JTLE  = 12,
  KTLS  = 1,
  KTLE  = 93,
  LTLS  = 1,
  LTLE  = 21,
  TLPAR1= 0.9,
  $END
$BCINP
  NBC   = 3,
  IBTYP = 12,   40,
  IBDIR = 2,   -3,
  JBCS  = 12,   -1,
  JBCE  = 1,   12,
  KBCS  = 93,  93,
  KBCE  = 1,   21,
  LBCS  = 21,  21,
  $END
$BCSINP $END

$GRDNAM
  NAME = ' Rear Cyl. & Mis. Body ( gr_4, 31x93x71 )', $END
$NITERS $END
$METPRM
  IRHS   = 1,    ILHS = 1,    IDISS = 1, $END
$TIMACU
  DT   = 0.10, ITIME= 1, CFLMIN=1, CFLMAX=200, TFOSO = 1.00, $END
$SMOACU
  ISPEC = 2, DIS2 = 2.00, DIS4 = 0.02,
  SMOO = 1.000, EPSE = 0.060, $END
$VISINP
  VISCJ = .F., VISCK = .T., VISCL = .T.,
  NTURB = 1,
  ITTYP = 1,
  ITDIR = 3,
  JTLS  = 1,
  JTLE  = 31,
  KTLS  = 1,
  KTLE  = 93,
  LTLS  = 1,
  LTLE  = 71,
  TLPAR1= 0.9,
  $END
$BCINP
  NBC   = 5,
  IBTYP = 12,   5,   40,   30,
  IBDIR = 2,   -1,   -3,   -1,
  JBCS  = 31,   1,   31,   31,
  KBCS  = 93,   93,   93,   93,
  KBCE  = 1,   1,
  LBCS  = 71,   71,   71,   71,
  $END
$BCSINP $END
```

77

```
$SCEINP $END


$GRDNAM
    NAME = 'Lower Canard Bod      5, 51x94x33 )', $END
$NITERS $END
$METPRM
    IRRS    = 0,    ILHS  = 2,      IDISS  = 2, $END
$TIMACU
    DT      = 0.04,  ITIME= 1,  CFLMIN=0, CFLMAX=200, TFOSO = 1.00, $END
$SMOACU
    ISPEC  = 2,  DIS2 = 2.00,  DIS4 = 0.02,
    SMOO   = 1.000, EPSE  = 0.060, $END
$VISINP
    VISCJ = .T.,  VISCK = .T.,  VISCL = .T.,
    NTURB =   2,
    ITTYP =   1,      1,
    ITDIR =   3,      1,
    JTLS  =   1,      1,
    JTLE  =  51,     51,
    KTLS  =   1,      1,
    KTLE  =  94,     94,
    LTLS  =   1,      1,
    LTLE  =  33,     33,
    TLPAR1= 0.9,    0.9,
    $END
$BCINP
    NBC    =   4,
    IBTYP =  15,    10,    5,    5,
    IBDIR =  -1,     2,    3,    1,
    JBCS  =  51,     1,    1,    1,
    JBCE  =  51,    51,   51,    1,
    KBCS  =   1,     1,    1,    1,
    KBCE  =  94,     1,   94,   94,
    LBCS  =   1,     1,    1,    1,
    LBCE  =  33,    33,    1,   33,
    $END
$SCEINP $END


$GRDNAM
    NAME = 'Upper Canard Body ( gr_6, 51x94x33 )', $END
$NITERS $END
$METPRM
    IRRS    = 0,    ILHS  = 2,      IDISS  = 2, $END
$TIMACU
    DT      = 0.04,  ITIME= 1,  CFLMIN=0, CFLMAX=200, TFOSO = 1.00, $END
$SMOACU
    ISPEC  = 2,  DIS2 = 2.00,  DIS4 = 0.02,
    SMOO   = 1.000, EPSE  = 0.060, $END
$VISINP
    VISCJ = .T.,  VISCK = .T.,  VISCL = .T.,
    NTURB =   2,
    ITTYP =   1,      1,
    ITDIR =   3,      1,
    JTLS  =   1,      1,
    JTLE  =  51,     51,
    KTLS  =   1,      1,
    KTLE  =  94,     94,
    LTLS  =   1,      1,
    LTLE  =  33,     33,
    TLPAR1= 0.9,    0.9,
    $END
$BCINP
    NBC    =   4,
    IBTYP =  15,    10,    5,    5,
    IBDIR =  -1,     2,    3,    1,
    JBCS  =  51,     1,    1,    1,
    JBCE  =  51,    51,   51,    1,
    KBCS  =   1,     1,    1,    1,
    KBCE  =  94,     1,   94,   94,
    LBCS  =   1,     1,    1,    1,
    LBCE  =  33,    33,    1,   33,
    $END
$SCEINP $END
```

78

APPENDIX H. PMARC INPUT FILE FOR A MISSILE FOREBODY

```
BODY (aoa 0 2, aos = 0.0, with rear flat base)
&BINP2  LSTINP=1,      LSTOUT= 1,    LSTFRQ= 0,    LENRUN= 0,      &END
        LFLITP=1,                                                  &END
&BINP3  LSTGEO=1,      LSTNAB= 1,    LSTNAM=0,     LSTCPV=0,       &END
&BINP4  MAXIT=200,     SOLRES=0.005,                               &END
&BINP5  NTSTPS= 3,     DTSTEP= 0.5,                                &END
&BINP6  RSYM= 1.0,     RGPR=0.0,     RFF=5.0,      RCORES=0.05     &END
        RCOREW=0.05,                                               &END
&BINP7  VINF= 335.19,  VSOUND= 1117.,                              &END
&BINP8  ALDEG= 0.0,    YANDEG=0.0,   PHIDOT=0.0,   THEDOT=0.0,     &END
        PSIDOT=0.0,                                                &END
&BINP8A PHIMAX=0.0,    THEMAX=0.0,   PSIMAX=0.0,                   &END
        WRX=0.0,       WRY=0.0,      WRZ=0.0,                      &END
&BINP8B DXMAX=0.0,     DYMAX=0.0,    DZMAX=0.0,                    &END
        WTX=0.0,       WTY=0.0,      WTZ=0.0,                      &END
&BINP9  CBAR=   1.00,  SREF=  0.7854       SSPAN=   1.00,          &END
&BINP10 RMPX= 0.0,     RMPY=0.00,    RMPZ=0.00,                    &END
        NORSEF=0,      NBCRGE=0,     NC2ONE=0,                     &END
&BINP11 NC2PCH=0,      CZDUB=0.0,    VREF=0.0,                     &END
        NORPCH=0,                                                  &END
        NORP=0,        NORL=0,                                     &END
        NOCF=0,        NOCL=0,                                     &END
        VNORM=0.0,                                                 &END
&BINP12 KPAN=0,        KSIDE=0,      NEWNAB=0,     NEWSID=0,       &END
&BINP13 NBLIT=0,                                                   &END
&ASEM1  ASEMX=-0.00,   ASEMX=0.00,   ASEMY=0.00,                   &END
        ASCAL=1.00,    ATHET=0.00,   NODEA= 5,                     &END
&ASEM2  APXX=-0.00,    APYX=0.00,    APZX=0.00,                    &END
        AHXX=0.00,     AHYY=1.00,    AHZZ=0.00,                    &END
&COMP1  COMPX= 0.0000, COMPY= 0.0000, COMPZ= 0.0000,               &END
        CSCAL= 1.000,  CTHET= 0.0,   NODEC= 5,                     &END
&COMP2  CPXX= 0.0000,  CPYX= 0.0,    CPZX= 0.0000,                 &END
        CHXX= 0.0000,  CHYX= 1.0000, CHZZ= 0.0000,                 &END
&PATCH1 IREV= 0, IDPAT= 1, MAKE=  0, KCOMP= 1, KASS= 1, IPATSYM=0, &END
        IPATCOP=0,
        CAN # 1, PAT # 1
&SECT1  STX= 0.0,  STY= 0.0,  STZ= 0.0,      SCALE=  1.0,          &END
        ALF=  0.0,  THETA=   0.0,                                  &END
        INNODE=  4,  TNODS=  0,  TNPS=  0,   TINTS= 3,
 0.484900E+01   0.353553E+00  -0.105613E+01
 0.473244E+01   0.325298E+00  -0.103334E+01
 0.451795E+01   0.325298E+00  -0.103334E+01
 0.432184E+01   0.325298E+00  -0.103334E+01
 0.418535E+01   0.325298E+00  -0.103334E+01
 0.404892E+01   0.325298E+00  -0.103334E+01
 0.384460E+01   0.325298E+00  -0.103334E+01
 0.331374E+01   0.325298E+00  -0.103334E+01
 0.281328E+01   0.325298E+00  -0.103334E+01
 0.260000E+01   0.325298E+00  -0.103334E+01
 0.281328E+01   0.379712E+00  -0.105613E+01
 0.331374E+01   0.379712E+00  -0.105613E+01
 0.384460E+01   0.379712E+00  -0.105613E+01
 0.404892E+01   0.379712E+00  -0.105613E+01
 0.418535E+01   0.379712E+00  -0.105613E+01
 0.432184E+01   0.379712E+00  -0.105613E+01
 0.451795E+01   0.379712E+00  -0.105613E+01
 0.473244E+01   0.379712E+00  -0.105613E+01
 0.484900E+01   0.353553E+00  -0.105613E+01
&BPNODE TNODE=3,   TNPC= 0,  TINTC= 3,                             &END
&SECT1  STX= 0.0,  STY= 0.0,      STZ= 0.0,                        &END
        ALF=  0.0,  THETA=   0.0,
        INNODE=  4,  TNODS=  3,  TNPS=  0,   TINTS= 3,
 0.506056E+01  -0.105613E+01   0.108334E+01
 0.501798E+01  -0.105613E+01   0.108334E+01
 0.497540E+01  -0.105613E+01   0.108334E+01
 0.493282E+01  -0.102892E+01   0.108334E+01
 0.489023E+01  -0.102892E+01   0.108334E+01
 0.484765E+01  -0.102892E+01   0.108334E+01
 0.480507E+01  -0.102892E+01   0.108334E+01
 0.476249E+01  -0.102892E+01   0.105613E+01
 0.471991E+01  -0.102892E+01   0.105613E+01
 0.467733E+01  -0.102892E+01   0.105613E+01
 0.476249E+01  -0.102892E+01   0.108334E+01
 0.484765E+01  -0.102892E+01   0.108334E+01
 0.480507E+01  -0.102892E+01   0.108334E+01
 0.484765E+01  -0.102892E+01   0.108334E+01
```

```
 0.489023E+01   0.108334E+01  -0.102892E+01
 0.493282E+01   0.108334E+01  -0.102892E+01
 0.497540E+01   0.108334E+01  -0.102892E+01
 0.501798E+01   0.105613E+01  -0.102892E+01
 0.506056E+01   0.105613E+01  -0.105613E+01
&BPNODE TNODE=3,   TNPC= 0,  TINTC= 3,                             &END
        IPATCOP=0,
        TIP # 1, PAT # 1.1
&SECT1  STX= 0.0,  STY= 0.0,     STZ= 0.0,    SCALE=  1.0,         &END
        ALF=  0.0,  THETA=   0.0,
        INNODE=  4,  TNODS=  0,  TNPS=  0,    TINTS= 3,
 0.506056E+01   0.105613E+01  -0.105613E+01
 0.501795E+01   0.102892E+01  -0.108334E+01
 0.497540E+01   0.102892E+01  -0.108334E+01
 0.493282E+01   0.102892E+01  -0.108334E+01
 0.489023E+01   0.102892E+01  -0.108334E+01
 0.484765E+01   0.102892E+01  -0.108334E+01
 0.480507E+01   0.102892E+01  -0.108334E+01
 0.476249E+01   0.102892E+01  -0.108334E+01
 0.471991E+01   0.105613E+01  -0.102892E+01
 0.467733E+01   0.105613E+01  -0.102892E+01
 0.476249E+01   0.108334E+01  -0.102892E+01
 0.484765E+01   0.108334E+01  -0.102892E+01
 0.480507E+01   0.108334E+01  -0.102892E+01
 0.484765E+01   0.108334E+01  -0.102892E+01
 0.489023E+01   0.108334E+01  -0.102892E+01
 0.493282E+01   0.108334E+01  -0.102892E+01
 0.497540E+01   0.108334E+01  -0.102892E+01
 0.501798E+01   0.105613E+01  -0.102892E+01
 0.506056E+01   0.105613E+01  -0.105613E+01
&BPNODE TNODE=3,   STX= 0.0,  STY= 0.0,   TINTC= 3,                &END
&SECT1  STX= 0.0,  STY= 0.0,   STZ= 0.0,    SCALE=  1.0,           &END
        ALF=  0.0,  THETA=   0.0,    TINTS= 3,
        INNODE=  4,  TNODS=  3,  TNPS=  0,
 0.508700E+01  -0.114395E+01
 0.507033E+01  -0.114395E+01
 0.505367E+01  -0.114395E+01
 0.503700E+01  -0.114395E+01
 0.502033E+01  -0.114395E+01
 0.500367E+01  -0.114395E+01
 0.498700E+01  -0.114395E+01
 0.497033E+01  -0.114395E+01
 0.495367E+01  -0.114395E+01
 0.493700E+01  -0.114395E+01
 0.497033E+01  -0.114395E+01
 0.498700E+01  -0.114395E+01
 0.500367E+01  -0.114395E+01
 0.502033E+01  -0.114395E+01
 0.503700E+01  -0.114395E+01
 0.505367E+01  -0.114395E+01
 0.507033E+01  -0.114395E+01
 0.508700E+01  -0.114395E+01
&BPNODE TNODE=3,   TNPC= 0,  TINTC= 3,                             &END
&PATCH1 IREV= 0, IDPAT= 1, MAKE=  0, KCOMP= 1, KASS= 1, IPATSYM=0, &END
        IPATCOP=0,
        CAN # 2, PAT # 2
&SECT1  STX= 0.0,  STY= 0.0,     STZ= 0.0,    SCALE=  1.0,         &END
        ALF=  0.0,  THETA=   0.0,    TINTS= 3,
        INNODE=  4,  TNODS=  0,  TNPS=  0,
 0.484900E+01   0.353553E+00
 0.473244E+01   0.379712E+00
 0.451795E+01   0.379712E+00
 0.432184E+01   0.379712E+00
 0.418535E+01   0.325298E+00
 0.404892E+01   0.325298E+00
 0.384460E+01   0.325298E+00
 0.331374E+01   0.325298E+00
 0.281328E+01   0.325298E+00
 0.260000E+01   0.325298E+00
 0.281328E+01   0.325298E+00
 0.331374E+01   0.379712E+00
 0.384460E+01   0.379712E+00
 0.404892E+01   0.379712E+00
 0.418535E+01   0.325298E+00
```

```
0.432181E+01   0.325298E+00   0.379712E+00
0.451795E+01   0.325298E+00   0.379712E+00
0.473244E+01   0.325298E+00   0.379712E+00
0.484900E+01   0.353553E+00   0.353553E+00
&BPNODE  TNODE=3,  TNPC= 0,   TINTC= 3,
&SECT1   STX= 0.0, STY= 0.0,    SCALE=  1.0,
         ALF=  0.0,  THETA=           TINTS= 3,
         INNODE=   4,  TNODE=  3,  STY= 0.0,
0.506056E+01   0.105613E+01   TNPS= 8,
0.501798E+01   0.108334E+01
0.497540E+01   0.108334E+01
0.493282E+01   0.102892E+01
0.489023E+01   0.102892E+01
0.484765E+01   0.102892E+01
0.480507E+01   0.102892E+01
0.476249E+01   0.102892E+01
0.471991E+01   0.102892E+01
0.467733E+01   0.105613E+01
0.476249E+01   0.108334E+01
0.480507E+01   0.108334E+01
0.489023E+01   0.108334E+01
0.493282E+01   0.108334E+01
0.497540E+01   0.108334E+01
0.501798E+01   0.105613E+01
0.506056E+01   0.105613E+01
&BPNODE  TNODE=3,  TNPC= 0,   TINTC= 3,                 &END
&PATCH1  IREV= 0,  IDPAT= 1, MAKE=   0, KCOMP= 1, KASS= 1, IPATSYM=0,
         IPATCOP=0,                                     &END
         TIP # 2, PAT # 2.1
&SECT1   STX= 0.0, STY= 0.0,    SCALE=  1.0,
         ALF=  0.0,  THETA=           TINTS= 3,
         INNODE=   4,  TNODE=  STY= 0.0,
0.506056E+01   0.105613E+01   TNPS= 0,
0.501798E+01   0.108334E+01
0.497540E+01   0.108334E+01
0.493282E+01   0.102892E+01
0.489023E+01   0.102892E+01
0.484765E+01   0.108334E+01
0.476249E+01   0.108334E+01
0.471991E+01   0.108334E+01
0.476249E+01   0.102892E+01
0.480507E+01   0.102892E+01
0.489023E+01   0.102892E+01
0.493282E+01   0.102892E+01
0.497540E+01   0.102892E+01
0.501798E+01   0.108334E+01
0.506056E+01   0.105613E+01
&BPNODE  TNODE=3,  TNPC= 0,   TINTC= 3,                 &END
&SECT1   STX= 0.0, STY= 0.0,    SCALE=  1.0,
         ALF=  0.0,  THETA=           TINTS= 3,
         INNODE=   4,  TNODE=  3,
0.508700E+01   0.114395E+01   TNPS= 0,
0.507033E+01   0.114395E+01
0.505367E+01   0.114395E+01
0.503700E+01   0.114395E+01
0.502033E+01   0.114395E+01
0.500367E+01   0.114395E+01
0.498700E+01   0.114395E+01
0.497033E+01   0.114395E+01
0.495367E+01   0.114395E+01
0.493700E+01   0.114395E+01
0.497033E+01   0.114395E+01
0.498700E+01   0.114395E+01
0.502033E+01   0.114395E+01
0.503700E+01   0.114395E+01
0.505367E+01   0.114395E+01
0.507033E+01   0.114395E+01
0.508700E+01   0.114395E+01
```

```
&BPNODE  TNODE=3,   TNPC= 0,   TINTC= 3,                &END
&PATCH1  IREV= -1,  IDPAT= 1, MAKE=   0, KCOMP= 1, KASS= 1, IPATSYM=0,
         IPATCOP=0,                                     &END
         CAM # 3, PAT # 3
&SECT1   STX= 0.0, STY= 0.0,    SCALE=  1.0,
         ALF=  0.0,  THETA=           TINTS= 3,
         INNODE=   4,  TNODE=  4,  TNPS= 0,
0.484900E+01  -0.353553E+00   0.353553E+00
0.473244E+01  -0.379712E+00   0.325298E+00
0.451795E+01  -0.379712E+00   0.325298E+00
0.432181E+01  -0.379712E+00   0.325298E+00
0.418535E+01  -0.379712E+00   0.325298E+00
0.404892E+01  -0.379712E+00   0.325298E+00
0.384460E+01  -0.379712E+00   0.325298E+00
0.331137E+01  -0.353530E+00   0.353530E+00
0.281132E+01  -0.379712E+00   0.325298E+00
0.260008E+01  -0.379712E+00   0.325298E+00
0.331137E+01  -0.325298E+00   0.379712E+00
0.384460E+01  -0.325298E+00   0.379712E+00
0.404892E+01  -0.325298E+00   0.379712E+00
0.418535E+01  -0.325298E+00   0.379712E+00
0.432181E+01  -0.325298E+00   0.379712E+00
0.451795E+01  -0.325298E+00   0.379712E+00
0.473244E+01  -0.353553E+00   0.353553E+00
0.484900E+01  -0.353553E+00   0.353553E+00
&BPNODE  TNODE=3,  STX= 0.0,   SCALE=  1.0,             &END
&SECT1   ALF=  0.0,  THETA=           TINTS= 3,
         INNODE=   4,  TNPS= 0,
0.506056E+01  -0.105613E+01   0.102892E+01
0.501798E+01  -0.108334E+01   0.102892E+01
0.497540E+01  -0.108334E+01   0.102892E+01
0.493282E+01  -0.102892E+01   0.102892E+01
0.489023E+01  -0.102892E+01   0.102892E+01
0.484765E+01  -0.108334E+01   0.105613E+01
0.476249E+01  -0.108334E+01   0.108334E+01
0.471991E+01  -0.108334E+01   0.102892E+01
0.476249E+01  -0.102892E+01   0.102892E+01
0.480507E+01  -0.102892E+01   0.102892E+01
0.489023E+01  -0.102892E+01   0.102892E+01
0.493282E+01  -0.102892E+01   0.102892E+01
0.497540E+01  -0.102892E+01   0.105613E+01
0.501798E+01  -0.105613E+01   0.105613E+01
0.506056E+01  -0.105613E+01   0.105613E+01
&BPNODE  TNODE=3,  TNPC= 0,   TINTC= 3,                 &END
&PATCH1  IREV= -1,  IDPAT= 1, MAKE=   0, KCOMP= 1, KASS= 1, IPATSYM=0,
         IPATCOP=0,                                     &END
         TIP # 3, PAT # 3.1
&SECT1   STX= 0.0, STY= 0.0,    SCALE=  1.0,
         ALF=  0.0,  THETA=           TINTS= 3,
         INNODE=   4,  TNPS= 0,
0.506056E+01   0.105613E+01   0.102892E+01
0.501798E+01  -0.108334E+01   0.102892E+01
0.497540E+01  -0.108334E+01   0.102892E+01
0.493282E+01  -0.102892E+01   0.102892E+01
0.489023E+01  -0.102892E+01   0.102892E+01
0.484765E+01  -0.108334E+01   0.102892E+01
0.476249E+01  -0.108334E+01   0.105613E+01
0.467733E+01  -0.108334E+01   0.108334E+01
0.471991E+01  -0.102892E+01   0.108334E+01
0.476249E+01  -0.102892E+01   0.108334E+01
0.484765E+01  -0.102892E+01   0.108334E+01
0.489023E+01  -0.102892E+01   0.108334E+01
0.493282E+01  -0.102892E+01   0.108334E+01
0.497540E+01  -0.102892E+01   0.108334E+01
0.501798E+01  -0.105613E+01   0.105613E+01
0.506056E+01  -0.105613E+01   0.105613E+01
&BPNODE  TNODE=3,  TNPC= 0,   TINTC= 3,                 &END
```

```
&SECT1  STX= 0.0,  STY= 0.0,  SCALE= 1.0,
        ALF=  0.0,  THETA=          TNPS= 0,
        INMODE=   4,   TNODS=  3,              TINTS= 3,
         0.508700E+01   -0.114395E+01
         0.507033E+01   -0.114395E+01
         0.505367E+01   -0.114395E+01
         0.503700E+01   -0.114395E+01
         0.502033E+01   -0.114395E+01
         0.500367E+01   -0.114395E+01
         0.498700E+01   -0.114395E+01
         0.497033E+01   -0.114395E+01
         0.495367E+01   -0.114395E+01
         0.493700E+01   -0.114395E+01
         0.497033E+01   -0.114395E+01
         0.498700E+01   -0.114395E+01
         0.500367E+01   -0.114395E+01
         0.502033E+01   -0.114395E+01
         0.503700E+01   -0.114395E+01
         0.505367E+01   -0.114395E+01
         0.507033E+01   -0.114395E+01
         0.508700E+01   -0.114395E+01                  &END
&BPNODE  TNODE=3,   TNPC= 0,   TINTC= 3,
&PATCH1  IREV= -1,  IDPAT= 1,  MAKE=  0, KCOMP= 1, KASS= 1, IPATSYM=0,  &END
         IPATCOP=0,                                    &END
                 CAN # 4, PAT # 4
&SECT1  ALF=  0.0,  STX= 0.0,  STY= 0.0,  SCALE= 1.0,
        INMODE=   4,   TNODS= 0             TNPS= 0,   TINTS= 3,
         0.484900E+01   -0.353553E+00
         0.473244E+01   -0.325529E+00
         0.451795E+01   -0.379712E+00
         0.432184E+01   -0.379712E+00
         0.418535E+01   -0.379712E+00
         0.404892E+01   -0.379712E+00
         0.384460E+01   -0.379712E+00
         0.331374E+01   -0.325529E+00
         0.281328E+01   -0.325529E+00
         0.260000E+01   -0.325529E+00
         0.331374E+01   -0.325529E+00
         0.384460E+01   -0.325529E+00
         0.404892E+01   -0.325529E+00
         0.418535E+01   -0.379712E+00
         0.432184E+01   -0.379712E+00
         0.451795E+01   -0.379712E+00
         0.473244E+01   -0.379712E+00
         0.484900E+01   -0.353553E+00                  &END
&BPNODE  TNODE=3,   TNPC= 0,   TINTC= 3,
&SECT1  STX= 0.0,  STY= 0.0,  SCALE= 1.0,
        ALF=  0.0,  THETA=          TNPS= 0,
        INMODE=   4,   TNODS=  3,              TINTS= 3,
         0.506056E+01   -0.105613E+01
         0.501798E+01   -0.108334E+01
         0.497540E+01   -0.108334E+01
         0.493282E+01   -0.102892E+01
         0.489023E+01   -0.102892E+01
         0.484765E+01   -0.102892E+01
         0.480507E+01   -0.108334E+01
         0.476249E+01   -0.108334E+01
         0.471991E+01   -0.102892E+01
         0.471991E+01   -0.102892E+01
         0.476249E+01   -0.102892E+01
         0.480507E+01   -0.108334E+01
         0.484765E+01   -0.108334E+01
         0.489023E+01   -0.102892E+01
         0.493282E+01   -0.102892E+01
         0.497540E+01   -0.102892E+01
         0.501798E+01   -0.108334E+01
         0.506056E+01   -0.105613E+01                  &END
&BPNODE  TNODE=3,   TNPC= 0,   TINTC= 3,
&PATCH1  IREV= -1,  IDPAT= 1,  MAKE=  0, KCOMP= 1, KASS= 1, IPATSYM=0,  &END
         IPATCOP=0,                                    &END
         TIP # 4, PAT # 4.1
&SECT1  STX= 0.0,  STY= 0.0,  SCALE= 1.0,
```

```
&SECT1  ALF=  0.0,  THETA= 0.0,  TNPS= 0,   TINTS= 3,
        INMODE=   4,   TNODS= 0
         0.506056E+01   -0.105613E+01
         0.501798E+01   -0.108334E+01
         0.497540E+01   -0.108334E+01
         0.493282E+01   -0.102892E+01
         0.489023E+01   -0.102892E+01
         0.484765E+01   -0.108334E+01
         0.480507E+01   -0.108334E+01
         0.476249E+01   -0.105613E+01
         0.471991E+01   -0.102892E+01
         0.471991E+01   -0.102892E+01
         0.476249E+01   -0.102892E+01
         0.480507E+01   -0.108334E+01
         0.484765E+01   -0.108334E+01
         0.489023E+01   -0.102892E+01
         0.493282E+01   -0.102892E+01
         0.497540E+01   -0.108334E+01
         0.501798E+01   -0.108334E+01
         0.506056E+01   -0.105613E+01                  &END
&BPNODE  TNODE=3,   TNPC= 0,   TINTC= 3,
&SECT1  STX= 0.0,   STY= 0.0,  SCALE= 1.0,
        ALF=  0.0,  THETA= 0.0,  TNPS= 0,   TINTS= 3,
        INMODE=   4,   TNODS=  3,
         0.508700E+01   -0.114395E+01
         0.505367E+01   -0.114395E+01
         0.503700E+01   -0.114395E+01
         0.502033E+01   -0.114395E+01
         0.500367E+01   -0.114395E+01
         0.498700E+01   -0.114395E+01
         0.497033E+01   -0.114395E+01
         0.495367E+01   -0.114395E+01
         0.493700E+01   -0.114395E+01
         0.497033E+01   -0.114395E+01
         0.498700E+01   -0.114395E+01
         0.500367E+01   -0.114395E+01
         0.502033E+01   -0.114395E+01
         0.503700E+01   -0.114395E+01
         0.505367E+01   -0.114395E+01
         0.507033E+01   -0.114395E+01
         0.508700E+01   -0.114395E+01                  &END
&BPNODE  TNODE=3,   TNPC= 0,   TINTC= 3,
&PATCH1  IREV=  0,  IDPAT= 2,  MAKE=  0, KCOMP= 1, KASS= 1, IPATSYM=0,  &END
         IPATCOP=0,
                 FOREBODY, PAT # 5
&SECT1  STX=  0.000000E+00, STY= 0.0,  STZ= 0.0,  SCALE=  0.0,
        ALF=  0.0,  TNODS=  4,  TNPS= 0,   TINTS= 3,
        INMODE=   4,
         0.000000E+00    0.192463E-02    0.391768E-01
         0.000000E+00    0.575536E-02    0.387995E-01
         0.000000E+00    0.953065E-02    0.380465E-01
         0.000000E+00    0.132142E-01    0.366311E-01
         0.000000E+00    0.167704E-01    0.354581E-01
         0.000000E+00    0.201652E-01    0.336435E-01
         0.000000E+00    0.233657E-01    0.315050E-01
         0.000000E+00    0.263412E-01    0.290631E-01
         0.000000E+00    0.290631E-01    0.263412E-01
         0.000000E+00    0.315050E-01    0.233657E-01
         0.000000E+00    0.336435E-01    0.201652E-01
         0.000000E+00    0.354581E-01    0.167704E-01
         0.000000E+00    0.369311E-01    0.132142E-01
         0.000000E+00    0.380465E-01    0.953066E-02
         0.000000E+00    0.387995E-01    0.575536E-02
         0.000000E+00    0.391768E-01    0.192463E-02
         0.000000E+00    0.380465E-01    0.953066E-02
         0.000000E+00    0.369311E-01    0.132142E-01
         0.000000E+00    0.354581E-01    0.167704E-01
         0.000000E+00    0.336435E-01    0.201652E-01
         0.000000E+00    0.315050E-01    0.233657E-01
         0.000000E+00    0.290631E-01    0.263412E-01
         0.000000E+00    0.263412E-01    0.290631E-01
         0.000000E+00    0.233657E-01    0.315050E-01
         0.000000E+00    0.201652E-01    0.336435E-01
         0.000000E+00    0.167704E-01    0.354581E-01
         0.000000E+00    0.132142E-01    0.369311E-01
         0.000000E+00    0.953066E-02    0.380465E-01
         0.000000E+00    0.575536E-02    0.387995E-01
         0.000000E+00    0.192463E-02    0.391768E-01
         0.000000E+00    0.263412E-01    0.290631E-01         &END
```

```
0.000000E+00    0.233657E-01    0.115050E-01
0.000000E+00    0.201652E-01    0.336435E-01
0.000000E+00    0.167704E-01    0.354581E-01
0.000000E+00    0.132142E-01    0.369311E-01
0.000000E+00    0.953066E-02    0.380485E-01
0.000000E+00    0.575536E-02    0.387995E-01
0.000000E+00    0.192463E-02    0.391768E-01
0.000000E+00   -0.192464E-02    0.391768E-01
0.000000E+00   -0.575535E-02    0.387995E-01
0.000000E+00   -0.953066E-02    0.380485E-01
0.000000E+00   -0.132142E-01    0.369311E-01
0.000000E+00   -0.167704E-01    0.354581E-01
0.000000E+00   -0.201652E-01    0.336435E-01
0.000000E+00   -0.233657E-01    0.315050E-01
0.000000E+00   -0.290631E-01    0.201652E-01
0.000000E+00   -0.336435E-01    0.192464E-01
0.000000E+00   -0.354581E-01    0.575535E-02
0.000000E+00   -0.369311E-01   -0.953066E-02
0.000000E+00   -0.380485E-01   -0.192464E-01
0.000000E+00   -0.387995E-01   -0.167704E-01
0.000000E+00   -0.391768E-01   -0.233657E-01
0.000000E+00   -0.391768E-01   -0.290631E-01
0.000000E+00   -0.387995E-01   -0.336435E-01
0.000000E+00   -0.380485E-01   -0.369311E-01
0.000000E+00   -0.369311E-01   -0.387995E-01
0.000000E+00   -0.354581E-01   -0.391768E-01
0.000000E+00   -0.336435E-01
0.000000E+00   -0.315050E-01
0.000000E+00   -0.290631E-01
0.000000E+00   -0.263412E-01
0.000000E+00   -0.233657E-01
0.000000E+00   -0.201652E-01
0.000000E+00   -0.132142E-01
0.000000E+00   -0.575537E-02
0.000000E+00    0.192463E-02
&BPNODE  TNODE=3,  TNPC= 0,
&SECT1   ALF= 0.0,  THETA=
         INNODE= 4,  TNODE=
0.000000E+00   -0.192463E-02
0.000000E+00    0.575536E-02
0.000000E+00    0.953065E-02
0.000000E+00    0.132142E-01
0.000000E+00    0.167704E-01
0.000000E+00    0.201652E-01
0.000000E+00    0.233657E-01
0.000000E+00    0.263412E-01
0.000000E+00    0.290631E-01
0.000000E+00    0.315050E-01
0.000000E+00    0.336435E-01
0.000000E+00    0.354581E-01
0.000000E+00    0.369311E-01
0.000000E+00    0.380485E-01
0.000000E+00    0.387995E-01
0.000000E+00    0.391768E-01
```

   THETA= 0.26720E-02,   STY= 0.0,   STZ= 0.0,   SCALE= 1.0,   &END

   TNPS= 0,   TINTS= 3,   &END

```
0.000000E+00   -0.192463E-02    0.391768E-01
0.000000E+00   -0.575536E-02    0.387995E-01
0.000000E+00   -0.953066E-02    0.380485E-01
0.000000E+00   -0.132142E-01    0.369311E-01
0.000000E+00   -0.167704E-01    0.354581E-01
0.000000E+00   -0.201652E-01    0.336435E-01
0.000000E+00   -0.233657E-01    0.315050E-01
0.000000E+00   -0.263412E-01    0.290631E-01
0.000000E+00   -0.290631E-01    0.263412E-01
0.000000E+00   -0.315050E-01    0.233657E-01
0.000000E+00   -0.336435E-01    0.201652E-01
0.000000E+00   -0.354581E-01    0.167704E-01
0.000000E+00   -0.369311E-01    0.132142E-01
0.000000E+00   -0.380485E-01    0.953066E-02
0.000000E+00   -0.387995E-01    0.575535E-02
0.000000E+00   -0.391768E-01    0.192464E-02
0.000000E+00   -0.391768E-01   -0.192464E-02
0.000000E+00   -0.387995E-01   -0.575535E-02
0.000000E+00   -0.380485E-01   -0.132142E-01
0.000000E+00   -0.354581E-01   -0.201652E-01
0.000000E+00   -0.315050E-01   -0.263412E-01
0.000000E+00   -0.290631E-01   -0.290631E-01
0.000000E+00   -0.263412E-01   -0.315050E-01
0.000000E+00   -0.201652E-01   -0.336435E-01
0.000000E+00   -0.132142E-01   -0.354581E-01
0.000000E+00   -0.575537E-02   -0.380485E-01
0.000000E+00    0.192463E-02   -0.387995E-01
                                -0.391768E-01
&BPNODE  TNODE=3,  TNPC= 3,
&SECT1   ALF= 0.0,  STY= 0.0,
         INNODE= 4,  THETA=
0.000000E+00    0.400059E-01   -0.814338E-01
0.000000E+00   -0.119632E-01   -0.806495E-01
0.000000E+00    0.198107E-01   -0.790886E-01
0.000000E+00    0.274673E-01   -0.767660E-01
0.000000E+00    0.348594E-01   -0.737041E-01
0.000000E+00    0.419158E-01   -0.699323E-01
0.000000E+00    0.485666E-01   -0.654871E-01
0.000000E+00    0.547535E-01   -0.604112E-01
0.000000E+00    0.604112E-01   -0.547535E-01
0.000000E+00    0.654871E-01   -0.485666E-01
0.000000E+00    0.699323E-01   -0.419158E-01
0.000000E+00    0.737041E-01   -0.348594E-01
0.000000E+00    0.767660E-01   -0.274673E-01
0.000000E+00    0.790886E-01   -0.198107E-01
0.000000E+00    0.806495E-01   -0.119632E-01
0.000000E+00    0.814338E-01   -0.400058E-02
0.000000E+00    0.806495E-01    0.119632E-01
0.000000E+00    0.790886E-01    0.198107E-01
0.000000E+00    0.767660E-01    0.274673E-01
0.000000E+00    0.737041E-01    0.348594E-01
0.000000E+00    0.699323E-01    0.419158E-01
0.000000E+00    0.654871E-01    0.547535E-01
0.000000E+00    0.604112E-01    0.604112E-01
0.000000E+00    0.547535E-01    0.654871E-01
0.000000E+00    0.485666E-01    0.699323E-01
0.000000E+00    0.419158E-01    0.737041E-01
0.000000E+00    0.348594E-01    0.767660E-01
0.000000E+00    0.274673E-01    0.790886E-01
0.000000E+00    0.198107E-01    0.806495E-01
0.000000E+00    0.119632E-01    0.814338E-01
0.000000E+00   -0.400059E-02    0.814338E-01
0.000000E+00   -0.119632E-01    0.806495E-01
0.000000E+00   -0.198107E-01    0.790886E-01
0.000000E+00   -0.274673E-01    0.767660E-01
0.000000E+00   -0.348594E-01    0.737041E-01
0.000000E+00   -0.419158E-01    0.654871E-01
```

   STZ= 0.0,   SCALE= 1.0,   &END

   TNPS= 0,   TINTS= 3,   &END

&BPNODE TNODE=3, TNPC= 0, STR= 0.0, STR= 0.0,
&SECT1 STX= .28994OE-01, TNPC= 0, STR= 0.0,
ALF= 0.0, THETA= 0.0, TNPS= 0,
INMODE= 4, TNODS= 3, TINTS= 3,

SCALE= 1.0, &END
&END

&BPNODE TNODE=3, TNPC= 0, STR= 0.0, STR= 0.0,
&SECT1 STX= .597930E-01, TNPC= 0, STR= 0.0,
ALF= 0.0, THETA= 0.0, TNPS= 0,
INMODE= 4, TNODS= 3, TINTS= 3,

SCALE= 1.0, &END
&END

&BPNODE   TNODE=3,   TNPC= 0,   STY= 0.0,   STX= 0.0,   TINTS= 3,
&SECT1   STX= 0.106384E+00,   THETA=   0.0,   TNPS= 0,
ALF=   0.0,   INMODE=   4,   TNODE=   0,

&BPNODE   TNODE=3,   TNPC= 0,   STY= 0.17620E+00,   STX= 0.0,   TINTC= 3,   SCALE=   1.0,
&SECT1   ALF=   0.0,   THETA=   0.0,   INMODE=   4,   TNODE=   0,   TNPS= 0,   TINTS= 3,

&BPNODE   TNODE=3,   TNPC= 0,   STY= 0.27552E+00,   STX= 0.0,   TINTC= 3,   SCALE=   1.0,
&SECT1   STX= 0.0,   TNPS= 0,   TINTS= 3,

```
ALF=  0.0,    THETA=  0.0,    TNPB=  0,    TINTB=  3,
  INMODE=  4,   TNODE=  0,
```

(numerical data columns — three columns of values in the form 0.000000E+00 and associated exponential values)

```
&BPNODE  TNODE=3,  TNPC=  0,    TINTC=  3,
&SECT1   STX=  0.41135E+00,  STY=  0.0,    STZ=  0.0,    SCALE=  1.0,    &END
  INMODE=  4,   THETA=  0.0,    TNPB=  0,    TINTB=  3,
```

(numerical data columns)

```
&END
```

(numerical data columns — three columns of values in the form 0.000000E+00 and associated exponential values)

```
&BPNODE  TNODE=3,  TNPC=  3,    TINTC=  3,
&SECT1   STX=  0.613692E+00,  STY=  0.0,    STZ=  0.0,    SCALE=  1.0,    &END
  INMODE=  4,   THETA=  0.0,    TNPB=  0,    TINTB=  3,
```

(numerical data columns)

```
&END
```

```
0.000000E+00   0.351058E+00  -0.125611E+00
...
(numeric data columns)
...
&BPMODE  TMODE=3,  TNPC= 0,  TINTC= 3,
&SECT1   STX=  0.835588E+00,  STY= 0.0,  STZ= 0.0,  SCALE=  1.0,  &END
         ALF=  0.0,  THETA=  0.0,
         INMODE=  4,  TNPS=  0,  TINTS= 3,  &END
```

```
0.000000E+00   0.388299E+00   0.138936E+00
...
(numeric data columns)
...
&BPMODE  TMODE=3,  TNPC= 0,  TINTC= 3,
&SECT1   STX=  0.933313E+00,  STY= 0.0,  STZ= 0.0,  SCALE=  1.0,  &END
         ALF=  0.0,  THETA=  0.0,
         INMODE=  4,  TNPS=  0,  TINTS= 3,  &END
```

86

&BPMODE TMODE=3, TNPC=3, STX= 0.0, STY= 0.0, SCALE= 1.0, &END
&SECT1 ALF= 0.0, THETA= 0.0, TNODE= 4, TNPS= 0, TINTS= 3, &END

&BPMODE TMODE=3, TNPC= 0.1291618E+01, STX= 0.0, STY= 0.0, SCALE= 1.0, &END
&SECT1 ALF= 0.0, THETA= 0.0, TNODE= 4, TNPS= 0, TINTS= 3, &END

&PNODE TNODE=3, TNPC= 0, TINTC= 1,
&SECT1 STX= 0.14653E+01, STY= 0.0, STZ= 0.0, SCALE= 1.0, &END
ALF= 0.0, THETA= 0.0, TNPS= 0, TINTS= 3,
INMODE= 4, TNODS= 0, &END

&PNODE TNODE=3, TNPC= 0, TINTC= 1,
&SECT1 STX= 0.17637E+01, STY= 0.0, STZ= 0.0, SCALE= 1.0, &END
ALF= 0.0, THETA= 0.0, TNPS= 0, TINTS= 3,
INMODE= 4, TNODS= 0, &END

&BPNODE   TNODE= 3,   TNPC= 0,   STX= 0.0,   TINTC= 3,
&SECT1   STX= 0.195193E+01,   STY= 0.0,   TINTS= 3,
    ALF=   0.0,   TNODS= 0,   TNPS= 0,
    INNODE= 4,   THETA=   0.0,

SCALE=   1.0,   &END

&END

[Columns of numerical data in scientific notation, e.g. 0.000000E+00, -0.393225E+00, -0.291635E+00, etc.]

&BPNODE   TNODE= 3,   TNPC= 0,   STX= 0.214924E+01,   STY= 0.0,   STZ= 0.0,   TINTC= 3,
&SECT1   STX= 0.0,   TNODS= 4,   TNPS= 0,
    ALF=   0.0,   THETA=   0.0,
    INNODE= 4,   TINTS= 3,

SCALE=   1.0,   &END

&END

&BPNODE   TNODE= 3,   TNPC= 0,   STX= 0.235533E+01,   STY= 0.0,   STZ= 0.0,   TINTC= 3,
&SECT1   STX= 0.0,   THETA=   0.0,
    ALF=   0.0,

SCALE=   1.0,   &END

[Columns of numerical data in scientific notation, e.g. 0.000000E+00, -0.120504E+00, -0.481079E+00, etc.]

INWODE= 4, TNODE= 0, TNPS= 0, TINTS= 3,

&END

&BPNODE   TNODE=3,   TNPC= 0,   TINTC= 3,
&SECT1   IREV= 0, IDPAT= 2, MAKE= 0, KCOMP= 1, KAS= 1, IPATSYM=0,
&PATCH1   IPATCON=0,
   MID # 1,   PAT # 6
&SECT1   STX= 0.260000E+01, STY= 0.0,   STZ= 0.0,   SCALE= 1.0,
   ALP=   0.0,   THETA=   0.0,
   INWODE= 4,   TNODE= 0,   TNPS= 0,   TINTS= 3,

&END

&BPNODE   TNODE=3,   TNPC= 0,   TINTC= 3,
&SECT1   STX= 0.281328E+01, STY= 0.0,   STZ= 0.0,   SCALE= 1.0,

&END

INWODE= 4, TNODE= 0, TNPS= 0, TINTS= 3,

&END

&BPNODE   TNODE=3,   TNPC= 0,   TINTC= 3,
&SECT1   STX= 0.260000E+01, STY= 0.0,   STZ= 0.0,   SCALE= 1.0,
   ALP=   0.0,   THETA=   0.0,
   INWODE= 4,   TNODE= 0,   TNPS= 0,   TINTS= 3,

&END

ALF= 0.0,   THETA= 0.0,   TNPS= 0,   TINTS= 3,
INMODE= 4,   TNODE= 4,
0.000000E+00   0.245338E-01   -0.499398E+00
0.000000E+00   0.733652E-01   -0.494588E+00
0.000000E+00   0.121490E+00   -0.485016E+00
0.000000E+00   0.166445E+00   -0.470772E+00
0.000000E+00   0.213778E+00   -0.451995E+00
0.000000E+00   0.257051E+00   -0.428864E+00
0.000000E+00   0.297850E+00   -0.401604E+00
0.000000E+00   0.325298E+00   -0.379712E+00
&BPNODE TNODE=3,   TNPC= 0,   STY= 0.0,   SCALE= 1.0,
&SECT1   STX= 0.331374E+01, STY= 0.0,   TINTS= 3,   &END
ALF= 0.0,   THETA= 0.0,   TNPS= 0,   TINTS= 3,
INMODE= 4,   TNODE= 4,
0.000000E+00   0.245338E-01   -0.499398E+00
0.000000E+00   0.733652E-01   -0.494588E+00
0.000000E+00   0.121490E+00   -0.485016E+00
0.000000E+00   0.166445E+00   -0.470772E+00
0.000000E+00   0.213778E+00   -0.451995E+00
0.000000E+00   0.257051E+00   -0.428864E+00
0.000000E+00   0.297850E+00   -0.401604E+00
0.000000E+00   0.325298E+00   -0.379712E+00
&BPNODE TNODE=3,   TNPC= 0,   STY= 0.0,   SCALE= 1.0,
&SECT1   STX= 0.384460E+01, STY= 0.0,   TINTS= 3,   &END
ALF= 0.0,   THETA= 0.0,   TNPS= 0,   TINTS= 3,
INMODE= 4,   TNODE= 4,
0.000000E+00   0.245338E-01   -0.499398E+00
0.000000E+00   0.733652E-01   -0.494588E+00
0.000000E+00   0.121490E+00   -0.485016E+00
0.000000E+00   0.166445E+00   -0.470772E+00
0.000000E+00   0.213778E+00   -0.451995E+00
0.000000E+00   0.257051E+00   -0.428864E+00
0.000000E+00   0.297850E+00   -0.401604E+00
0.000000E+00   0.325298E+00   -0.379712E+00
&BPNODE TNODE=3,   TNPC= 0,   STY= 0.0,   SCALE= 1.0,
&SECT1   STX= 0.404892E+01, STY= 0.0,   TINTS= 3,   &END
ALF= 0.0,   THETA= 0.0,   TNPS= 0,   TINTS= 3,
INMODE= 4,   TNODE= 4,
0.000000E+00   0.245338E-01   -0.499398E+00
0.000000E+00   0.733652E-01   -0.494588E+00
0.000000E+00   0.121490E+00   -0.485016E+00
0.000000E+00   0.166445E+00   -0.470772E+00
0.000000E+00   0.213778E+00   -0.451995E+00
0.000000E+00   0.257051E+00   -0.428864E+00
0.000000E+00   0.297850E+00   -0.401604E+00
0.000000E+00   0.325298E+00   -0.379712E+00
&BPNODE TNODE=3,   TNPC= 0,   STY= 0.0,   SCALE= 1.0,
&SECT1   STX= 0.418635E+01, STY= 0.0,   TINTS= 3,   &END
ALF= 0.0,   THETA= 0.0,   TNPS= 0,   TINTS= 3,
INMODE= 4,   TNODE= 4,
0.000000E+00   0.245338E-01   -0.499398E+00
0.000000E+00   0.733652E-01   -0.494588E+00
0.000000E+00   0.121490E+00   -0.485016E+00
0.000000E+00   0.166445E+00   -0.470772E+00
0.000000E+00   0.213778E+00   -0.451995E+00
0.000000E+00   0.257051E+00   -0.428864E+00
0.000000E+00   0.297850E+00   -0.401604E+00
0.000000E+00   0.325298E+00   -0.379712E+00
&BPNODE TNODE=3,   TNPC= 0,   STY= 0.0,   SCALE= 1.0,
&SECT1   STX= 0.432184E+01, STY= 0.0,   TINTS= 3,   &END
ALF= 0.0,   THETA= 0.0,   TNPS= 0,   TINTS= 3,
INMODE= 4,   TNODE= 4,
0.000000E+00   0.245338E-01   -0.499398E+00
0.000000E+00   0.733652E-01   -0.494588E+00
0.000000E+00   0.121490E+00   -0.485016E+00
0.000000E+00   0.166445E+00   -0.470772E+00
0.000000E+00   0.213778E+00   -0.451995E+00
0.000000E+00   0.257051E+00   -0.428864E+00
0.000000E+00   0.297850E+00   -0.401604E+00
0.000000E+00   0.325298E+00   -0.379712E+00
&BPNODE TNODE=3,   TNPC= 0,   STY= 0.0,   SCALE= 1.0,
&SECT1   STX= 0.451795E+01, STY= 0.0,   TINTS= 3,   &END
ALF= 0.0,   THETA= 0.0,   TNPS= 0,   TINTS= 3,
INMODE= 4,   TNODE= 4,
0.000000E+00   0.245338E-01   -0.499398E+00
0.000000E+00   0.733652E-01   -0.494588E+00

0.000000E+00   0.121490E+00   -0.485016E+00
0.000000E+00   0.166445E+00   -0.470772E+00
0.000000E+00   0.257051E+00   -0.451995E+00
0.000000E+00   0.213778E+00   -0.428864E+00
0.000000E+00   0.297850E+00   -0.401604E+00
0.000000E+00   0.325298E+00   -0.379712E+00
&BPNODE TNODE=3,   TNPC= 0,   STY= 0.0,   STZ= 0.0,   SCALE= 1.0,   &END
&SECT1   STX= 0.473244E+01, STY= 0.0,   TNPS= 0,   TINTS= 3,
ALF= 0.0,   THETA= 0.0,
INMODE= 4,   TNODE= 0,
0.000000E+00   0.245338E-01   -0.499398E+00
0.000000E+00   0.733652E-01   -0.494588E+00
0.000000E+00   0.121490E+00   -0.485016E+00
0.000000E+00   0.166445E+00   -0.470772E+00
0.000000E+00   0.213778E+00   -0.451995E+00
0.000000E+00   0.297850E+00   -0.401604E+00
0.000000E+00   0.325298E+00   -0.379712E+00
&BPNODE TNODE=3,   TNPC= 0,   STY= 0.0,   STZ= 0.0,   SCALE= 1.0,   &END
&SECT1   STX= 0.484900E+01, STY= 0.0,   TNPS= 0,   TINTS= 3,
ALF= 0.0,   THETA= 0.0,
INMODE= 4,   TNODE= 3,
0.000000E+00   0.245338E-01   -0.499398E+00
0.000000E+00   0.733652E-01   -0.494588E+00
0.000000E+00   0.121490E+00   -0.485016E+00
0.000000E+00   0.213778E+00   -0.470772E+00
0.000000E+00   0.257051E+00   -0.428864E+00
0.000000E+00   0.297850E+00   -0.401604E+00
0.0   -0.353553E+00   -0.353553E+00
&BPNODE TNODE=3,   TNPC= 0,   TINTC= 3,
&PATCH1 IREV= 0,   IDPAT= 2,   MAKE= 0,   KCOMP= 1, KA8S= 1, IPATSYN=0,   &END
MID # 2, PAT # 7
IPATCOP=0,
&SECT1   STX= 0.260000E+01, STY= 0.0,   STZ= 0.0,   SCALE= 1.0,
ALF= 0.0,   THETA= 0.0,   TNPS= 0,   TINTS= 3,
INMODE= 4,   TNODE= 3,
0.0   -0.353553E+00   -0.353553E+00
0.000000E+00   0.401604E+00   -0.428864E+00
0.000000E+00   0.451995E+00   -0.451995E+00
0.000000E+00   0.470772E+00   -0.470772E+00
0.000000E+00   0.485016E+00   -0.485016E+00
0.000000E+00   0.494588E+00   -0.494588E+00
0.000000E+00   0.499398E+00   -0.499398E+00
0.0   0.353553E+00   -0.353553E+00
&BPNODE TNODE=3,   TNPC= 0,   TINTC= 3,   &END
&SECT1   STX= 0.261120E+01, STY= 0.0,   THETA= 0.0,
ALF= 0.0,   THETA= 0.0,   TNPS= 0,   TINTS= 3,
INMODE= 4,   TNODE= 3,
0.000000E+00   0.379712E+00   -0.325298E+00
0.000000E+00   0.401604E+00   -0.297850E+00
0.000000E+00   0.428864E+00   -0.257051E+00
0.000000E+00   0.451995E+00   -0.213778E+00
0.000000E+00   0.470772E+00   -0.168445E+00
0.000000E+00   0.485016E+00   -0.121490E+00
0.000000E+00   0.494588E+00   -0.733652E-01
0.000000E+00   0.499398E+00   -0.245338E-01
0.000000E+00   0.499398E+00   0.245338E-01
0.000000E+00   0.494588E+00   0.733652E-01
0.000000E+00   0.485016E+00   0.121490E+00
0.000000E+00   0.470772E+00   0.168445E+00
0.000000E+00   0.451995E+00   0.213778E+00
0.000000E+00   0.428864E+00   0.257051E+00
0.000000E+00   0.401604E+00   0.297850E+00
0.000000E+00   0.379712E+00   0.325298E+00
&BPNODE TNODE=3,   TNPC= 0,   STY= 0.0,   STZ= 0.0,   SCALE= 1.0,   &END
&SECT1   STX= 0.331374E+01, STY= 0.0,   TINTC= 3,
ALF= 0.0,   THETA= 0.0,

INMODE= 4, TNODE= 0, TNPS= 0, TINTS= 3, &END
0.000000E+00 0.379712E+00 -0.325298E+00
0.000000E+00 0.401604E+00 -0.297850E+00
0.000000E+00 0.428864E+00 -0.257051E+00
0.000000E+00 0.451995E+00 -0.213778E+00
0.000000E+00 0.470772E+00 -0.168445E+00
0.000000E+00 0.485016E+00 -0.121490E+00
0.000000E+00 0.493398E+00 -0.733652E-01
0.000000E+00 0.494588E+00 -0.245338E-01
0.000000E+00 0.494588E+00 0.245338E-01
0.000000E+00 0.485016E+00 0.121490E+00
0.000000E+00 0.470772E+00 0.168445E+00
0.000000E+00 0.451995E+00 0.213778E+00
0.000000E+00 0.428864E+00 0.257051E+00
0.000000E+00 0.401604E+00 0.297850E+00
0.000000E+00 0.379712E+00 0.325298E+00

&BPNODE TNODE=3, TNPC= 0, TINTC= 3,
&SECT1 STX= 0.384460E+01, STY= 0.0, STZ= 0.0, SCALE= 1.0,
ALF= 0.0, THETA=

INMODE= 4, TNODE= 0, TNPS= 0, TINTS= 3, &END
0.000000E+00 0.379712E+00 -0.325298E+00
0.000000E+00 0.401604E+00 -0.297850E+00
0.000000E+00 0.428864E+00 -0.257051E+00
0.000000E+00 0.451995E+00 -0.213778E+00
0.000000E+00 0.470772E+00 -0.168445E+00
0.000000E+00 0.485016E+00 -0.121490E+00
0.000000E+00 0.493398E+00 -0.733652E-01
0.000000E+00 0.494588E+00 -0.245338E-01
0.000000E+00 0.494588E+00 0.245338E-01
0.000000E+00 0.485016E+00 0.121490E+00
0.000000E+00 0.470772E+00 0.168445E+00
0.000000E+00 0.451995E+00 0.213778E+00
0.000000E+00 0.428864E+00 0.257051E+00
0.000000E+00 0.401604E+00 0.297850E+00
0.000000E+00 0.379712E+00 0.325298E+00

&BPNODE TNODE=3, TNPC= 0, TINTC= 3,
&SECT1 STX= 0.404892E+01, STY= 0.0, STZ= 0.0, SCALE= 1.0,
ALF= 0.0, THETA=

INMODE= 4, TNODE= 0, TNPS= 0, TINTS= 3, &END
0.000000E+00 0.379712E+00 -0.325298E+00
0.000000E+00 0.401604E+00 -0.297850E+00
0.000000E+00 0.428864E+00 -0.257051E+00
0.000000E+00 0.451995E+00 -0.213778E+00
0.000000E+00 0.470772E+00 -0.168445E+00
0.000000E+00 0.485016E+00 -0.121490E+00
0.000000E+00 0.493398E+00 -0.733652E-01
0.000000E+00 0.494588E+00 -0.245338E-01
0.000000E+00 0.494588E+00 0.245338E-01
0.000000E+00 0.485016E+00 0.121490E+00
0.000000E+00 0.470772E+00 0.168445E+00
0.000000E+00 0.451995E+00 0.213778E+00
0.000000E+00 0.428864E+00 0.257051E+00
0.000000E+00 0.401604E+00 0.297850E+00
0.000000E+00 0.379712E+00 0.325298E+00

&BPNODE TNODE=3, TNPC= 0, TINTC= 3,
&SECT1 STX= 0.416335E+01, STY= 0.0, STZ= 0.0, SCALE= 1.0,
ALF= 0.0, THETA=

INMODE= 4, TNODE= 0, TNPS= 0, TINTS= 3, &END
0.000000E+00 0.379712E+00 -0.325298E+00
0.000000E+00 0.401604E+00 -0.297850E+00
0.000000E+00 0.428864E+00 -0.257051E+00
0.000000E+00 0.451995E+00 -0.213778E+00
0.000000E+00 0.470772E+00 -0.168445E+00
0.000000E+00 0.485016E+00 -0.121490E+00
0.000000E+00 0.493398E+00 -0.733652E-01
0.000000E+00 0.494588E+00 -0.245338E-01
0.000000E+00 0.494588E+00 0.245338E-01
0.000000E+00 0.485016E+00 0.121490E+00
0.000000E+00 0.470772E+00 0.168445E+00
0.000000E+00 0.451995E+00 0.213778E+00
0.000000E+00 0.428864E+00 0.257051E+00
0.000000E+00 0.401604E+00 0.297850E+00

0.000000E+00 0.379712E+00 0.325298E+00

&BPNODE TNODE=3, TNPC= 0, TINTC= 3,
&SECT1 STX= 0.432184E+01, STY= 0.0, STZ= 0.0, SCALE= 1.0,
ALF= 0.0, THETA=

INMODE= 4, TNODE= 0, TNPS= 0, TINTS= 3, &END
0.000000E+00 0.379712E+00 -0.325298E+00
0.000000E+00 0.401604E+00 -0.297850E+00
0.000000E+00 0.428864E+00 -0.257051E+00
0.000000E+00 0.451995E+00 -0.213778E+00
0.000000E+00 0.470772E+00 -0.168445E+00
0.000000E+00 0.485016E+00 -0.121490E+00
0.000000E+00 0.493398E+00 -0.733652E-01
0.000000E+00 0.494588E+00 -0.245338E-01
0.000000E+00 0.494588E+00 0.245338E-01
0.000000E+00 0.485016E+00 0.121490E+00
0.000000E+00 0.470772E+00 0.168445E+00
0.000000E+00 0.451995E+00 0.213778E+00
0.000000E+00 0.428864E+00 0.257051E+00
0.000000E+00 0.401604E+00 0.297850E+00
0.000000E+00 0.379712E+00 0.325298E+00

&BPNODE TNODE=3, TNPC= 0, TINTC= 3,
&SECT1 STX= 0.451795E+01, STY= 0.0, STZ= 0.0, SCALE= 1.0,
ALF= 0.0, THETA=

INMODE= 4, TNODE= 0, TNPS= 0, TINTS= 3, &END
0.000000E+00 0.379712E+00 -0.325298E+00
0.000000E+00 0.401604E+00 -0.297850E+00
0.000000E+00 0.428864E+00 -0.257051E+00
0.000000E+00 0.451995E+00 -0.213778E+00
0.000000E+00 0.470772E+00 -0.168445E+00
0.000000E+00 0.485016E+00 -0.121490E+00
0.000000E+00 0.493398E+00 -0.733652E-01
0.000000E+00 0.494588E+00 -0.245338E-01
0.000000E+00 0.494588E+00 0.245338E-01
0.000000E+00 0.485016E+00 0.121490E+00
0.000000E+00 0.470772E+00 0.168445E+00
0.000000E+00 0.451995E+00 0.213778E+00
0.000000E+00 0.428864E+00 0.257051E+00
0.000000E+00 0.401604E+00 0.297850E+00
0.000000E+00 0.379712E+00 0.325298E+00

&BPNODE TNODE=3, TNPC= 0, TINTC= 3,
&SECT1 STX= 0.473244E+01, STY= 0.0, STZ= 0.0, SCALE= 1.0,
ALF= 0.0, THETA=

INMODE= 4, TNODE= 0, TNPS= 0, TINTS= 3, &END
0.000000E+00 0.379712E+00 -0.325298E+00
0.000000E+00 0.401604E+00 -0.297850E+00
0.000000E+00 0.428864E+00 -0.257051E+00
0.000000E+00 0.451995E+00 -0.213778E+00
0.000000E+00 0.470772E+00 -0.168445E+00
0.000000E+00 0.485016E+00 -0.121490E+00
0.000000E+00 0.493398E+00 -0.733652E-01
0.000000E+00 0.494588E+00 -0.245338E-01
0.000000E+00 0.494588E+00 0.245338E-01
0.000000E+00 0.485016E+00 0.121490E+00
0.000000E+00 0.470772E+00 0.168445E+00
0.000000E+00 0.451995E+00 0.213778E+00
0.000000E+00 0.428864E+00 0.257051E+00
0.000000E+00 0.401604E+00 0.297850E+00
0.000000E+00 0.379712E+00 0.325298E+00

&BPNODE TNODE=3, TNPC= 0, TINTC= 3,
&SECT1 STX= 0.494900E+01, STY= 0.0, STZ= 0.0, SCALE= 1.0,
ALF= 0.0, THETA=

INMODE= 4, TNODE= 0, TNPS= 0, TINTS= 3, &END
0.0   0.353553E+00 -0.353553E+00
0.000000E+00 0.401604E+00 -0.297850E+00
0.000000E+00 0.428864E+00 -0.257051E+00
0.000000E+00 0.451995E+00 -0.213778E+00
0.000000E+00 0.470772E+00 -0.168445E+00
0.000000E+00 0.485016E+00 -0.121490E+00
0.000000E+00 0.493398E+00 -0.733652E-01
0.000000E+00 0.494588E+00 -0.245338E-01
0.000000E+00 0.494588E+00 0.245338E-01
0.000000E+00 0.485016E+00 0.121490E+00

```
0.000000E+00   0.470772E+00   0.168445E+00
0.000000E+00   0.451995E+00   0.213778E+00
0.000000E+00   0.428864E+00   0.257051E+00
0.000000E+00   0.401604E+00   0.297850E+00
0.0            0.353553E+00   0.353553E+00
&BPNODE  TNODE=3,  TNPC= 0,  TINTS= 3,
&PATCH1  IREV= 0,  IDPAT= 2, MAKE=  0, KCOMP= 1, KABS= 1, IPATSYM=0,  &END
         IPATCOP=0,                                                   &END
         MID # 3, PAT # 8
&SECT1   STX= 0.260000E+01,  STY= 0.0,  STZ= 0.0,   SCALE=   1.0,     &END
         ALF=  0.0,  THETA=  0.0,
         INMODE= 4,  TNODS= 0,  TNPS= 0,  TINTS= 3,
0.000000E+00   0.353553E+00   0.353553E+00
0.000000E+00   0.297850E+00   0.401604E+00
0.000000E+00   0.257051E+00   0.428864E+00
0.000000E+00   0.213778E+00   0.451995E+00
0.000000E+00   0.168445E+00   0.470772E+00
0.000000E+00  -0.733653E-01   0.485016E+00
0.000000E+00   0.121490E+00   0.494588E+00
0.000000E+00   0.245339E-01   0.499398E+00
0.000000E+00  -0.733652E-01   0.499398E+00
0.000000E+00  -0.121490E+00   0.494588E+00
0.000000E+00  -0.168445E+00   0.485016E+00
0.000000E+00  -0.213778E+00   0.470772E+00
0.000000E+00  -0.257051E+00   0.451995E+00
0.000000E+00  -0.297850E+00   0.428864E+00
0.000000E+00  -0.353553E+00   0.401604E+00
0.000000E+00  -0.333553E+00   0.353553E+00
&BPNODE  TNODE=3,  TNPC= 0,  TINTS= 3,
&SECT1   STX= 0.281328E+01,  STY= 0.0,  STZ= 0.0,   SCALE=   1.0,     &END
         ALF=  0.0,  THETA=  0.0,                                     &END
         INMODE= 4,  TNODS= 0,  TNPS= 0,  TINTS= 3,
0.000000E+00   0.325298E+00   0.379712E+00
0.000000E+00   0.297850E+00   0.401604E+00
0.000000E+00   0.257051E+00   0.428864E+00
0.000000E+00   0.213778E+00   0.470772E+00
0.000000E+00   0.168445E+00   0.485016E+00
0.000000E+00   0.733653E-01   0.494588E+00
0.000000E+00   0.121490E+00   0.499398E+00
0.000000E+00  -0.245339E-01   0.499398E+00
0.000000E+00  -0.733652E-01   0.494588E+00
0.000000E+00  -0.168445E+00   0.485016E+00
0.000000E+00  -0.121490E+00   0.470772E+00
0.000000E+00  -0.257051E+00   0.428864E+00
0.000000E+00  -0.213778E+00   0.451995E+00
0.000000E+00  -0.297850E+00   0.401604E+00
0.000000E+00  -0.325298E+00   0.379712E+00
&BPNODE  TNODE=3,  TNPC= 0,  TINTS= 3,
&SECT1   STX= 0.311374E+01,  STY= 0.0,  STZ= 0.0,   SCALE=   1.0,     &END
         ALF=  0.0,  THETA=  0.0,                                     &END
         INMODE= 4,  TNODS= 0,  TNPS= 0,  TINTS= 3,
0.000000E+00   0.325298E+00   0.379712E+00
0.000000E+00   0.297850E+00   0.401604E+00
0.000000E+00   0.257051E+00   0.428864E+00
0.000000E+00   0.213778E+00   0.470772E+00
0.000000E+00   0.121490E+00   0.485016E+00
0.000000E+00   0.733653E-01   0.494588E+00
0.000000E+00  -0.245339E-01   0.499398E+00
0.000000E+00  -0.121490E+00   0.494588E+00
0.000000E+00  -0.213778E+00   0.470772E+00
0.000000E+00  -0.257051E+00   0.451995E+00
0.000000E+00  -0.297850E+00   0.428864E+00
0.000000E+00  -0.325298E+00   0.379712E+00
&BPNODE  TNODE=3,  TNPC= 0,  TINTS= 3,
&SECT1   STX= 0.384460E+01,  STY= 0.0,  STZ= 0.0,   SCALE=   1.0,     &END
         ALF=  0.0,  THETA=  0.0,                                     &END
         INMODE= 4,  TNODS= 0,  TNPS= 0,  TINTS= 3,
0.000000E+00   0.325298E+00   0.379712E+00
0.000000E+00   0.297850E+00   0.401604E+00
0.000000E+00   0.257051E+00   0.428864E+00
0.000000E+00   0.213778E+00   0.451995E+00
```

```
0.000000E+00   0.168445E+00   0.470772E+00
0.000000E+00   0.121490E+00   0.485016E+00
0.000000E+00   0.733653E-01   0.494588E+00
0.000000E+00  -0.245339E-01   0.499398E+00
0.000000E+00  -0.733652E-01   0.494588E+00
0.000000E+00  -0.168445E+00   0.485016E+00
0.000000E+00  -0.121490E+00   0.470772E+00
0.000000E+00  -0.213778E+00   0.451995E+00
0.000000E+00  -0.257051E+00   0.428864E+00
0.000000E+00  -0.297850E+00   0.401604E+00
0.000000E+00  -0.325298E+00   0.379712E+00
&BPNODE  TNODE=3,  TNPC= 0,  TINTS= 3,
&SECT1   STX= 0.404892E+01,  STY= 0.0,  STZ= 0.0,   SCALE=   1.0,     &END
         ALF=  0.0,  THETA=  0.0,
         INMODE= 4,  TNODS= 0,  TNPS= 0,  TINTS= 3,
0.000000E+00   0.325298E+00   0.379712E+00
0.000000E+00   0.297850E+00   0.401604E+00
0.000000E+00   0.257051E+00   0.428864E+00
0.000000E+00   0.213778E+00   0.451995E+00
0.000000E+00   0.168445E+00   0.470772E+00
0.000000E+00   0.121490E+00   0.485016E+00
0.000000E+00   0.733653E-01   0.494588E+00
0.000000E+00  -0.245339E-01   0.499398E+00
0.000000E+00  -0.733652E-01   0.494588E+00
0.000000E+00  -0.121490E+00   0.485016E+00
0.000000E+00  -0.168445E+00   0.470772E+00
0.000000E+00  -0.213778E+00   0.451995E+00
0.000000E+00  -0.257051E+00   0.428864E+00
0.000000E+00  -0.297850E+00   0.401604E+00
0.000000E+00  -0.325298E+00   0.379712E+00
&BPNODE  TNODE=3,  TNPC= 0,  TINTS= 3,
&SECT1   STX= 0.416535E+01,  STY= 0.0,  STZ= 0.0,   SCALE=   1.0,     &END
         ALF=  0.0,  THETA=  0.0,                                     &END
         INMODE= 4,  TNODS= 0,  TNPS= 0,  TINTS= 3,
0.000000E+00   0.325298E+00   0.379712E+00
0.000000E+00   0.297850E+00   0.401604E+00
0.000000E+00   0.257051E+00   0.428864E+00
0.000000E+00   0.213778E+00   0.470772E+00
0.000000E+00   0.168445E+00   0.485016E+00
0.000000E+00   0.121490E+00   0.494588E+00
0.000000E+00   0.733653E-01   0.499398E+00
0.000000E+00  -0.245339E-01   0.499398E+00
0.000000E+00  -0.733652E-01   0.494588E+00
0.000000E+00  -0.168445E+00   0.485016E+00
0.000000E+00  -0.121490E+00   0.470772E+00
0.000000E+00  -0.213778E+00   0.451995E+00
0.000000E+00  -0.257051E+00   0.428864E+00
0.000000E+00  -0.297850E+00   0.401604E+00
0.000000E+00  -0.325298E+00   0.379712E+00
&BPNODE  TNODE=3,  TNPC= 0,  TINTS= 3,
&SECT1   STX= 0.432184E+01,  STY= 0.0,  STZ= 0.0,   SCALE=   1.0,     &END
         ALF=  0.0,  THETA=  0.0,                                     &END
         INMODE= 4,  TNODS= 0,  TNPS= 0,  TINTS= 3,
0.000000E+00   0.325298E+00   0.379712E+00
0.000000E+00   0.297850E+00   0.401604E+00
0.000000E+00   0.257051E+00   0.428864E+00
0.000000E+00   0.213778E+00   0.470772E+00
0.000000E+00   0.168445E+00   0.485016E+00
0.000000E+00   0.121490E+00   0.494588E+00
0.000000E+00   0.733653E-01   0.499398E+00
0.000000E+00  -0.245339E-01   0.499398E+00
0.000000E+00  -0.733652E-01   0.494588E+00
0.000000E+00  -0.168445E+00   0.485016E+00
0.000000E+00  -0.121490E+00   0.470772E+00
0.000000E+00  -0.213778E+00   0.451995E+00
0.000000E+00  -0.257051E+00   0.428864E+00
0.000000E+00  -0.297850E+00   0.401604E+00
0.000000E+00  -0.325298E+00   0.379712E+00
&BPNODE  TNODE=3,  TNPC= 0,  TINTS= 3,
&SECT1   STX= 0.451195E+01,  STY= 0.0,  STZ= 0.0,   SCALE=   1.0,     &END
         ALF=  0.0,  THETA=  0.0,                                     &END
         INMODE= 4,  TNODS= 0,  TNPS= 0,  TINTS= 3,
```

&BPNODE   TNODE=3, TNPC= 0, STX= 0.472441E+01, STY= 0.0,   STZ= 0.0,   TINTC= 3,   SCALE= 1.0,   &END
&SECT1   STX= 0.0,   THETA= 0.0,
   ALF= 0.0,
   INMODE= 4,   TNODE= 3,

&BPNODE   TNODE=3, TNPC= 0, STX= 0.404900E+01, STY= 0.0,   STZ= 0.0,   TINTC= 3,   SCALE= 1.0,   &END
&SECT1   STX= 0.0,   THETA= 0.0,
   ALF= 0.0,
   INMODE= 4,   TNODE= 3,

&BPNODE   TNODE=3, IREY=0, IDPAT= 2, MAKE= 0, KCOMP= 1, KASS= 1, IPATSYM=0,   &END
&PATCH1   IPATCOP=0, PAT # 4
   MID # 4, PAT # 4
&SECT1   STX= 0.260000E+01, STY= 0.0,   STZ= 0.0,   TINTS= 3,   SCALE= 1.0,   &END
   THETA= 0.0,
   INMODE= 4,   TNODE= 3,

&BPNODE   TNODE=3, TNPC= 0, STX= 0.281328E-01, STY= 0.0,   STZ= 0.0,   TINTS= 3,   SCALE= 1.0,   &END
&SECT1   STX= 0.0,   THETA= 0.0,
   ALF= 0.0,
   INMODE= 4,   TNODE= 0,

&BPNODE   TNODE=3, TNPC= 0, STX= 0.331374E+01, STY= 0.0,   STZ= 0.0,   TINTS= 3,   SCALE= 1.0,   &END
&SECT1   STX= 0.0,   THETA= 0.0,
   ALF= 0.0,
   INMODE= 4,   TNODE= 0,

&BPNODE   TNODE=3, TNPC= 0, STX= 0.384460E+01, STY= 0.0,   STZ= 0.0,   TINTS= 3,   SCALE= 1.0,   &END
&SECT1   STX= 0.0,   THETA= 0.0,
   ALF= 0.0,
   INMODE= 4,   TNODE= 0,

&BPNODE   TNODE=3, TNPC= 0, STX= 0.404892E+01, STY= 0.0,   STZ= 0.0,   TINTS= 3,   SCALE= 1.0,   &END
&SECT1   STX= 0.0,   THETA= 0.0,
   ALF= 0.0,
   INMODE= 4,   TNODE= 0,

&BPNODE TNODE=3, TNPC= 0, TINTC= 3,
&SECT1   STX= 0.418535E+01, STY= 0.0, STZ= 0.0,
    ALF= 0.0, THETA= 0.0,
    INMODE= 4, TNODE= 0,   TNPS= 0,   TINTS= 3,
    SCALE= 1.0,
&END

&BPNODE TNODE=3, TNPC= 0, TINTC= 3,
&SECT1   STX= 0.432184E+01, STY= 0.0, STZ= 0.0,
    ALF= 0.0, THETA= 0.0,
    INMODE= 4, TNODE= 0,   TNPS= 0,   TINTS= 3,
    SCALE= 1.0,
&END

&BPNODE TNODE=3, TNPC= 0, TINTC= 3,
&SECT1   STX= 0.473244E+01, STY= 0.0, STZ= 0.0,
    ALF= 0.0, THETA= 0.0,
    INMODE= 4, TNODE= 0,   TNPS= 0,   TINTS= 3,
    SCALE= 1.0,
&END

&BPNODE TNODE=3, TNPC= 0, TINTC= 3,
&SECT1   STX= 0.484900E+01, STY= 0.0, STZ= 0.0,
    ALF= 0.0, THETA= 0.0,
    INMODE= 4, TNODE= 3,   TNPS= 0,   TINTS= 3,
    SCALE= 1.0,
&END

MID # 5, PAT # 10
&PATCH1 IREV= 0, IDPAT= 2, MAKE= 0, KCOMP= 1, KASS= 1, IPATSYM=0,
    IPATCOP=0,
&SECT1   STX= 0.260000E+01, STY= 0.0, STZ= 0.0,
    ALF= 0.0, THETA= 0.0,
    INMODE= 4, TNODE= 0,   TNPS= 0,   TINTS= 3,
    SCALE= 1.0,
&END

&BPNODE TNODE=3, TNPC= 0, TINTC= 3,
&SECT1   STX= 0.281128E+01, STY= 0.0, STZ= 0.0,
    ALF= 0.0, THETA= 0.0,
    INMODE= 4, TNODE= 0,   TNPS= 0,   TINTS= 3,
    SCALE= 1.0,
&END

&BPNODE TNODE=3, TNPC= 0, TINTC= 3,
&SECT1   STX= 0.311374E+01, STY= 0.0, STZ= 0.0,
    ALF= 0.0, THETA= 0.0,
    INMODE= 4, TNODE= 0,   TNPS= 0,   TINTS= 3,
    SCALE= 1.0,
&END

&BPNODE TNODE=3, TNPC= 0, TINTC= 3,
&SECT1   STX= 0.364460E+01, STY= 0.0, STZ= 0.0,
    ALF= 0.0, THETA=
&END

95

```
INMODE=   4,    TNODE=   0,    TNPB=   0,    TINTS=  3,                      &END
0.000000E+00  -0.325298E+00  -0.379712E+00
0.000000E+00  -0.297850E+00  -0.401604E+00
0.000000E+00  -0.257051E+00  -0.428864E+00
0.000000E+00  -0.213778E+00  -0.451995E+00
0.000000E+00  -0.168445E+00  -0.470772E+00
0.000000E+00  -0.121490E+00  -0.485016E+00
0.000000E+00  -0.733654E-01  -0.494588E+00
0.000000E+00  -0.245338E-01  -0.499398E+00
0.000000E+00   0.245338E-01  -0.499398E+00
&BPNODE  TNODE=3    TNPC=   0,    TINTC=  3,
&SECT1   STX= 0.404892E+01,  STY= 0.0,   STZ= 0.0,   SCALE=  1.0,
ALF=  0.0,    THETA=   0.0,
INMODE=   4,    TNODE=   0,    TNPB=   0,    TINTS=  3,                      &END
0.000000E+00  -0.325298E+00  -0.379712E+00
0.000000E+00  -0.297850E+00  -0.401604E+00
0.000000E+00  -0.257051E+00  -0.428864E+00
0.000000E+00  -0.213778E+00  -0.451995E+00
0.000000E+00  -0.168445E+00  -0.470772E+00
0.000000E+00  -0.121490E+00  -0.485016E+00
0.000000E+00  -0.733654E-01  -0.494588E+00
0.000000E+00  -0.245338E-01  -0.499398E+00
0.000000E+00   0.245338E-01  -0.499398E+00
&BPNODE  TNODE=3    TNPC=   0,    TINTC=  3,
&SECT1   STX= 0.416535E+01,  STY= 0.0,   STZ= 0.0,   SCALE=  1.0,
ALF=  0.0,    THETA=   0.0,
INMODE=   4,    TNODE=   0,    TNPB=   0,    TINTS=  3,                      &END
0.000000E+00  -0.325298E+00  -0.379712E+00
0.000000E+00  -0.297850E+00  -0.401604E+00
0.000000E+00  -0.257051E+00  -0.428864E+00
0.000000E+00  -0.213778E+00  -0.451995E+00
0.000000E+00  -0.168445E+00  -0.470772E+00
0.000000E+00  -0.121490E+00  -0.485016E+00
0.000000E+00  -0.733654E-01  -0.494588E+00
0.000000E+00  -0.245338E-01  -0.499398E+00
0.000000E+00   0.245338E-01  -0.499398E+00
&BPNODE  TNODE=3    TNPC=   0,    TINTC=  3,
&SECT1   STX= 0.432184E+01,  STY= 0.0,   STZ= 0.0,   SCALE=  1.0,
ALF=  0.0,    THETA=   0.0,
INMODE=   4,    TNODE=   0,    TNPB=   0,    TINTS=  3,                      &END
0.000000E+00  -0.325298E+00  -0.379712E+00
0.000000E+00  -0.297850E+00  -0.401604E+00
0.000000E+00  -0.257051E+00  -0.428864E+00
0.000000E+00  -0.213778E+00  -0.451995E+00
0.000000E+00  -0.168445E+00  -0.470772E+00
0.000000E+00  -0.121490E+00  -0.485016E+00
0.000000E+00  -0.733654E-01  -0.494588E+00
0.000000E+00  -0.245338E-01  -0.499398E+00
0.000000E+00   0.245338E-01  -0.499398E+00
&BPNODE  TNODE=3    TNPC=   0,    TINTC=  3,
&SECT1   STX= 0.451795E+01,  STY= 0.0,   STZ= 0.0,   SCALE=  1.0,
ALF=  0.0,    THETA=   0.0,
INMODE=   4,    TNODE=   0,    TNPB=   0,    TINTS=  3,                      &END
0.000000E+00  -0.325298E+00  -0.379712E+00
0.000000E+00  -0.297850E+00  -0.401604E+00
0.000000E+00  -0.257051E+00  -0.428864E+00
0.000000E+00  -0.213778E+00  -0.451995E+00
0.000000E+00  -0.168445E+00  -0.470772E+00
0.000000E+00  -0.121490E+00  -0.485016E+00
0.000000E+00  -0.733654E-01  -0.494588E+00
0.000000E+00  -0.245338E-01  -0.499398E+00
0.000000E+00   0.245338E-01  -0.499398E+00
&BPNODE  TNODE=3    TNPC=   0,    TINTC=  3,
&SECT1   STX= 0.473244E+01,  STY= 0.0,   STZ= 0.0,   SCALE=  1.0,
ALF=  0.0,    THETA=   0.0,
INMODE=   4,    TNODE=   0,    TNPB=   0,    TINTS=  3,                      &END
0.000000E+00  -0.325298E+00  -0.379712E+00
0.000000E+00  -0.297850E+00  -0.401604E+00
0.000000E+00  -0.257051E+00  -0.428864E+00
0.000000E+00  -0.213778E+00  -0.451995E+00
0.000000E+00  -0.168445E+00  -0.470772E+00
0.000000E+00  -0.121490E+00  -0.485016E+00
0.000000E+00  -0.722864E+00  -0.494588E+00
0.000000E+00  -0.245338E-01  -0.499398E+00
0.000000E+00   0.245338E-01  -0.499398E+00
&BPNODE  TNODE=3    TNPC=   0,    TINTC=  3,
```

```
&SECT1   STX= 0.484900E+01,  STY= 0.0,   STZ= 0.0,   SCALE=  1.0,
ALF=  0.0,    THETA=   0.0,    TNPB=   0,    TINTS=  3,
INMODE=   4,    TNODE=   0,    -0.353553E+00
0.000000E+00  -0.297850E+00  -0.401604E+00
0.000000E+00  -0.257051E+00  -0.428864E+00
0.000000E+00  -0.213778E+00  -0.451995E+00
0.000000E+00  -0.168445E+00  -0.470772E+00
0.000000E+00  -0.121490E+00  -0.485016E+00
0.000000E+00  -0.733654E-01  -0.494588E+00
0.000000E+00  -0.245338E-01  -0.499398E+00
0.000000E+00   0.245338E-01  -0.499398E+00
&BPNODE  TNODE=3    TNPC=   0,    TINTC=  3,                                  &END
&PATCH1  IREV=   0,    IDPAT=  2,    MAKE=   0,    KCOMP=  1,  KASB=  1,  IPATSYM=0,  &END
IPATCOP=   0,
APTBODY, PAT # 11
&SECT1   STX= 0.484900E+01,  STY= 0.0,   STZ= 0.0,   SCALE=  1.0,
ALF=  0.0,    THETA=   0.0,    TNPB=   0,    TINTS=  3,
INMODE=   4,    TNODE=   0,    -0.499398E+00
0.000000E+00   0.245338E-01  -0.733652E-01
0.000000E+00   0.733652E-01  -0.245338E-01
0.000000E+00   0.121490E+00   0.245338E-01
0.000000E+00   0.168445E+00   0.121490E+00
0.000000E+00   0.213778E+00   0.213778E+00
0.000000E+00   0.257051E+00  -0.257051E+00
0.000000E+00   0.297850E+00   0.297850E+00
0.000000E+00   0.353553E+00   0.353553E+00
0.000000E+00   0.401604E+00  -0.401604E+00
0.000000E+00   0.428864E+00   0.428864E+00
0.000000E+00   0.451995E+00   0.451995E+00
0.000000E+00   0.470772E+00  -0.470772E+00
0.000000E+00   0.485016E+00   0.485016E+00
0.000000E+00   0.494588E+00  -0.494588E+00
0.000000E+00   0.499398E+00   0.499398E+00
0.0           0.499398E+00  -0.499398E+00
0.0           0.485016E+00  -0.485016E+00
0.0           0.470772E+00  -0.470772E+00
0.0           0.451995E+00  -0.451995E+00
0.0           0.428864E+00  -0.428864E+00
0.0           0.401604E+00  -0.401604E+00
0.0           0.353553E+00  -0.353553E+00
0.0           0.297850E+00  -0.297850E+00
0.0           0.257051E+00  -0.257051E+00
0.0           0.213778E+00  -0.213778E+00
0.0           0.168445E+00  -0.168445E+00
0.0           0.121490E+00  -0.121490E+00
0.0           0.733652E-01  -0.733652E-01
0.0           0.245339E-01  -0.245339E-01
0.0          -0.245339E-01  -0.121490E+00
0.0          -0.733652E-01  -0.213777E+00
0.0          -0.121490E+00  -0.257051E+00
0.0          -0.168445E+00  -0.297850E+00
0.0          -0.213778E+00  -0.401604E+00
0.0          -0.257051E+00  -0.428864E+00
0.0          -0.297850E+00  -0.451995E+00
0.0          -0.353553E+00  -0.470772E+00
0.0          -0.401604E+00  -0.485016E+00
0.0          -0.428864E+00  -0.494588E+00
0.0          -0.451995E+00  -0.499398E+00
0.0          -0.470772E+00  -0.257051E+00
0.0          -0.485016E+00  -0.213777E+00
0.0          -0.494588E+00  -0.121490E+00
0.0          -0.499398E+00  -0.733652E-01
0.0          -0.485016E+00  -0.245339E-01
0.0          -0.470772E+00   0.121490E+00
0.0          -0.428864E+00   0.168445E+00
0.0          -0.401604E+00  -0.213777E+00
0.0          -0.353553E+00  -0.257051E+00
0.0          -0.297850E+00  -0.353553E+00
0.0          -0.257051E+00  -0.353553E+00
```

&BPNODE TNODE=3, TNPC= 0, TINTC= 3,
&SECT1   STX= 0.490969E+01, STY= 0.0, STZ= 0.0, SCALE= 1.0,
         ALF= 0.0, THETA= 0.0, TNPS= 0,
         INMODE= 4, TNODE= 0, TINTS= 3,
&END

&BPNODE TNODE=3, TNPC= 0, TINTC= 3,
&SECT1   STX= 0.506251E+01, STY= 0.0, STZ= 0.0, SCALE= 1.0,
         ALF= 0.0, THETA= 0.0, TNPS= 0,
         INMODE= 4, TNODE= 0, TINTS= 3,
&END

&BPNODE TNODE=3, TNPC= 0, TINTC= 3,
&SECT1   STX= 0.524336E+01, STY= 0.0, STZ= 0.0, SCALE= 1.0,
         ALF= 0.0, THETA= 0.0, TNPS= 0,
         INMODE= 4, TNODE= 0, TINTS= 3,
&END

0.000000E+00   0.499398E+00   0.245338E-01
0.000000E+00   0.494588E+00   0.733652E-01
0.000000E+00   0.485016E+00   0.121490E+00
...
&BPNODE TNODE=3, TNFC= 0, TINTC= 0,
&SECT1   STX= 0.706453E+01, STY= 0.0, STZ= 0.0, SCALE= 1.0,
   ALF= 0.0, THETA= 0.0, TNPS= 0, TINTS= 3,
   INMODE= 4, TNODE= 3, &END
&END

0.000000E+00   0.370476E+00   0.335779E+00
0.000000E+00   0.335780E+00   0.370476E+00
0.000000E+00   0.297850E+00   0.401604E+00
...
&BPNODE TNODE=3, TNFC= 0, TINTC= 0, SCALE= 1.0,
&SECT1   STX= 0.79516SE+01, STY= 0.0, STZ= 0.0,
   ALF= 0.0, THETA= 0.0, TNPS= 0, TINTS= 3,
   INMODE= 4, TNODE= 3, &END
&END

99

&BPNODE TNODE=3, TNPC= 0, STX= 0.0, STZ= 0.0, SCALE= 1.0,   &END
&SECT1   STX= 0.0, TNPC= 0,
         ALF= 0.0, THETA= 0.862412E+01, TINTS= 3,
         INMODE= 4, TNODB= 0, TNFS= 0,   &END

&BPNODE TNODE=3, TNPC= 0, STX= 0.0, STZ= 0.0, SCALE= 1.0,   &END
&SECT1   STX= 0.0, TNPC= 0,
         ALF= 0.0, THETA= 0.96621E+01, TINTS= 3,
         INMODE= 4, TNODB= 0, TNFS= 0,   &END

Page 45

```
&BPNODE  TNODE=3,  TNPC= 0,  STT= 0.0,  STZ= 0.0,  SCALE= 1.0,
&SECT1   STX= 0.105261E+02,  TINTC= 3,
         ALF= 0.0,  THETA= 0.0,  TINTS= 3,
         INMODE= 4,  TNODB= 0,  TNPB= 0,
                                                        &END
                                                        &END
```

Page 46

```
&BPNODE  TNODE=3,  TNPC= 0,  STT= 0.0,  STZ= 0.0,  SCALE= 1.0,
&SECT1   STX= 0.111560E+02,  TINTC= 3,
         ALF= 0.0,  THETA= 0.0,  TINTS= 3,
         INMODE= 4,  TNODB= 0,  TNPB= 0,
                                                        &END
                                                        &END
```

&BPNODE TNODE=3, TNPC= 0, TINTC= 3, STX= 0.0, SCALE= 1.0,
&SECT1 STX= 0.121723E+02, STY= 0.0, TINTS= 3,
     ALF= 0.0, THETA= 0.0, TNPS= 0,
     INNODE= 4, TNODE= 0,
0.000000E+00   -0.257051E+00   -0.428864E+00   &END
0.000000E+00   -0.213778E+00   -0.451995E+00   &END
0.000000E+00   -0.168445E+00   -0.470772E+00
0.000000E+00   -0.121490E+00   -0.485016E+00
0.000000E+00   -0.733654E-01   -0.494588E+00
0.000000E+00   -0.245338E-01   -0.499398E+00
0.000000E+00   0.245338E-01   -0.499398E+00
0.000000E+00   0.733654E-01   -0.494588E+00
0.000000E+00   0.121490E+00   -0.485016E+00
0.000000E+00   0.168445E+00   -0.470772E+00
0.000000E+00   0.213778E+00   -0.451995E+00
0.000000E+00   0.257051E+00   -0.428864E+00
0.000000E+00   0.297850E+00   -0.401604E+00
0.000000E+00   0.335779E+00   -0.370476E+00
0.000000E+00   0.370476E+00   -0.335779E+00
0.000000E+00   0.401604E+00   -0.297850E+00
0.000000E+00   0.428864E+00   -0.257051E+00
0.000000E+00   0.451995E+00   -0.213778E+00
0.000000E+00   0.470772E+00   -0.168445E+00
0.000000E+00   0.485016E+00   -0.121490E+00
0.000000E+00   0.494588E+00   -0.733654E-01
0.000000E+00   0.499398E+00   -0.245338E-01
0.000000E+00   0.499398E+00   0.245338E-01
0.000000E+00   0.494588E+00   0.733654E-01
0.000000E+00   0.485016E+00   0.121490E+00
0.000000E+00   0.470772E+00   0.168445E+00
0.000000E+00   0.451995E+00   0.213778E+00
0.000000E+00   0.428864E+00   0.257051E+00
0.000000E+00   0.401604E+00   0.297850E+00
0.000000E+00   0.370476E+00   0.335779E+00
0.000000E+00   0.335779E+00   0.370476E+00
0.000000E+00   0.297850E+00   0.401604E+00
0.000000E+00   0.257051E+00   0.428864E+00
0.000000E+00   0.213778E+00   0.451995E+00
0.000000E+00   0.168445E+00   0.470772E+00
0.000000E+00   0.121490E+00   0.485016E+00
0.000000E+00   0.733654E-01   0.494588E+00
0.000000E+00   0.245338E-01   0.499398E+00
0.000000E+00   -0.245338E-01   0.499398E+00

&BPNODE TNODE=3, TNPC= 0, TINTC= 3, STX= 0.0, SCALE= 1.0,
&SECT1 STX= 0.129750E+02, STY= 0.0, TINTS= 3,
     ALF= 0.0, THETA= 0.0, TNPS= 0,
     INNODE= 4, TNODE= 0,
0.000000E+00   0.245338E-01   -0.499398E+00   &END
0.000000E+00   0.733654E-01   -0.494588E+00   &END
0.000000E+00   0.121490E+00   -0.485016E+00
0.000000E+00   0.168445E+00   -0.470772E+00
0.000000E+00   0.213778E+00   -0.451995E+00
0.000000E+00   0.257051E+00   -0.428864E+00
0.000000E+00   0.297850E+00   -0.401604E+00
0.000000E+00   0.335779E+00   -0.370476E+00
0.000000E+00   0.370476E+00   -0.335779E+00
0.000000E+00   0.401604E+00   -0.297850E+00
0.000000E+00   0.428864E+00   -0.257051E+00
0.000000E+00   0.451995E+00   -0.213778E+00
0.000000E+00   0.470772E+00   -0.168445E+00
0.000000E+00   0.485016E+00   -0.121490E+00
0.000000E+00   0.494588E+00   -0.733654E-01
0.000000E+00   0.499398E+00   -0.245338E-01
0.000000E+00   0.499398E+00   0.245338E-01
0.000000E+00   0.494588E+00   0.733654E-01
0.000000E+00   0.485016E+00   0.121490E+00
0.000000E+00   0.470772E+00   0.168445E+00
0.000000E+00   0.451995E+00   0.213778E+00
0.000000E+00   0.428864E+00   0.257051E+00
0.000000E+00   0.401604E+00   0.297850E+00
0.000000E+00   0.370476E+00   0.335779E+00
0.000000E+00   0.335779E+00   0.370476E+00
0.000000E+00   0.297850E+00   0.401604E+00
0.000000E+00   0.257051E+00   0.428864E+00
0.000000E+00   0.213778E+00   0.451995E+00
0.000000E+00   0.168445E+00   0.470772E+00
0.000000E+00   0.121490E+00   0.485016E+00
0.000000E+00   0.733654E-01   0.494588E+00
0.000000E+00   0.245338E-01   0.499398E+00
0.000000E+00   -0.245338E-01   0.499398E+00
0.000000E+00   -0.733654E-01   0.494588E+00
0.000000E+00   -0.121490E+00   0.485016E+00

&BPNODE TNODE=3, TNPC= 0, TINTC= 3, STX= 0.0, SCALE= 1.0,
&SECT1 STX= 0.137645E+02, STY= 0.0, TINTS= 3,
     ALF= 0.0, THETA= 0.0, TNPS= 0,
     INNODE= 4, TNODE= 0,
0.000000E+00   0.245338E-01   -0.499398E+00   &END
0.000000E+00   0.733654E-01   -0.494588E+00   &END
0.000000E+00   0.121490E+00   -0.485016E+00

0.000000E+00 0.168445E+00 -0.470772E+00
0.000000E+00 0.213778E+00 -0.451995E+00
0.000000E+00 0.257051E+00 -0.428864E+00
0.000000E+00 0.335779E+00 -0.401604E+00
0.000000E+00 0.370476E+00 -0.370476E+00
0.000000E+00 0.401604E+00 -0.335779E+00
0.000000E+00 0.428864E+00 -0.297850E+00
0.000000E+00 0.451995E+00 -0.257051E+00
0.000000E+00 0.470772E+00 -0.213778E+00
0.000000E+00 0.485016E+00 -0.168445E+00
0.000000E+00 0.494588E+00 -0.121490E+00
0.000000E+00 0.499398E+00 -0.733652E-01
0.000000E+00 0.494588E+00 -0.245338E-01
0.000000E+00 0.470772E+00 0.245338E-01
0.000000E+00 0.428864E+00 0.733652E-01
0.000000E+00 0.370476E+00 0.121490E+00
0.000000E+00 0.297850E+00 0.168445E+00
0.000000E+00 0.213778E+00 0.257051E+00
0.000000E+00 0.121490E+00 0.297850E+00
0.000000E+00 0.245339E-01 0.335779E+00
0.000000E+00 -0.733652E-01 0.370476E+00
0.000000E+00 -0.168445E+00 0.401604E+00
0.000000E+00 -0.257051E+00 0.428864E+00
0.000000E+00 -0.335779E+00 0.451995E+00
0.000000E+00 -0.401604E+00 0.470772E+00
0.000000E+00 -0.451995E+00 0.485016E+00
0.000000E+00 -0.485016E+00 0.494588E+00
0.000000E+00 -0.499398E+00 0.499398E+00
0.000000E+00 -0.494588E+00 0.485016E+00
0.000000E+00 -0.470772E+00 0.470772E+00
0.000000E+00 -0.428864E+00 0.428864E+00
0.000000E+00 -0.370476E+00 0.401604E+00
0.000000E+00 -0.297850E+00 0.370476E+00
0.000000E+00 -0.213778E+00 0.335779E+00
0.000000E+00 -0.121490E+00 0.297850E+00
0.000000E+00 -0.245339E-01 0.257051E+00
0.000000E+00 0.733652E-01 0.213778E+00
0.000000E+00 0.168445E+00 0.168445E+00
0.000000E+00 0.257051E+00 -0.733652E-01
0.000000E+00 0.335779E+00 -0.245338E-01
0.000000E+00 0.401604E+00 -0.370476E+00
0.000000E+00 0.451995E+00 -0.401604E+00
0.000000E+00 0.485016E+00 -0.428864E+00
0.000000E+00 0.499398E+00 -0.470772E+00
&BPNODE TNODE=3, TNPC=0, TINTC=0, STY= 0.0, STZ= 0.0, SCALE= 1.0, &END
&SECT1 STY= 0.145410E+02, THETA= 0.0, TNPS= 0, TINTS= 3,
         ALF= 0.0, TNODE= 4,
         INMODE= 4, 0.245338E-01
0.000000E+00 0.733652E-01 0.121490E+00
0.000000E+00 0.168445E+00 0.213778E+00
0.000000E+00 0.257051E+00 0.297850E+00
0.000000E+00 0.335779E+00 0.370476E+00
0.000000E+00 0.401604E+00 -0.297850E+00

0.000000E+00 0.428864E+00 -0.257051E+00
0.000000E+00 0.451995E+00 -0.213778E+00
0.000000E+00 0.470772E+00 -0.168445E+00
0.000000E+00 0.485016E+00 -0.121490E+00
0.000000E+00 0.499398E+00 -0.733652E-01
0.000000E+00 0.494588E+00 -0.245338E-01
0.000000E+00 0.485016E+00 0.245339E-01
0.000000E+00 0.470772E+00 0.121490E+00
0.000000E+00 0.451995E+00 0.213778E+00
0.000000E+00 0.428864E+00 0.257051E+00
0.000000E+00 0.335780E+00 0.297850E+00
0.000000E+00 0.257051E+00 0.335779E+00
0.000000E+00 0.168445E+00 0.370476E+00
0.000000E+00 0.733653E-01 0.401604E+00
0.000000E+00 -0.245338E-01 0.428864E+00
0.000000E+00 -0.121490E+00 0.451995E+00
0.000000E+00 -0.213778E+00 0.470772E+00
0.000000E+00 -0.297850E+00 0.485016E+00
0.000000E+00 -0.370476E+00 0.494588E+00
0.000000E+00 -0.428864E+00 0.499398E+00
0.000000E+00 -0.451995E+00 0.485016E+00
0.000000E+00 -0.485016E+00 0.451995E+00
0.000000E+00 -0.499398E+00 0.401604E+00
0.000000E+00 -0.494588E+00 0.335779E+00
0.000000E+00 -0.470772E+00 0.257051E+00
0.000000E+00 -0.445808E+00 0.168445E+00
0.000000E+00 -0.399398E+00 0.733652E-01
0.000000E+00 -0.335779E+00 -0.245339E-01
0.000000E+00 -0.257051E+00 -0.121490E+00
0.000000E+00 -0.168445E+00 -0.213778E+00
0.000000E+00 -0.733652E-01 -0.297850E+00
0.000000E+00 0.245338E-01 -0.370476E+00
0.000000E+00 0.121490E+00 -0.428864E+00
0.000000E+00 0.213777E+00 -0.470772E+00
0.000000E+00 0.257051E+00 -0.485016E+00
0.000000E+00 0.335780E+00 -0.494588E+00
0.000000E+00 0.401604E+00 -0.499398E+00
&BPNODE TNODE=3, TNPC=0, TINTC=02, STY= 0.0, STZ= 0.0, SCALE= 1.0, &END
&SECT1 STY= 0.153047E+02, THETA= 0.0, TNPS= 0, TINTS= 3,
         ALF= 0.0, TNODE= 4,
         INMODE= 4, 0.245338E-01
0.000000E+00 0.733652E-01 -0.485016E+00
0.000000E+00 0.168445E+00 -0.470772E+00
0.000000E+00 0.257051E+00 -0.451995E+00
0.000000E+00 0.335779E+00 -0.428864E+00
0.000000E+00 0.401604E+00 -0.370476E+00
0.000000E+00 0.451995E+00 -0.335779E+00
0.000000E+00 0.485016E+00 -0.297850E+00
0.000000E+00 0.470772E+00 -0.257051E+00
0.000000E+00 0.494588E+00 -0.213778E+00
0.000000E+00 0.499398E+00 -0.168445E+00
0.000000E+00 0.499398E+00 -0.121490E+00
0.000000E+00 0.493398E+00 -0.733652E-01
0.000000E+00 0.499398E+00 0.245338E-01

0.000000E+00 0.494588E+00 0.733652E-01
0.000000E+00 0.485016E+00 0.121490E+00
0.000000E+00 0.470772E+00 0.168445E+00
0.000000E+00 0.451995E+00 0.213778E+00
0.000000E+00 0.401604E+00 0.257051E+00
0.000000E+00 0.370476E+00 0.297850E+00
0.000000E+00 0.335780E+00 0.335779E+00
0.000000E+00 0.297850E+00 0.370476E+00
0.000000E+00 0.257051E+00 0.401604E+00
0.000000E+00 0.213778E+00 0.428864E+00
0.000000E+00 0.168445E+00 0.451995E+00
0.000000E+00 0.121490E+00 0.470772E+00
0.000000E+00 0.733652E-01 0.485016E+00
0.000000E+00 -0.245339E-01 0.493398E+00
0.000000E+00 -0.121490E+00 0.499398E+00
0.000000E+00 -0.168445E+00 0.494588E+00
0.000000E+00 -0.257051E+00 0.485016E+00
0.000000E+00 -0.335780E+00 0.470772E+00
0.000000E+00 -0.401604E+00 0.451995E+00
0.000000E+00 -0.428864E+00 0.428864E+00
0.000000E+00 -0.451995E+00 0.401604E+00
0.000000E+00 -0.470772E+00 0.370476E+00
0.000000E+00 -0.494588E+00 0.335779E+00
0.000000E+00 -0.493398E+00 0.297850E+00
0.000000E+00 -0.499398E+00 0.257051E+00
0.000000E+00 -0.335779E+00 0.213777E+00
0.000000E+00 -0.257051E+00 0.168445E+00
0.000000E+00 -0.213777E+00 0.121490E+00
0.000000E+00 -0.168445E+00 0.245339E-01
0.000000E+00 -0.121490E+00 -0.733652E-01
0.000000E+00 -0.733653E-01 -0.245338E-01
0.000000E+00 -0.245339E-01 -0.470772E+00
0.000000E+00 -0.733652E-01 -0.485016E+00
0.000000E+00 -0.257051E+00 -0.493398E+00
0.000000E+00 -0.451995E+00 -0.499398E+00

&BPNODE   TNODE=3,   TNPC=0,   TINTC=3,
&SECT1 STX= 0.160557E+02, STY= 0.0,   STZ= 0.0,   SCALE= 1.0,
  ALP= 0.0,   THETA= 0.0,
   INMODE= 4,   TNODS= 3, TNPS= 0,   TINTS= 3,
0.000000E+00 0.245338E-01 -0.499398E+00
0.000000E+00 0.733652E-01 -0.494588E+00
0.000000E+00 0.121490E+00 -0.485016E+00
0.000000E+00 0.168445E+00 -0.470772E+00
0.000000E+00 0.213778E+00 -0.451995E+00
0.000000E+00 0.257051E+00 -0.428864E+00
0.000000E+00 0.297850E+00 -0.401604E+00
0.000000E+00 0.335780E+00 -0.370476E+00
0.000000E+00 0.370476E+00 -0.335779E+00
0.000000E+00 0.401604E+00 -0.257051E+00
0.000000E+00 0.428864E+00 -0.213778E+00
0.000000E+00 0.451995E+00 -0.168445E+00
0.000000E+00 0.470772E+00 -0.121490E+00
0.000000E+00 0.485016E+00 -0.733652E-01
0.000000E+00 0.493398E+00 0.245338E-01
0.000000E+00 0.499398E+00 0.733652E-01
0.000000E+00 0.485016E+00 0.121490E+00
0.000000E+00 0.451995E+00 0.213778E+00
0.000000E+00 0.401604E+00 0.257051E+00
0.000000E+00 0.370476E+00 0.297850E+00
&END

&END

0.000000E+00 0.335780E+00 0.370476E+00
0.000000E+00 0.297850E+00 0.401604E+00
0.000000E+00 0.257051E+00 0.428864E+00
0.000000E+00 0.213778E+00 0.451995E+00
0.000000E+00 0.168445E+00 0.470772E+00
0.000000E+00 0.733653E-01 0.485016E+00
0.000000E+00 -0.245339E-01 0.494588E+00
0.000000E+00 -0.733652E-01 0.499398E+00
0.000000E+00 -0.245338E-01 0.494588E+00
0.000000E+00 -0.121490E+00 0.485016E+00
0.000000E+00 -0.168445E+00 0.470772E+00
0.000000E+00 -0.257051E+00 0.451995E+00
0.000000E+00 -0.297850E+00 0.401604E+00
0.000000E+00 -0.335779E+00 0.370476E+00
0.000000E+00 -0.370476E+00 0.335779E+00
0.000000E+00 -0.401604E+00 0.297850E+00
0.000000E+00 -0.428864E+00 0.257051E+00
0.000000E+00 -0.451995E+00 0.213777E+00
0.000000E+00 -0.470772E+00 0.168445E+00
0.000000E+00 -0.494588E+00 0.733652E-01
0.000000E+00 -0.499398E+00 -0.245339E-01
0.000000E+00 -0.485016E+00 -0.733652E-01
0.000000E+00 -0.470772E+00 -0.121490E+00
0.000000E+00 -0.428864E+00 -0.213777E+00
0.000000E+00 -0.401604E+00 -0.257051E+00
0.000000E+00 -0.370476E+00 -0.297850E+00
0.000000E+00 -0.335780E+00 -0.335780E+00
0.000000E+00 -0.257051E+00 -0.370476E+00
0.000000E+00 -0.168445E+00 -0.401604E+00
0.000000E+00 -0.121490E+00 -0.428864E+00
0.000000E+00 -0.733654E-01 -0.470772E+00
0.000000E+00 -0.245338E-01 -0.494588E+00
0.000000E+00 0.245338E-01 -0.499398E+00

&BPNODE   TNODE=3,   TNPC=0,   TINTC=3,
&SECT1 STX= 0.167943E+02, STY= 0.0,   STZ= 0.0,   SCALE= 1.0,
  ALP= 0.0,   THETA= 0.0,
   INMODE= 4,   TNODS= 3, TNPS= 0,   TINTS= 3,
0.000000E+00 0.245339E-01 -0.499398E+00
0.000000E+00 0.733652E-01 -0.494588E+00
0.000000E+00 0.121490E+00 -0.485016E+00
0.000000E+00 0.168445E+00 -0.470772E+00
0.000000E+00 0.213778E+00 -0.451995E+00
0.000000E+00 0.257051E+00 -0.428864E+00
0.000000E+00 0.297850E+00 -0.401604E+00
0.000000E+00 0.335779E+00 -0.370476E+00
0.000000E+00 0.370476E+00 -0.335779E+00
0.000000E+00 0.401604E+00 -0.257051E+00
0.000000E+00 0.428864E+00 -0.213778E+00
0.000000E+00 0.451995E+00 -0.168445E+00
0.000000E+00 0.470772E+00 -0.121490E+00
0.000000E+00 0.485016E+00 -0.733652E-01
0.000000E+00 0.493398E+00 0.245338E-01
0.000000E+00 0.499398E+00 0.733652E-01
0.000000E+00 0.485016E+00 0.121490E+00
0.000000E+00 0.451995E+00 0.213778E+00
0.000000E+00 0.401604E+00 0.257051E+00
0.000000E+00 0.370476E+00 0.297850E+00
0.000000E+00 0.335780E+00 0.370476E+00
0.000000E+00 0.297850E+00 0.401604E+00
0.000000E+00 0.257051E+00 0.428864E+00
0.000000E+00 0.213778E+00 0.451995E+00
0.000000E+00 0.168445E+00 0.470772E+00
0.000000E+00 0.121490E+00 0.485016E+00
0.000000E+00 -0.733653E-01 0.494588E+00
&END

&END

0.000000E+00   0.245339E-01   0.499398E+00
0.000000E+00 -0.245338E-01   0.499398E+00
0.000000E+00 -0.733652E-01   0.494588E+00
0.000000E+00 -0.121490E+00   0.485016E+00
0.000000E+00 -0.168445E+00   0.470772E+00
0.000000E+00 -0.213778E+00   0.451995E+00
0.000000E+00 -0.257051E+00   0.428864E+00
0.000000E+00 -0.297850E+00   0.401604E+00
0.000000E+00 -0.335779E+00   0.370476E+00
0.000000E+00 -0.370476E+00   0.335779E+00
0.000000E+00 -0.401604E+00   0.297850E+00
0.000000E+00 -0.428864E+00   0.257051E+00
0.000000E+00 -0.451995E+00   0.213778E+00
0.000000E+00 -0.470772E+00   0.168445E+00
0.000000E+00 -0.485016E+00   0.121490E+00
0.000000E+00 -0.494588E+00   0.733652E-01
0.000000E+00 -0.499398E+00   0.245339E-01
0.000000E+00 -0.499398E+00 -0.245338E-01
0.000000E+00 -0.494588E+00 -0.733652E-01
0.000000E+00 -0.485016E+00 -0.121490E+00
0.000000E+00 -0.470772E+00 -0.168445E+00
0.000000E+00 -0.451995E+00 -0.213777E+00
0.000000E+00 -0.428864E+00 -0.257051E+00
0.000000E+00 -0.401604E+00 -0.297850E+00
0.000000E+00 -0.370476E+00 -0.335779E+00
0.000000E+00 -0.335779E+00 -0.370476E+00
0.000000E+00 -0.297850E+00 -0.401604E+00
0.000000E+00 -0.257051E+00 -0.428864E+00
0.000000E+00 -0.213778E+00 -0.451995E+00
0.000000E+00 -0.168445E+00 -0.470772E+00
0.000000E+00 -0.121490E+00 -0.485016E+00
0.000000E+00 -0.733652E-01 -0.494588E+00
0.000000E+00 -0.245338E-01 -0.499398E+00

&BPNODE TNODE=3,   TNPC=0,   TINTC= 3,   STX= 0.0,   STY= 0.0,
&SECT1   STX=   0.175208E+02,   THETA=   0.0,   SCALE=   1.0,   &END
         ALF=   0.0,   TNP8= 0,   TINTS= 3,
         INNODE=   4,   TNODS= 0,

0.000000E+00 -0.499398E+00   0.245339E-01
0.000000E+00 -0.494588E+00   0.121490E+00
0.000000E+00 -0.485016E+00   0.168445E+00
0.000000E+00 -0.470772E+00   0.213778E+00
0.000000E+00 -0.451995E+00   0.257051E+00
0.000000E+00 -0.428864E+00   0.297850E+00
0.000000E+00 -0.401604E+00   0.335779E+00
0.000000E+00 -0.370476E+00   0.370476E+00
0.000000E+00 -0.335779E+00   0.401604E+00
0.000000E+00 -0.297850E+00   0.428864E+00
0.000000E+00 -0.257051E+00   0.451995E+00
0.000000E+00 -0.213778E+00   0.470772E+00
0.000000E+00 -0.168445E+00   0.485016E+00
0.000000E+00 -0.121490E+00   0.494588E+00
0.000000E+00 -0.733652E-01   0.494588E+00
0.000000E+00   0.245338E-01   0.499398E+00
0.000000E+00   0.733652E-01   0.494588E+00
0.000000E+00   0.121490E+00   0.485016E+00
0.000000E+00   0.168445E+00   0.470772E+00
0.000000E+00   0.213778E+00   0.451995E+00
0.000000E+00   0.257051E+00   0.428864E+00

&END

0.000000E+00 -0.297850E+00   0.401604E+00
0.000000E+00 -0.335779E+00   0.370476E+00
0.000000E+00 -0.370476E+00   0.335779E+00
0.000000E+00 -0.401604E+00   0.297850E+00
0.000000E+00 -0.428864E+00   0.257051E+00
0.000000E+00 -0.451995E+00   0.213777E+00
0.000000E+00 -0.485016E+00   0.168445E+00
0.000000E+00 -0.493398E+00   0.121490E+00
0.000000E+00 -0.494588E+00   0.733652E-01
0.000000E+00 -0.499398E+00   0.245339E-01
0.000000E+00 -0.499398E+00 -0.245338E-01
0.000000E+00 -0.485016E+00 -0.733652E-01
0.000000E+00 -0.470772E+00 -0.121490E+00
0.000000E+00 -0.451995E+00 -0.168445E+00
0.000000E+00 -0.428864E+00 -0.257051E+00
0.000000E+00 -0.401604E+00 -0.297850E+00
0.000000E+00 -0.370476E+00 -0.335780E+00
0.000000E+00 -0.335779E+00 -0.370476E+00
0.000000E+00 -0.297850E+00 -0.401604E+00
0.000000E+00 -0.257051E+00 -0.428864E+00
0.000000E+00 -0.213777E+00 -0.451995E+00
0.000000E+00 -0.168445E+00 -0.470772E+00
0.000000E+00 -0.121490E+00 -0.485016E+00
0.000000E+00 -0.733654E-01 -0.494588E+00
0.000000E+00 -0.245338E-01 -0.499398E+00

&BPNODE TNODE=3,   TNPC=0,   TINTC= 3,   STX= 0.0,   STY= 0.0,
&SECT1   STX=   0.179788E+02,   THETA=   0.0,   SCALE=   1.0,   &END
         ALF=   0.0,   TNP8= 0,   TINTS= 3,
         INNODE=   4,   TNODS= 0,

0.000000E+00 -0.245316E-01 -0.499352E+00
0.000000E+00   0.733585E-01 -0.494543E+00
0.000000E+00   0.121479E+00 -0.484971E+00
0.000000E+00   0.168429E+00 -0.470729E+00
0.000000E+00   0.213758E+00 -0.451953E+00
0.000000E+00   0.257028E+00 -0.428825E+00
0.000000E+00   0.297822E+00 -0.401567E+00
0.000000E+00   0.335749E+00 -0.370441E+00
0.000000E+00   0.370441E+00 -0.335749E+00
0.000000E+00   0.401567E+00 -0.297822E+00
0.000000E+00   0.428825E+00 -0.257028E+00
0.000000E+00   0.451953E+00 -0.213758E+00
0.000000E+00   0.470729E+00 -0.168429E+00
0.000000E+00   0.484971E+00 -0.121479E+00
0.000000E+00   0.494543E+00 -0.733585E-01
0.000000E+00   0.499352E+00 -0.245316E-01
0.000000E+00   0.499352E+00   0.245316E-01
0.000000E+00   0.484971E+00   0.121479E+00
0.000000E+00   0.470729E+00   0.168429E+00
0.000000E+00   0.451953E+00   0.213758E+00
0.000000E+00   0.428825E+00   0.257028E+00
0.000000E+00   0.401567E+00   0.335749E+00
0.000000E+00   0.370441E+00   0.370441E+00
0.000000E+00   0.335749E+00   0.401567E+00
0.000000E+00   0.297822E+00   0.428825E+00
0.000000E+00   0.257028E+00   0.451953E+00
0.000000E+00   0.213758E+00   0.470729E+00
0.000000E+00   0.168429E+00   0.484971E+00

&END

0.000000E+00 -0.484971E+00   0.121479E+00
0.000000E+00 -0.494543E+00   0.733585E-01
0.000000E+00 -0.499352E+00   0.245316E-01
0.000000E+00 -0.493352E+00 -0.245317E-01
0.000000E+00 -0.494543E+00 -0.733585E-01
0.000000E+00 -0.484971E+00 -0.121479E+00
0.000000E+00 -0.470729E+00 -0.168429E+00
0.000000E+00 -0.451953E+00 -0.213758E+00
0.000000E+00 -0.428825E+00 -0.257028E+00
0.000000E+00 -0.401567E+00 -0.297822E+00
0.000000E+00 -0.370441E+00 -0.335749E+00
0.000000E+00 -0.335749E+00 -0.370441E+00
0.000000E+00 -0.297822E+00 -0.401567E+00
0.000000E+00 -0.257028E+00 -0.428825E+00
0.000000E+00 -0.213758E+00 -0.451953E+00
0.000000E+00 -0.168429E+00 -0.470729E+00
0.000000E+00 -0.121479E+00 -0.484971E+00
0.000000E+00 -0.733586E-01 -0.494543E+00
0.000000E+00 -0.245316E-01 -0.499352E+00

&RPNODE TNODE=3, TNPC= 0, TINTC= 3,
&SECT1   STY= 0.0, STZ= 0.0, THETA= 0.0,
     ALP= 0.0, TNODE= 4, TNPE= 0, TINTE= 3,
     INMODE= 4,   SCALE= 1.0,

0.000000E+00 -0.244765E-01 -0.499352E+00
0.000000E+00 -0.731938E-01 -0.493433E+00
0.000000E+00 -0.121206E+00 -0.483883E+00
0.000000E+00 -0.168051E+00 -0.469672E+00
0.000000E+00 -0.213278E+00 -0.450939E+00
0.000000E+00 -0.256451E+00 -0.427862E+00
0.000000E+00 -0.297154E+00 -0.406666E+00
0.000000E+00 -0.334995E+00 -0.369610E+00
0.000000E+00 -0.369610E+00 -0.334995E+00
0.000000E+00 -0.406666E+00 -0.297154E+00
0.000000E+00 -0.427862E+00 -0.256451E+00
0.000000E+00 -0.450939E+00 -0.213278E+00
0.000000E+00 -0.469672E+00 -0.168051E+00
0.000000E+00 -0.483883E+00 -0.121206E+00
0.000000E+00 -0.493433E+00 -0.731938E-01
0.000000E+00 -0.498231E+00 -0.244765E-01
0.000000E+00 -0.498231E+00   0.244765E-01
0.000000E+00 -0.493433E+00   0.731938E-01
0.000000E+00 -0.483883E+00   0.121206E+00
0.000000E+00 -0.469672E+00   0.168051E+00
&END

&END

0.000000E+00 -0.450939E+00 -0.213278E+00
0.000000E+00 -0.427862E+00 -0.256451E+00
0.000000E+00 -0.406666E+00 -0.297154E+00
0.000000E+00 -0.369610E+00 -0.334995E+00
0.000000E+00 -0.334995E+00 -0.369610E+00
0.000000E+00 -0.297154E+00 -0.406666E+00
0.000000E+00 -0.256451E+00 -0.427862E+00
0.000000E+00 -0.213278E+00 -0.450939E+00
0.000000E+00 -0.168051E+00 -0.469672E+00
0.000000E+00 -0.121206E+00 -0.483883E+00
0.000000E+00 -0.731940E-01 -0.493433E+00
0.000000E+00 -0.244765E-01 -0.498231E+00
0.000000E+00   0.244764E-01 -0.498231E+00

&RPNODE TNODE=3, TNPC= 0, TINTC= 3,
&SECT1   STY= 0.183821E+02, STZ= 0.0,   SCALE= 1.0,
     ALP= 0.0, TNODE= 4, TNPE= 0, TINTE= 3,
     INMODE= 4, THETA= 0.0,

0.000000E+00   0.243347E-01 -0.495345E+00
0.000000E+00   0.727698E-01 -0.490574E+00
0.000000E+00   0.120504E+00 -0.481079E+00
0.000000E+00   0.167078E+00 -0.466951E+00
0.000000E+00   0.212043E+00 -0.448326E+00
0.000000E+00   0.254965E+00 -0.425384E+00
0.000000E+00   0.295432E+00 -0.398344E+00
0.000000E+00   0.333054E+00 -0.367469E+00
0.000000E+00   0.367469E+00 -0.333054E+00
0.000000E+00   0.398344E+00 -0.295432E+00
0.000000E+00   0.425384E+00 -0.254965E+00
0.000000E+00   0.448326E+00 -0.212043E+00
0.000000E+00   0.466951E+00 -0.167078E+00
0.000000E+00   0.481079E+00 -0.120504E+00
0.000000E+00   0.490574E+00 -0.727698E-01
0.000000E+00   0.495345E+00 -0.243347E-01
0.000000E+00   0.495345E+00   0.243347E-01
0.000000E+00   0.490574E+00   0.727698E-01
0.000000E+00   0.481079E+00   0.120504E+00
0.000000E+00   0.466951E+00   0.167078E+00
0.000000E+00   0.448326E+00   0.212043E+00
0.000000E+00   0.425384E+00   0.254965E+00
0.000000E+00   0.398344E+00   0.295432E+00
0.000000E+00   0.367469E+00   0.333054E+00
0.000000E+00   0.333054E+00   0.367469E+00
0.000000E+00   0.295432E+00   0.398344E+00
0.000000E+00   0.254965E+00   0.425384E+00
0.000000E+00   0.212043E+00   0.448326E+00
0.000000E+00   0.167078E+00   0.466951E+00
0.000000E+00   0.120504E+00   0.481079E+00
0.000000E+00   0.727699E-01   0.490574E+00
0.000000E+00   0.243347E-01   0.495345E+00
&END

&END

Aug 8 1995 09:51   DATA5

```
&BPNODE  TNODE=3,  TNPC= 0,   TINTC= 3,
&SECT1   STX= 0.185704E+02, STY= 0.0,  STZ= 0.0,   SCALE= 1.0,
   ALF=  0.0,   THETA=  0.0,
      INMODE= 4,  TNODE= 3,  TNPS= 0,  TINTS= 3,
```

Aug 8 1995 09:51   DATA5

```
&SECT1   STX= 0.185704E+02, STY= 0.0,  STZ= 0.0,   SCALE= 1.0,
   ALF=  0.0,   THETA=  0.0,
      INMODE= 4,  TNODE= 3,  TNPS= 0,  TINTS= 3,
```

&END

&BPNODE TNODE=3, TNPC= 0,   TINTC= 3,
&SECT1   STX= 0.185704E+02, STY= 0.0, STZ= 0.0,   SCALE= 1.0,
   ALF= 0.0,   THETA= 0.0,
      INMODE= 4, TNODE= 3, TNPS= 0, TINTS= 3,

&END

&END

```
0.000000E+00   0.196594E+00  -0.415663E+00
0.000000E+00   0.236390E+00  -0.394392E+00
0.000000E+00   0.273908E+00  -0.369323E+00
0.000000E+00   0.308790E+00  -0.340697E+00
0.000000E+00   0.340697E+00  -0.308790E+00
0.000000E+00   0.369323E+00  -0.273908E+00
0.000000E+00   0.394392E+00  -0.236390E+00
0.000000E+00   0.415663E+00  -0.196594E+00
0.000000E+00   0.432931E+00  -0.154905E+00
0.000000E+00   0.446030E+00  -0.111172E+00
0.000000E+00   0.454833E+00  -0.671662E-01
0.000000E+00   0.459256E+00  -0.225618E-01
0.000000E+00   0.454833E+00   0.671662E-01
0.000000E+00   0.446030E+00   0.111172E+00
0.000000E+00   0.432931E+00   0.154905E+00
0.000000E+00   0.415663E+00   0.196594E+00
0.000000E+00   0.394392E+00   0.236390E+00
0.000000E+00   0.369323E+00   0.273908E+00
0.000000E+00   0.340697E+00   0.308790E+00
0.000000E+00   0.308790E+00   0.340697E+00
0.000000E+00   0.273908E+00   0.369323E+00
0.000000E+00   0.236390E+00   0.394392E+00
0.000000E+00   0.196594E+00   0.415663E+00
0.000000E+00   0.154905E+00   0.432931E+00
0.000000E+00   0.111172E+00   0.446030E+00
0.000000E+00   0.671662E-01   0.454833E+00
0.000000E+00   0.225618E-01   0.459256E+00
0.000000E+00  -0.111172E+00   0.446030E+00
0.000000E+00  -0.154905E+00   0.432931E+00
0.000000E+00  -0.196594E+00   0.415663E+00
0.000000E+00  -0.236390E+00   0.394392E+00
0.000000E+00  -0.273908E+00   0.369323E+00
0.000000E+00  -0.308790E+00   0.340697E+00
0.000000E+00  -0.340697E+00   0.308790E+00
0.000000E+00  -0.369323E+00   0.273908E+00
0.000000E+00  -0.394392E+00   0.236390E+00
0.000000E+00  -0.415663E+00   0.196594E+00
0.000000E+00  -0.432931E+00   0.154905E+00
0.000000E+00  -0.446030E+00   0.111172E+00
0.000000E+00  -0.454833E+00   0.671662E-01
0.000000E+00  -0.459256E+00   0.225618E-01
0.000000E+00  -0.459256E+00  -0.225617E-01
```

&BPNODE TNODE=3, STY= 0.0, TNPC= 0, TINTC=3,
&SECT1   STY= 0.185704E+02, STT= 0.0, STZ= 0.0,
         ALF= 0.0, THETA= 0.0,
         INMODE= 4, TNODE= 0, TNPS= 0, TINTS= 3,
0.000000E+00   0.217421E-01 -0.438309E+00
0.000000E+00   0.650170E-01 -0.429826E+00
0.000000E+00   0.107666E+00 -0.417203E+00
0.000000E+00   0.149278E+00 -0.400562E+00
0.000000E+00   0.189452E+00 -0.380064E+00
0.000000E+00   0.227802E+00 -0.355905E+00
0.000000E+00   0.263957E+00 -0.328319E+00
0.000000E+00   0.297571E+00 -0.297571E+00
0.000000E+00   0.328319E+00 -0.263957E+00
0.000000E+00   0.355905E+00 -0.227802E+00
0.000000E+00   0.380064E+00 -0.189452E+00
                                            SCALE= 1.0,   &END
                                                           &END

```
0.000000E+00   0.400562E+00  -0.189452E+00
0.000000E+00   0.417203E+00  -0.149278E+00
0.000000E+00   0.429826E+00  -0.107666E+00
0.000000E+00   0.438309E+00  -0.650170E-01
0.000000E+00   0.442571E+00  -0.217421E-01
0.000000E+00   0.442571E+00   0.217421E-01
0.000000E+00   0.438309E+00   0.650170E-01
0.000000E+00   0.429826E+00   0.107666E+00
0.000000E+00   0.417203E+00   0.149278E+00
0.000000E+00   0.400562E+00   0.189452E+00
0.000000E+00   0.380064E+00   0.227802E+00
0.000000E+00   0.355905E+00   0.263957E+00
0.000000E+00   0.328319E+00   0.297571E+00
0.000000E+00   0.297571E+00   0.328319E+00
0.000000E+00   0.263957E+00   0.355905E+00
0.000000E+00   0.227802E+00   0.380064E+00
0.000000E+00   0.189452E+00   0.400562E+00
0.000000E+00   0.149278E+00   0.417203E+00
0.000000E+00   0.107666E+00   0.429826E+00
0.000000E+00   0.650170E-01   0.438309E+00
0.000000E+00   0.217421E-01   0.442571E+00
0.000000E+00  -0.217421E-01   0.442571E+00
0.000000E+00  -0.650170E-01   0.438309E+00
0.000000E+00  -0.107666E+00   0.429826E+00
0.000000E+00  -0.149278E+00   0.417203E+00
0.000000E+00  -0.189452E+00   0.400562E+00
0.000000E+00  -0.227802E+00   0.380064E+00
0.000000E+00  -0.263957E+00   0.355905E+00
0.000000E+00  -0.297571E+00   0.328319E+00
0.000000E+00  -0.328319E+00   0.297571E+00
0.000000E+00  -0.355905E+00   0.263957E+00
0.000000E+00  -0.380064E+00   0.227802E+00
0.000000E+00  -0.400562E+00   0.189452E+00
0.000000E+00  -0.417203E+00   0.149278E+00
0.000000E+00  -0.429826E+00   0.107666E+00
0.000000E+00  -0.438309E+00   0.650170E-01
0.000000E+00  -0.442571E+00   0.217421E-01
0.000000E+00  -0.442571E+00  -0.217421E-01
```

&BPNODE TNODE=3, STY= 0.0, TNPC= 0, TINTC= 3,
&SECT1   STY= 0.185704E+02, STT= 0.0, STZ= 0.0,
         ALF= 0.0, THETA= 0.0,
         INMODE= 4, TNODE= 0, TNPS= 0, TINTS= 3,
0.000000E+00   0.208489E-01 -0.424388E+00
0.000000E+00   0.623458E-01 -0.420301E+00
0.000000E+00   0.103242E+00 -0.412166E+00
0.000000E+00   0.143144E+00 -0.400062E+00
0.000000E+00   0.181666E+00 -0.384105E+00
0.000000E+00   0.218442E+00 -0.364449E+00
0.000000E+00   0.253113E+00 -0.341283E+00
0.000000E+00   0.285345E+00 -0.314830E+00
0.000000E+00   0.314830E+00 -0.285345E+00
0.000000E+00   0.341283E+00 -0.253113E+00
0.000000E+00   0.364449E+00 -0.218442E+00
0.000000E+00   0.384105E+00 -0.181666E+00
0.000000E+00   0.400062E+00 -0.143144E+00
0.000000E+00   0.412166E+00 -0.103242E+00
0.000000E+00   0.420301E+00 -0.623458E-01
0.000000E+00   0.424388E+00 -0.208489E-01
0.000000E+00   0.420301E+00   0.623458E-01
                                            SCALE= 1.0,   &END
                                                           &END

DATA5

Aug 8 1995 09:51

&BPNODE TNODE= 3, TNPC= 0, TINTC= 3,
&SECT1 STX= 0.18570IE+02, STY= 0.0, STZ= 0.0, SCALE= 1.0,
    ALF= 0.0, THETA= 0.0, TNPS= 0, TINTS= 3,
    INMODE= 4, TNODE= 3,
&END

&END

DATA5

Aug 8 1995 09:51

&BPNODE TNODE= 3, TNPC= 0, TINTC= 3,
&SECT1 STX= 0.18570IE+02, STY= 0.0, STZ= 0.0, SCALE= 1.0,
    ALF= 0.0, THETA= 0.0, TNPS= 0, TINTS= 3,
    INMODE= 4, TNODE= 3,
&END

&END

&BPMODE TNODE=3, TNPC= 0,   STX= 0.185704E+02, STE= 0.0,   SCALE= 1.0,   &END
&SECT1 STX= 0.0, THETA= 0.0, TNODE= 3,   TNPM= 0,   TINTS= 3,   &END
        INMODE= 4, TNODE= 0,

&BPMODE TNODE=3, TNPC= 0,   STX= 0.185704E+02, STE= 0.0,   SCALE= 1.0,   &END
&SECT1 STX= 0.0, THETA= 0.0, TNODE= 3,   TNPM= 0,   TINTS= 3,   &END
        INMODE= 4, TNODE= 0,

111

&BPNODE   TNODE=3,   TNPC= 0,   STX= 0.0,   TINTC= 3,
&SECT1   STX= 0.185704E+02,   STY= 0.0,   STZ= 0.0,   SCALE= 1.0,
&END

ALF=   0.0,   THETA=   0.0,   TNPS=   0,
INMODE=   4,   TNODE=   0,   TINTS= 3,

```
0.000000E+00  -0.746561E-01  -0.208650E+00
0.000000E+00  -0.538454E-01  -0.214963E+00
0.000000E+00  -0.325161E-01  -0.219205E+00
0.000000E+00  -0.198736E-01  -0.221337E+00
0.000000E+00  -0.490073E-01  -0.221337E+00
```

&BPNODE
&SECT1

ALF= 0.0, THETA= 0.0, TNPS= 0,
INMODE= 4, TNODE= 0, TINTS= 3,

```
0.000000E+00  -0.855343E-02  -0.174109E+00
0.000000E+00  -0.255779E-01  -0.174109E+00
0.000000E+00  -0.423561E-01  -0.169095E+00
0.000000E+00  -0.587263E-01  -0.164129E+00
0.000000E+00  -0.745310E-01  -0.157563E+00
0.000000E+00  -0.896179E-01  -0.149518E+00
0.000000E+00  -0.103842E+00  -0.140014E+00
0.000000E+00  -0.117065E+00  -0.129162E+00
0.000000E+00  -0.129162E+00  -0.117065E+00
0.000000E+00  -0.140014E+00  -0.103842E+00
0.000000E+00  -0.149518E+00  -0.896179E-01
0.000000E+00  -0.157563E+00  -0.745310E-01
0.000000E+00  -0.164129E+00  -0.587263E-01
0.000000E+00  -0.169095E+00  -0.423561E-01
0.000000E+00  -0.172432E+00  -0.255779E-01
0.000000E+00  -0.174109E+00  -0.855342E-02
0.000000E+00  -0.174109E+00   0.855342E-02
0.000000E+00  -0.172432E+00   0.255779E-01
0.000000E+00  -0.169095E+00   0.423561E-01
0.000000E+00  -0.164129E+00   0.587263E-01
0.000000E+00  -0.157563E+00   0.745310E-01
0.000000E+00  -0.149518E+00   0.896179E-01
0.000000E+00  -0.140014E+00   0.103842E+00
0.000000E+00  -0.129162E+00   0.117065E+00
0.000000E+00  -0.117065E+00   0.129162E+00
0.000000E+00  -0.103842E+00   0.140014E+00
0.000000E+00  -0.896179E-01   0.149518E+00
0.000000E+00  -0.745310E-01   0.157563E+00
0.000000E+00  -0.587263E-01   0.164129E+00
0.000000E+00  -0.423561E-01   0.169095E+00
0.000000E+00  -0.255779E-01   0.172432E+00
0.000000E+00  -0.855342E-02   0.174109E+00
```

&BPNODE   TNODE=3,   TNPC= 0,   STX= 0.0,   TINTC= 3,
&SECT1   STX= 0.185704E+02,   STY= 0.0,   STZ= 0.0,   SCALE= 1.0,
&END

ALF=   0.0,   THETA=   0.0,   TNPS=   0,
INMODE=   4,   TNODE=   0,   TINTS= 3,

```
0.000000E+00   0.622335E-02  -0.126679E+00
0.000000E+00   0.186101E-01  -0.125459E+00
0.000000E+00   0.308177E-01  -0.123031E+00
0.000000E+00   0.427284E-01  -0.119418E+00
0.000000E+00   0.542277E-01  -0.114655E+00
0.000000E+00   0.652047E-01  -0.108787E+00
0.000000E+00   0.755537E-01  -0.101872E+00
0.000000E+00   0.851752E-01  -0.939763E-01
0.000000E+00   0.939763E-01  -0.851752E-01
0.000000E+00   0.101872E+00  -0.755537E-01
0.000000E+00   0.108787E+00  -0.652047E-01
0.000000E+00   0.114655E+00  -0.542277E-01
0.000000E+00   0.119418E+00  -0.427284E-01
0.000000E+00   0.123031E+00  -0.308177E-01
0.000000E+00   0.125459E+00  -0.186101E-01
0.000000E+00   0.126679E+00  -0.622334E-02
0.000000E+00   0.126679E+00   0.622334E-02
0.000000E+00   0.125459E+00   0.186101E-01
0.000000E+00   0.123031E+00   0.308177E-01
0.000000E+00   0.119418E+00   0.427284E-01
0.000000E+00   0.114655E+00   0.542277E-01
0.000000E+00   0.108787E+00   0.652047E-01
0.000000E+00   0.101872E+00   0.755537E-01
0.000000E+00   0.939763E-01   0.851752E-01
0.000000E+00   0.851752E-01   0.939763E-01
0.000000E+00   0.755537E-01   0.101872E+00
0.000000E+00   0.652047E-01   0.108787E+00
0.000000E+00   0.542277E-01   0.114655E+00
0.000000E+00   0.427284E-01   0.119418E+00
0.000000E+00   0.308177E-01   0.123031E+00
0.000000E+00   0.186101E-01   0.125459E+00
0.000000E+00   0.622335E-02   0.126679E+00
0.000000E+00  -0.622335E-02   0.126679E+00
0.000000E+00  -0.186101E-01   0.125459E+00
0.000000E+00  -0.308177E-01   0.123031E+00
0.000000E+00  -0.427284E-01   0.119418E+00
0.000000E+00  -0.542277E-01   0.114655E+00
0.000000E+00  -0.652047E-01   0.108787E+00
0.000000E+00  -0.755537E-01   0.101872E+00
0.000000E+00  -0.851752E-01   0.939763E-01
0.000000E+00  -0.939763E-01   0.851752E-01
0.000000E+00  -0.101872E+00   0.755537E-01
0.000000E+00  -0.108787E+00   0.652047E-01
0.000000E+00  -0.114655E+00   0.542277E-01
0.000000E+00  -0.119418E+00   0.427284E-01
0.000000E+00  -0.123031E+00   0.308177E-01
0.000000E+00  -0.125459E+00   0.186101E-01
0.000000E+00  -0.126679E+00   0.622335E-02
```

&BPNODE   TNODE=3,   TNPC= 0,   STX= 0.185704E+02,   STY= 0.0,   STZ= 0.0,   SCALE= 1.0,
&SECT1   STX= 0.0,   TINTC= 3,
&END

ALF=   0.0,   THETA=   0.0,   TNPS=   0,
INMODE=   4,   TNODE=   0,   TINTS= 3,

```
0.000000E+00   0.400059E-02  -0.814338E-01
0.000000E+00   0.119632E-01  -0.806495E-01
0.000000E+00   0.198107E-01  -0.790886E-01
0.000000E+00   0.274673E-01  -0.767660E-01
0.000000E+00   0.348594E-01  -0.737044E-01
```

&END

(Page 69 — DATA5: dense columns of numeric data, each row in the form `0.000000E+00` with associated values such as `0.419158E-01 -0.699312E-01`, etc.)

```
&BPNODE  TNODE=3,  TNPC= 0,  STY= 0,  STY= 0,  TINTC= 3,
&SECT1   STY= 0.185704E+02,  TNPC= 0,            SCALE= 1.0,   &END
ALF= 0.0,        THETA=                                         &END
INMODE= 4,  TNODE= 4,
```

(Page 70 — DATA5: dense columns of numeric data, each row in the form `0.000000E+00` with associated values such as `0.369311E-01 -0.132142E-01`, etc.)

```
&BPNODE  TNODE=3,  TNPC= 0,  STY= 0.0,  STY= 0.0,  TINTC= 3,
&SECT1   STY= 0.185704E+02,  TNPC= 0,            SCALE= 0.0,   &END
ALF= 0.0,        THETA=                                         &END
INMODE= 4,  TNODE= 5,  TNPS= 0,  TINTS= 3,
```

```
0.000000E+00    0.369311E-01    0.132142E-01
0.000000E+00    0.354581E-01    0.167704E-01
0.000000E+00    0.336435E-01    0.201652E-01
0.000000E+00    0.315050E-01    0.233657E-01
0.000000E+00    0.290631E-01    0.263412E-01
0.000000E+00    0.263412E-01    0.290631E-01
0.000000E+00    0.233657E-01    0.315050E-01
0.000000E+00    0.201652E-01    0.336435E-01
0.000000E+00    0.167704E-01    0.354581E-01
0.000000E+00    0.132142E-01    0.369311E-01
0.000000E+00    0.953066E-02    0.380485E-01
0.000000E+00    0.575536E-02    0.387995E-01
0.000000E+00    0.192463E-02    0.391768E-01
0.000000E+00   -0.192463E-02    0.391768E-01
0.000000E+00   -0.575536E-02    0.387995E-01
0.000000E+00   -0.953066E-02    0.380485E-01
0.000000E+00   -0.132142E-01    0.369311E-01
0.000000E+00   -0.167704E-01    0.354581E-01
0.000000E+00   -0.201652E-01    0.336435E-01
0.000000E+00   -0.233657E-01    0.315050E-01
0.000000E+00   -0.263412E-01    0.290631E-01
0.000000E+00   -0.290631E-01    0.263412E-01
0.000000E+00   -0.315050E-01    0.233657E-01
0.000000E+00   -0.336435E-01    0.201652E-01
0.000000E+00   -0.354581E-01    0.167704E-01
0.000000E+00   -0.369311E-01    0.132142E-01
0.000000E+00   -0.380485E-01    0.953066E-02
0.000000E+00   -0.387995E-01    0.575535E-02
0.000000E+00   -0.391768E-01    0.192464E-02
0.000000E+00   -0.391768E-01   -0.192464E-02
0.000000E+00   -0.387995E-01   -0.575535E-02
0.000000E+00   -0.380485E-01   -0.953064E-02
0.000000E+00   -0.369311E-01   -0.132142E-01
0.000000E+00   -0.354581E-01   -0.167704E-01
0.000000E+00   -0.336435E-01   -0.201652E-01
0.000000E+00   -0.315050E-01   -0.233657E-01
0.000000E+00   -0.290631E-01   -0.263412E-01
0.000000E+00   -0.263412E-01   -0.290631E-01
0.000000E+00   -0.233657E-01   -0.315050E-01
0.000000E+00   -0.201652E-01   -0.336435E-01
0.000000E+00   -0.167704E-01   -0.354581E-01
0.000000E+00   -0.132142E-01   -0.369311E-01
0.000000E+00   -0.953066E-02   -0.380485E-01
0.000000E+00   -0.575537E-02   -0.387995E-01
0.000000E+00   -0.192463E-02   -0.391768E-01
0.000000E+00    0.192462E-02   -0.391768E-01
&BPNODE   TNODE=3,    TNPC= 0,      TINTC= 3,                          &END
&WAKE1    IDWAK= 0,     IFLXW= 0,        ITRFTZ= 0,   INTRW=  0,       &END
 NO WAKES
&WAKE2    KWPACH= 0,    KWSIDE= 0,       KWLINE= 0,   KWPAN1= 0,
          KWPAN2= 0,    NODEW= 0,        INITIAL= 0,                   &END
&CONSTRM  NONSL = 0,    KPSL = 0,                                      &END
&BLPARAM  RN = 2000000.0, VISC = 0.00001422, NSLBL = 0,               &END
&VS1      NVOLR= 1,        NVOLC= 0,                                   &END
&VS2      X0=   -0.0050, Y0=      0.0000, Z0=    0.0000, INTVSR= 1,    &END
&VS3      X1=  -39.7335, Y1=      0.0000, Z1=    0.0000, NPT1=  20,    &END
&VS4      X2=    0.0000, Y2=      0.0000, Z2=    0.0000, NPT2=   0,    &END
&VS5      X3=    0.0000, Y3=      0.0000, Z3=    0.0000, NPT3=   0,    &END
&VS6      XR0=   0.0000, YR0=     0.0000, ZR0=   0.0000, INTVSC= 0,    &END
&VS7      XR1=   0.0000, YR1=     0.0000, ZR1=   0.0000,
          XR2=   0.0000, YR2=     0.0000, ZR2=   0.0000,              &END
&VS8      R1=    0.0000, R2=      0.0000, PHI1=  0.0,   PHI2=  0.0,   &END
&VS9      NRAD=  0,        NPHI=  0,        NLEN=  0,                   &END
&SLIN1    NSTLIN= 0,                                                   &END
&SLIN2    SX0=   0.0,    SY0=    0.0,    SZ0=   0.0,
          SU=    0.0,    SD=     0.0,    DS=    0.0,    INTSL= 0      &END
```

114

LIST OF REFERENCES

1. Hemsch, M. J., Nielsen, J. N., and Mendenhall, M. R., *"Tactical Missile Aerodynamics,"* Progress in Astronautics and Aeronautics, Volumes 104, 141, and 142, AIAA, 1986 and 1992.

2. Ying, S. X., Baganoff, D., Steger, J. L., and Schiff, L. B., "Numerical Simulation of Unsteady, Viscous, High Angle-of-Attack Flows Using a Partially Flux-Split Algorithm," AIAA Paper 86-2179-CP, AIAA Atmospheric Flight Mechanics Conference, August 1986.

3. Ying, S. X., Schiff, L. B., and Steger, J. L., "A Numerical Study of Three-Dimensional Separated Flow Past a Hemisphere Cylinder," AIAA Paper 87-1207, AIAA 19th Fluid Dynamics, Plasma Dynamics and Lasers Conference, June 1987.

4. Degani, D., Schiff, L. B., "Numerical Simulation of the Effect of Spatial Disturbances on Vortex," AIAA Paper 89-0340, AIAA 27th Aerospace Sciences, January 1989.

5. Schiff, L. B., Degani, D., and Gavali, S., "Numerical Simulation of Vortex Unsteadiness on Slender Bodies of Revolution at Large Incidence," AIAA Paper 89-0195, AIAA 27th Aerospace Sciences Meeting, January 1989.

6. Ekaterinaris, J. A., "Computation of Flow fields Over Missile Configurations" AIAA Paper 94-1915, AIAA 12th Applied Aerodynamics Conference, June 1994.

7. Smith, E. H., Hebbar, S. K., and Platzer, M., "Aerodynamic Characteristics of a Canard-Controlled Missile at High Angles of Attack," AIAA Paper 93-0763, AIAA 31st Aerospace Sciences Meeting, January 1993.

8. Chin, S. S., *"Missile Configuration Design,"* McGraw-Hill, 1961.

9. Karamcheti, K., *"Principle of Ideal-Fluid Aerodynamics,"* John Wiley, 1966.

10. Oswatitsch, K., *"Gasdynamik,"* Springer-Verlag, 1952.

11. Char, B. W., Geddes, K. O., Gonnet, G. H., Leong, B. L., Monagan, M. B., Watt, S. M., *"First Leaves: A Tutorial Introduction to Maple V,"* Springer-Verlag, 1992.

12. von Karman, T., *"Calculation of Pressure Distribution on Airship Hulls,"* NACA, Technical Memorandum No. 574, 1927.

13. Chow, C. Y., *"An Introduction to Computational Fluid Mechanics,"* Seminole Publishing Company, 1983.

115

14. Ashby, D. L., Dudley, M. R., Iguchi, S. K., Browne, L., Katz, J., *"Potential Flow Theory and Operation Guide for the Panel Code PMARC_12,"* COSMIC, Program ARC-13362, The University of Georgia, Athens, Georgia, December 1992.

15. Conversations between Max Platzer, Mark Lambert and author, Naval Postgraduate School, April - August 1995.

16. Ashby, D. L., Dudley, M. R., Iguchi, S. K., *"Development and Validation of an Advanced Low-Order Panel Method,"* NASA, Technical Memorandum No. 101024, October 1988.

17. Rixey, J. W., *"A Multi-Faceted Engineering Study of Aerodynamic Errors of the Service Aircraft Instrumentation Package (SAIP),"* Engineer's Degree, Naval Postgraduate School, Monterey, Ca, September 1992.

18. Porter, D. B., *"A Numerical Study of Airplanes Flying in Proximity,"* Master's Thesis, Naval Postgraduate School, Monterey, Ca, September 1993.

19. Edge, D. C., Perkins, J. N., "Three-Dimensional Aerodynamic Analysis of a Subsonic High-Lift Transport Configuration Using PMARC," AIAA Paper 95-0039, AIAA 33rd Aerospace Sciences Meeting, January 1995.

20. Buning, P. G., Chan, W. M., Renze, K. J., Sondak, D. L., Chiu, I., Soltnick, J. P., *"OVERFLOW User's Manual,"* NASA Ames Research Center, 30 April 1993.

21. Anderson, J. D., *"Fundamentals of Aerodynamics,"* McGraw-Hill, 1991.

22. Anderson, D. A., Tannehill, J. C., Pletcher, R. H., *"Computational Fluid Mechanics and Heat Transfer,"* Hemisphere Publishing, 1984.

23. Suhs, N. E., Tramel, R. W., *"Pegsus 4.0 User's Manual,"* Arnold Engineering Development Center, AEDC-TR-91-8, June 1991.

24. Conversations between John Ekaterinaris, NASA Ames Research Center, and author, January 1995.

INITIAL DISTRIBUTION LIST

1. Defense Technical Information Center...2
    Cameron Station
    Alexandria, VA 22304-6145

2. Library Code 52 2
    Naval Postgraduate School
    Monterey, CA 93943-5101

3. Chairman, Code AA/CO..1
    Naval Postgraduate School
    Monterey, CA 93943-5000

4. Dr. Max F. Platzer..5
    Dept. of Aeronautics and Astronautics, Code AA/Pl
    Naval Postgraduate School
    Monterey, CA 93943-5000

5. Dr. Garth V. Hobson...1
    Dept. of Aeronautics and Astronautics, Code AA/Hb
    Naval Postgraduate School
    Monterey, CA 93943-5000

6. Dr. Kevin Jones...1
    Dept. of Aeronautics and Astronautics, Code AA/Jo
    Naval Postgraduate School
    Monterey, CA 93943-5000

7. Dr. Ismail Tuncer 1
    Dept. of Aeronautics and Astronautics, Code AA/Tu
    Naval Postgraduate School
    Monterey, CA 93943-5000

8. Mr. Ronald E. Marvin 2
    818 Kevin Way
    Ridgecrest, CA 93555